# ANALYSIS WITH UNCERTAINTY OF HYDROLOGICAL EXTREME EVENTS

**Dissertation**

submitted to and approved by the

Department of Architecture, Civil Engineering and Environmental Sciences
University of Braunschweig – Institute of Technology

and the

Department of Civil and Environmental Engineering
University of Florence

in candidacy for the degree of a
**Doktor-Ingenieur (Dr.-Ing.) /**
**Dottore di Ricerca in Civil and Environmental Engineering*)**

by
Valentina Chiarello
born 15.07.1984
from Galatina (LE), Italy

| | |
|---|---|
| Submitted on | 01/08/2016 |
| Oral examination on | 09/11/2016 |
| Professorial advisors | Prof. Enrica Caporali<br>Prof. Hermann Matthies |

**2017**

*) Either the German or the Italian form of the title may be used.

# Acknowledgements

*If we could know enough about the nature of the sources of uncertainties, we could devise ways of dealing with them. Without that knowledge, every approach will be an approximation.*
*(Beven and Binley, 2014, GLUE: 20 years on)*

The first thanks are for you prof., you take always care of me, and when I said always is definitely true, in every hour of the day, in every moment of my research work, since my first dissertation. She really trusts her favorite PhD. I am deeply grateful to my advisor prof. Enrica Caporali, she has always pushed me, supported me, she is by my side having an immeasurable confidence in me.
I would like to express my thankfulness to Prof. Hermann G. Matthies for supervising my thesis, I very much appreciate his valuable suggestions. Moreover, I've learned more than maths during the fruitful discussions on rodent animals with him.
I would really like to thank Bojana Rosic who kindly helped me in this work, for having provided all the mathematical knowledge and the valuable Matlab tools. I am sincerely grateful to her, I've taken advantage of her helpfulness $10^6$ time moments and more.
I would like to express my thankfulness to prof. Castelli for providing the MOBIDIC model and to Giulia for teaching me the fundamental of the model simulation.
I am grateful to prof. Llasat for assisting me during my stay in Barcelona, she truly hosted me in her research group at the University of Barcelona.
A giant thanks is for Cosima, the perfect secretary, the Mother of efficiency, the best citizen of Braunschweig. I am indebted to you, maybe forever, since you've helped me to find an accommodation, a bike, a Birkenstock shop, and so on, when we became friends going out for a drink or enjoying our time eating taralli baresi. I am indebted to you for the biggest help that you've always gave to me, I hope that my true love for you can pay some of my debt.
My greatest gratitude goes to my family, who always supporting me, particularly during my staying abroad. You are always by my side, you have even learned to use Skype, you could not stay much closer to me. I wish to thank my best friends that always let me feel home right the day I came back from my periods abroad, especially Martina. A special thank for Daniela, Wolfenbuttel would not been so beautiful without you.
Above all my deepest gratitude I owe to you Alessandro, saying that you support me is not enough, your love is more and more than a support, your patience is not evaluable. Thanks forever.

# Abstract

In engineering practice for flood risk assessment it is of primary importance to provide an accurate design flood estimate corresponding to a given risk level. Developing efficient methodologies for assessing flood quantiles in ungauged river basins means to focus on Uncertainty Quantification (UQ). Uncertainty of the model parameters and observed measures is the subject of a relevant and ongoing research activity, in assessing the uncertainty in the design flood we deal with the uncertainty of the model output. In this thesis, the evaluations of the flood quantiles and the predictive uncertainty of these variables are provided by two different models. Within the framework of regional flood frequency analysis approaches, the Top-Kriging interpolation technique is used and the results are compared with the estimates of flood quantiles provided by an at-site flood frequency analysis. Moreover, identification procedure of the uncertain parameters of the distributed hydrological model MOBIDIC (MOdello di Bilancio Idrologico DIstribuito e Continuo) was developed.

Efficient tools to tackle the parameter identification and the evolution of uncertainty in hydrological modelling have been researched. Monte Carlo and related techniques, i.e. the sampling or ensembles procedures, are well-known, methods based on functional approximation, where the unknown Random Variables (RVs) are represented as functions of known and more simple independent RVs, are very recent and can help to accelerate the Bayesian update. In order to find the Bayesian solution of inverse problem, the Ensemble Kalman filter (EnKF) and Wiener's Polynomial Chaos Expansion (PCE) methods are compared. The numerical evaluation of the analyzed Bayesian updating methods is carried out with reference to the hydrological model MOBIDIC. The proposed methodologies are applied to the case study of the Arno river basin, in Tuscany Region, Italy.

The actual value of some model parameters is described in a Bayesian way through a probabilistic model: the parameters are considered as RVs, the impact of errors, or uncertainty, in the data are investigated. The quantification of the accuracy of the different models and the comparison of results from the interpolation techniques and from the hydrological model MOBIDIC are evaluated. Finally, a preliminary discussion on the ways to convey the results of UQ to stakeholders and to communicate the outcomes for flood risk assessment is carried out.

# Abstract

In der technischen Praxis der Bewertung von Hochwasserrisikos ist es wichtig, eine präzise Wasserstandsvorhersage zusammen mit der Wahrscheinlichkeit ihres Auftretens zu liefern. Um effektive Methoden zur Bewertung von Hochwasserquantilen in Flüssen ohne Pegelmessung zu entwickeln, muss man den Fokus auf die Quantifizierung von Unsicherheit legen.
Unsicherheiten bei Modellparametern und Messungen ist das Thema gegenwärtiger relevanter Forschungstätigkeit; bei der Einschätzung von Unsicherheiten in der Hochwassersimulation betrachten wir die Unsicherheit des Modells.
In dieser Dissertation erfolgt die Evaluation der Quantile des Hochwasser und die Vorhersageunsicherheit dieser Variablen durch zwei unterschiedliche Modelle. Im Rahmen von Ansätzen zur regionalen Hochwasserfrequenzanalyse werden Top-Kriging Interpolationstechniken benutzt, und die Resulate werden mit Schätzungen der Hochwasserquantile verglichen, die durch eine Vorort-Hochwasserfrequenzanalyse gewonnen wurden. Zusätzlich wird das räumliche hydrologische Modell MOBIDIC (MOdello di Bilancio Idrologico DIstribuito e Continuo), durch das die unsicheren Parameter identifiziert werden, eingeführt.
Effiziente Werkzeuge zur Parameteridentifikation und Entwicklung von Unsicherheiten in hydrologischen Modellen werden identifiziert. Während Monte Carlo- und verwandte Techniken, z. B. Ensemble-Verfahren, wohlbekannt sind, sind Methoden der funktionalen Approximation, bei der die unbekannten Zufallsgrößen als Funktionen von bekannten und einfacheren Zufallsgrößen repräsentiert werden, relativ neu und können dazu dienen, Bayes´sche Aktualisierung zu beschleunigen.
Um eine Bayes´sche Lösung des inversen Problems zu finden, werden der Ensemble Kalman Filter und Wieners Polynome Chaos-Entwicklungs verglichen. Die numerische Auswertung der analysierten Methoden zur Bayes´schen Aktualisierung wird in Bezug auf das hydrologische Modell MOBIDIC durchgeführt.
Die vorgeschlagenen Methoden werden auf eine Fallstudie des Flußbettes des Arno in der Toskana, Italien, angewandt. Die Werte einiger Modellparameter werden auf Bayes´sche Weise anhand eines Wahrscheinlichkeitsmodells beschrieben: Die Parameter werden als Zufallsgrößen betrachtet und die Auswirkung von Fehlern oder Unsicherheiten bezüglich der Daten werden untersucht. Die Quantifikation der Genauigkeit der verschiedenen Modelle und der Vergleich der Resultate mit Hilfe von Interpolationstechniken und des MOBIDIC-Modells werden ausgewertet. Anschließend folgt eine vorläufige Diskussion über die Art und Weise, die Resultate der Quantifizierung von Unsicherheiten an Betroffene zu übermitteln und die Ergebnisse dieser Bewertung von Hochwasserrisiken zu veröffentlichen.

# Contents

# List of Figures

# List of Tables

# List of Symbols

| Symbol | Description |
|---|---|
| $T_r$ | Return period |
| $Q$ | Discharge |
| Q10 | 10-years return period flood quantile |
| Q50 | 50-years return period flood quantile |
| Q100 | 100-years return period flood quantile |
| Q200 | 200-years return period flood quantile |
| Q500 | 500-years return period flood quantile |
| Q10/A | Q10 normalized by catchment area |
| Q50/A | Q50 normalized by catchment area |
| Q100/A | Q100 normalized by catchment area |
| Q200/A | Q200 normalized by catchment area |
| Q500/A | Q500 normalized by catchment area |

| Acronym | *Acronym description* |
|---|---|
| AEP | Annual Exceedance Probability |
| AIC | Akaike Information Criterion |
| AMALGAM | Multialgorithm Genetically Adaptive Method for Multiobjective Optimization |
| ARF | Areal Reduction Factor |
| BATEA | BAyesian Total Error Analysis |
| BFS | Bayesian Forecasting System |
| BIC | Bayesian Information Criterion |
| BLUE | Best Linear Unbiased Estimator |
| BMA | Bayesian Model Averaging |
| BU | Bayesian Update |
| CCA | Canonical Correlation Analysis |
| CFR | Regional Functional Centre |
| CK | Canonical Kriging |
| DYNIA | DYNamic Identifiability Analysis |
| DREAM | Differential Evolution Adaptive Metropolis |
| EnKF | Ensemble Kalman Filter |
| ERT | Electrical Resistivity Tomography |
| GIS | Geographical Information Systems |
| GLUE | Generalized Likelihood Uncertainty Estimation |
| IAHS | International Association of Hydrological Science |
| IBUNE | Integrated Bayesian Uncertainty Estimator |
| IDF | rainfall Intensity-Duration Frequency curve |
| MAE | Mean Absolute Error |

| | |
|---|---|
| MCS | Monte Carlo Sampling |
| ME | Mean Error |
| ML | Maximum Likelihood |
| MLBMA | Maximum Likelihood version of Bayesian Model Averaging |
| MOBIDIC | MOdello di Bilancio Idrologico DIstribuito |
| MOSCEM-UA | MultiObjective Shuffled Complex Evolution University of Arizona |
| NSE | Nash-Sutcliffe Efficiency |
| PCA | Principal Component Analysis |
| PCE | Wiener's Polynomial Chaos Expansion |
| PGRA | Flood Risk Management Plans |
| PSBI | Physiographical-Space-Based Interpolation |
| PTF | Pedo Transfer Functions |
| PUB | Predictions in Ungauged Basins |
| RFFA | Regional Flood Frequency Analysis |
| RMSE | Root Mean Square Error |
| RV | Random Variable |
| SCEM-UA | Shuffled Complex Evolution Metropolis University of Arizona |
| SIR | Regional Hydrologic Service of Tuscany |
| szi | Sullo zero idrometrico (on zero gauge) |
| UA | Uncertainty Assessment |
| UoM | Unit of Management |
| UQ | Uncertainty Quantification |
| USGS | United States Geological Survey |

# Chapter 1

# Introduction

## 1.1 Motivation

Extreme river floods have been already a substantial natural hazard over the past centuries and now the impacts of human activities are leading to changes in the magnitudes and frequency of floods and droughts at even remote locations.
In developing countries extreme floods can result in many fatalities, while in developed countries, more often, extreme floods cause material damage in the billions and tens of billions of dollars. Destructive floods in the last decade across the globe have led to record high material damage. For the first time, global annual losses from natural disasters exceeded $200 billion in 2005, 2008, and 2011 (National Academies of Sciences, 2012). Data on loss of life, on the other hand, has no clear trend but an analysis of global statistics showed that inland floods (river floods, flash floods and drainage floods) caused 175,000 fatalities and affected more than 2.2 billion people between 1975 and 2002 (Jonkman, 2005). In the above statistics, the consequences of other types of floods such as coastal floods and tsunamis are not included although coastal flood events are even more catastrophic than inland floods in terms of loss of life. For example, flooding caused hurricane Katrina in the year 2005 caused, according to the Louisiana Department of Health, 1,464 fatalities or the estimated death toll from the Indian Ocean tsunami in the year 2004 is approximately 230,000, making it one of the most catastrophic disasters in history.
The national science academies from 15 countries issued the so-called "G-Science" statements: one of this, "Building Resilience to Disasters of Natural and Technological Origin", emphasizes that a more effective guide to building resilience can be based on systematic scientific risk surveillance and ranking.
While experience from recent disasters provides useful lessons, the challenge for the hydrological community is to identify appropriate responses to these threats. In this framework, a considerable attention has been given in the last decades in studying, understanding and predicting the nature of environmental extreme events. Hydro-meteorological phenomena such as floods, heavy rain, hailstorms, snowfall, hurricanes, heat waves, and droughts, are mainly investigated. Extreme hydro-meteorological events, in fact, are paramount for the massive impacts that they might cause on everyday life as well as because of their possible link with climate change.

**Figure 1.1: An episode of high streamflow occurred on 30.01.2014 in Florence.**

a) 

b) 

c) 

**Figure 1.2: Flood events occurred in Tuscany in recent years: a) Albegna river flood on November 2012 (http://www.greenreport.it/news/albegna-2-anni-dallalluvione-ce-protocollo-dintesa-per-messa-in-sicurezza-fiume/) b) Ombrone Grossetano river flood on August 2015 (http://www.meteosiena24.it/4968-2/) c) Orcia river flood (http://www.inmeteo.net/blog/2012/11/13/alluvione-toscana-13-novembre-2012-grosseto/)**

## 1.2 Scope of the research

The present dissertation aims to investigate several methods for predictions in ungauged basins. The main purpose is to provide an accurate design flood estimate corresponding to a given risk level even in ungauged river basins.
Numerous predictive tools such as lumped models, distributed models and statistical regionalization to predict runoff in ungauged catchments have been developed. Therefore, the estimate of flood quantiles in ungauged river basins and in sites characterized by short or discontinuous time series are provided by two methods:

- the use of geostatistical spatial interpolation techniques, which allow estimation of a variable including its uncertainty, like Top-kriging (Skøien et al., 2006);

- the use of the distributed and raster-based hydrological balance model MOBIDIC (MOdello di Bilancio Idrologico DIstribuito e Continuo) (Campo et al., 2006; Castelli et al., 2009).

Since predictions of extreme stream flow related variables at sites where little or no data are available are highly uncertain, this research activity focuses on the estimation of predictive uncertainty, and its subsequent reduction. Each estimates of the design variable of interest should be accompanied by an assessment of its predictive uncertainty usually reported in terms of errors in an overall goodness of fit procedure in poorly gauged river basins.
The application of a hydrological model that describes the key processes of interest during a flood event, means take into account a set of parameters that represent the physical phenomena and govern critical processes as well as appropriate meteorological inputs and geographic data. Each of these datasets required by the hydrological model MOBIDIC for the prediction system, is either not known at all, or at best known imperfectly, due to the inherent multi-scale space-time heterogeneity of the hydrologic system, especially in ungauged basins.
As it is becoming increasingly hard to ignore the presence of uncertainty in the hydrologic systems, the main scope of this research is to improve the existing mathematical models of flood phenomena by including the uncertainties into the problem itself. In particular, an effort is done to propose a methodology where the hydrological modeling is efficiently coupled with the assessment of parameter uncertainty.
In applications, it is frequently of interest to solve inverse problems: to find an input to a mathematical model, given an observation of the solution of the model. The problem of updating the knowledge of an uncertain quantity in a sequential way from noisy and incomplete data is a so-called inverse problem of identification. The parameter identification and the evolution of uncertainty in the model can be approached in different ways, both classical optimisation approach and Bayesian

update approach. This study aims to investigate several numerical approaches for the numerical evaluation of the Linear Bayesian Update, Ensemble Kalman filter (EnKF) method as well as functional approximation based method (PCE) are tested for compute the posterior.

The knowledge of how data uncertainty and variability might affect hydrological models for flow predictions in ungauged basins represents a crucial challenge. This becomes more challenging considering we deal mainly with nonlinear problems. The vast majority of applied geosciences like hydrology have adopted risk assessment as a standard practice. Any flood risk analysis must be probabilistic and any probabilistic floods hazard analysis must focus on uncertainty quantification.

The original contribution of the research activity is to identify in the framework of flood risk assessment efficient tools to tackle the parameter identification problem in hydrological modelling, where the patterns are complex because involving significant unknowns and uncertainties.

## 1.3 Expected results

The assessment of the desired stream flow index (i.e., the flood quantile associated with a given non-exceedance probability, usually expressed in terms of return period) is carried out by means of different methodologies: an at-site flood frequency analysis, a regionalization approach, a hydrological model application. Regarding the regional flood frequency analysis, it has been studied the possibility to apply Top-kriging, a quite recent spatial interpolation technique developed for the regionalization of streamflow regime. By means of Top-kriging application, it is possible to achieve a complete characterization of the design floods used for planning and floodplain management investigations. In particular, the application in ungauged sites, the most common situation in real world, is carried out. The Top-kriging outcomes are compared with the results obtained by means of the new MOBIDIC module for design hydrograph application. These simulations show the possibility to use for design hydrograph estimations the results of a regional frequency analysis of extreme rainfall, given in the form of parameters of the rainfall Intensity-Duration Frequency (IDF) curve for assigned return periods ($T_r$). Moreover, the comparison of results from different methodologies allows to assess model performance in order to identify the most suitable strategy for streamflow extremes assessment in ungauged river basins.

Regarding the parameter identification procedure, the attention is focused on investigate different numerical approaches for the Bayesian solution of inverse problem. One result of this study is to propose a methodology for flood risk mitigation that investigates the presence of model parameter uncertainty and explain how it is possible to identify the parameters of a hydrological model through the comparison of different Bayesian updating methods.

In this dissertation, the value of some MOBIDIC model parameters to be identified is described in a Bayesian way through a probabilistic model: they are described as RVs, the randomness reflecting the uncertainty about the true values. The impact of errors, or uncertainty, in the data such as parameter values and initial conditions are investigated. Different ways of numerically computing the Bayesian update (BU) are considered, via Monte Carlo methods, i.e. EnKF procedure, as well as via functional approximation, i.e. PCE, where the unknown RVs are represented as functions of known RVs. An original procedure for couple flood risk assessment and uncertainty quantification is proposed: the identification of the parameter of a hydrological model considered uncertainty is carried out with PCE based method. The method is very recent and may be well combined with the Monte Carlo methods for the forward problem. Moreover, as BU may be numerically very demanding, the computational procedure based on PCE of stochastic problems, could be helpful to accelerate the update. A comparison between PCE based methods and Monte-Carlo based methods in hydrological modelling that focuses on the prediction of the design flood in ungauged river basins is not available in the literature yet. Therefore, both methodologies are applied on the case study.

## 1.4 Thesis outline

The thesis is organized as follows: we first introduce the objectives and the expected results of the research, later in part I we look at methodologies for assessing flood quantiles in ungauged river basins in the framework of regional flood frequency analysis, in Part II we consider the design flood estimates provided by the hydrological model MOBIDIC. In both cases the predictive uncertainty is quantified. Chapter 2 gives an overview of the Geostatistical spatial interpolation techniques for regionalization of hydrometric information, provides a description of the basic concepts of Kriging procedure and presents the Top-kriging methodology in detail. In Chapter 3 the study area, data, and flood quantiles are described. We illustrate the Top-kriging technique for the case of estimating the flood quantiles corresponding to several return periods in Tuscany Region (Italy). This includes an analysis of the estimation uncertainties in ungauged river basins. The mathematical theory of Uncertainty Quantification (UQ), the topic of UQ in hydrology as well as the reasons for the Presence of Uncertainty in hydrology are reviewed in Chapter 4. The methods for model parameter identification and the numerical approaches for Bayesian updating to inverse problems considered in this study are illustrated in Chapter 5.
In Chapter 6 we define the dataset used in the hydrological model MOBIDIC and we illustrate the UQ of the parameters of MOBIDIC through the comparison of different Bayesian updating approaches. This includes the numerical implementation considering different RV representations, which may take the form of sampling as well as functional approximations such as PCE.

Chapter 7 provides a brief discussion on the best flood risk management strategy in order to define the ways to communicate the outcomes of UQ and flood risk assessment. Finally, in Chapter 8 some concluding remarks, the main results obtained by the two methodologies are summarized and an outlook to future research activities is given.

# Chapter 2

# Regional flood frequency analysis

## 2.1 Related work

According to the Predictions in Ungauged Basins - PUB science initiative of the International Association of Hydrological Science - IAHS (Hrachowitz et al., 2013; Sivapalan et al., 2003), hydrologists have developed numerous predictive tools such as empirical models, lumped models, distributed models and statistical regionalization to predict runoff in ungauged catchments. The most widely used tools (unit hydrographs, flood frequency curves, flow duration curves) are essentially data driven, and are estimated from hydrometric data at basin scales. In cases where no at-site data are available, data collected at gauged neighboring catchments, or at catchments with similar hydrologic regimes may be used (see e.g. Brath et al., 2003; Cunderlik and Burn, 2006; GREHYS, 1996a; Ouarda et al., 2001).
Methods for estimating runoff at ungauged locations such as the Rational Method and the index-flood method have been in practical use for a long time. However, for many purposes, empirical methods do not suffice and process understanding needs to be invoked in order to make predictions that are reliable for a diverse set of hydrological conditions (Blöschl, 2016).
The assessment of extreme hydrological events at sites characterized by short time series or where no data record exists, has been mainly obtained by regional models. The regionalization of the streamflow regime is a central topic in this research field, several regional estimation procedures and techniques have been proposed (Burn, 1990; GREHYS, 1996b; Pandey and Nguyen, 1999; Rosbjerg and Madsen, 1995; Shu and Burn, 2004a, 2004b). In general, the steps involved in Regional Flood Frequency Analysis (RFFA) are:

1. Delineation of homogeneous regions;
2. At-site frequency analysis;
3. Regional relationship development.

The index flood method, introduced by Dalrymple (1960), is the most widely used method of RFFA. This requires a two-step procedure. The first step is the identification of groups of hydrologically homogeneous regions within a common probability model of annual maximum peak flows can be assumed to be invariant.

The second step provides a scale factor represented by the index flood. The flood discharges of given return periods relative to the selected site, indeed, are expressed as the product of two terms: the scale factor of the examined site (the index flood) and the dimensionless growth factor, which has regional validity. The literature contains numerous studies on the identification of homogeneous regions and the estimation of the growth factor (see for instance Burn and Goel, 2000; Castellarin et al., 2001; Reed et al., 1999), and relatively few on estimating the index flood. Homogeneous regions can be assessed with different approaches, often with multivariate analysis tools such as Principal Component Analysis (PCA), Canonical Correlation Analysis (CCA) and Cluster Analysis. Several studies use a hierarchical approach as a method of identification of homogeneous regions (Gottschalk et al., 2011; Sauquet, 2006).

Recent studies show that techniques, which have been originally applied for the spatial interpolation of point data (e.g. kriging interpolators, De Marsily and Ahmed, 1987), can be effectively applied for regionalization of hydrometric information (Castiglioni et al., 2011; Chokmani and Ouarda, 2004; Skøien et al., 2006; Skøien and Blöschl, 2007). A general framework and methodological approach which integrate concepts and techniques of RFFA, geostatistical theory and analytical Geographical Information Systems (GIS) are proposed in Daviau et al. (2000). The purpose of this study is to extend the non-parametric (Gingras and Adamowski, 1993) and L-moment (Hosking and Wallis, 1997, 1993) methods for RFFA by treating at-site flood parameters as spatially continuous random variables. This is done using GIS and geostatistical methods such as visualization, semi-variograms and kriging. The L-moment and kriging techniques provide both the parameter estimates and the error associated with these estimates (variance) for diagnostic purposes.

Gottschalk and co-workers (Gottschalk, 1993a, 1993b; Sauquet et al., 2000) have extended geostatistical concepts to river catchments. Considering that observations are structured along stream networks and the runoff process is non-homogenous along rivers as the basin areas are nested (Gottschalk, 1993a), it is not obvious define a measure of distance between catchments. The author suggests to replace the Euclidean distance with a "geostatistics" distance, a relevant distance measure called Ghosh distance. In Gottschalk et al. (2011) the temporal, spatial and cross-covariances of runoff, rather than spatial and spatio-temporal semivariograms is mainly investigated.

Gottschalk (1993b) first developed a method for calculating covariance along a river network and used this for interpolation along the network (Gottschalk, 1993b). Sauquet et al. (2000) further developed this method for mapping annual runoff along the river network using water balance constraints in the estimation procedure.

Skøien et al. (2006), extending the work of Sauquet et al. (2000), proposed a method of geostatistical estimation on stream networks known as Top-kriging, or topological kriging. Their method is a kriging interpolation procedure that takes into account the geometric organization and structure of hydrographic network, the catchment area

and the stronger spatial correlation between nested catchments. According to the authors, this method can be used for a range of stream flow-related variables including variables that do not aggregate linearly and are non-stationary. The authors exploited also short records considering local uncertainties of the measurements that may differ between locations, providing the estimation of predictive uncertainty in ungauged catchments.

Top-kriging interpolation of runoff characteristics for PUB has been tested for the estimation of flow duration curves (Pugliese et al., 2014), flood statistics (Archfield et al., 2013; Salinas et al., 2013), flood hydrographs (Skøien et al., 2008; Skøien and Blöschl, 2007). The latter authors report an improved runoff prediction compared to estimates of regionalized hydrologic model simulations. Such findings are confirmed in a recent study of Viglione et al. (2013). This study shows that, in Austria, a direct interpolation of daily runoff by Top-kriging is superior to simulations obtained by hydrologic model driven by transferred model parameters. With the aim to relate this finding to the density of gauging stations, the role of station density for predicting daily runoff by Top-kriging interpolation in Austria has been investigated too (Parajka et al., 2015). The main objective of this study was to evaluate predictive accuracy of Top-kriging interpolation driven by different number of stations (i.e. station densities) in an input dataset. The idea was to interpolate daily runoff for different station densities in Austria and to evaluate the minimum number of stations needed for accurate runoff predictions. The results of the cross-validation indicate that, in Austria, Top-kriging interpolation is superior to hydrological model regionalization if station density exceeds approximately 2 stations per 1000 km$^2$ instead lower runoff efficiency is found for low station densities (less than 1 station/1000 km$^2$) and in some smaller headwater basins.

Furthermore, in the context of low flow regionalization, a comparison of Top-kriging with regional regression method is applied by Laaha et al. (2014). To apply the regional model, the authors subdivided study area, in Austria, into eight geographically adjoining regions of similar low flow seasonality and a multiple regression relationship between low flow and catchment characteristics is found for each region. Results obtained by the regional model suggest that precipitation is strictly related with low flows in Austria and the topography seems to have an important control of low flows, because of its strong influence on precipitation. Geology has positive or negative effects on low flows depending on the porosity of the formations, while the role of land use appears subordinate. The spatial estimates obtained by Top-kriging and regional regression are similar on a larger scale, while there are clear differences if the small-scale variability is considered: in particular, Top-kriging procedure generates more heterogeneous patterns. These differences in estimates depend entirely on the spatial variability of the predictors related to topography and the climate of the study area. As concerns the uncertainties estimated by the two methods, many differences are found for most of the stream network. While the errors of regression are almost constant over large areas, the ones

of Top-kriging are more heterogeneous, as in the case of the spatial estimates. This means that the performance of Top-kriging depends on the intrinsic homogeneity of observation data and the density of the gauging network in the study area, while the performance of the regression model depends on the availability of catchment characteristics and how these characteristics are related with the low flows. The choice between Top-kriging and regression model should be affected by the data availability and the characteristics of the observations, but the authors affirm that considering the stream flow generation processes, the distribution of kriging weights and of uncertainty along the stream network, Top-kriging appears well adapted for the river network problems.

Another approach for regional flood frequency estimation, termed Canonical Kriging (CK), or Physiographical-Space-Based Interpolation (PSBI), is proposed by Chokmani and Ouarda (2004). This methodology, using physiographical and meteorological characteristics of gauging stations and multivariate analysis techniques such as Principal Components Analysis (PCA) and Canonical Correlation Analysis (CCA), interpolates flow quantiles with Ordinary kriging through the continuous physiographical space (physiographical space-based kriging method). The PSBI approach, unlike other methods, does not consider the coordinates in the geographical space, but it is based on the use of the catchments coordinates in the physiographical spaces. This choice is related to the determination to interpolate the involved hydrological variables over the physiographical domain. The method starts from a set of hydrological and physiographic variables that, in the case studied by the authors correspond, respectively, to streamflow quantiles and climatic variables. The aim of the CCA is to connect the two groups using vectors of canonical variables, while PCA is used to generate a new set of variables. After obtaining the physiographical and climatic characteristics of the ungauged basins, these basins can be placed in a CCA or a PCA physiographic/climatic space. The position of the ungauged basin in the transformed physiographical space and the information about the hydrological variable in the surrounding basins, are necessary to estimate the values of the variable for the ungauged basins. This could be done if the hydrological variable is continuous over the transformed physiographical space. Geostatistical techniques were so far used to estimate flood flow quantiles because it was widely demonstrated that hydrological variables can be considered as continuous. The kriging procedure is then applied to interpolate the variables over the physiographical space. Finally, according to the authors, the physiographical-space-based interpolation is effective to estimate flow quantiles and it results extremely satisfactory in the case of high-frequency quantiles within the CCA physiographical space.

Castiglioni et al. (2011) compared PSBI with Top-kriging for low flow predictions in ungauged sites, observing the complementary utility of the two methods for headwater and larger scale catchments, focusing on the prediction of low flow index $Q_{355}$ the daily streamflow that, on average, is equaled or exceeded 355 days in a year.

The authors evaluated the performance of Top-kriging and PSBI with the further purpose to compare advantages and disadvantages related to the application of each methodology. In the context of the prediction in ungauged basins this study tries to find out additional details on the usefulness of the two spatial interpolation techniques for the prediction of streamflow indices. The decision of the authors to focus only on kriging-based approaches is justified by the presence of a previous analysis performed for the same study area: results show that predictions of low-flow indices in ungauged basins are more accurate if the PSBI method is used instead of a traditional multiregression model (Castiglioni et al., 2009). In this case, excluding a small number of basins characterized by a particular low flow frequency regime, findings obtained by the two methodologies are very similar: this means that both can be considered as an effective alternative to traditional regionalization approaches, such as multiregression models. Nevertheless, the performance of the two methods strictly depend on the topological characteristics of the river network: Top-kriging outperforms PSBI at larger river branches and PSBI outperforms Top-kriging for headwater catchments. The main difference between the two methodologies is the different support they use for performing the interpolation: PSBI is based on the use of the catchments coordinates in the physiographical spaces, while Top-kriging estimates the values of the involved variable directly along the river network. This latter is based only on spatial information and for this reason requires local data as accurate as possible: in fact, heterogeneity not covered by local data will cause higher uncertainties. It remains to point out that the methods are complementary in terms of the basic principle of spatial interpolation, in terms of data requirements and finally in terms of predictive performances. Implicitly, the authors suggested the possibility of improving the prediction accuracy by blending the two methods but the analysis performed by Archfield et al. (2013) shown that coupling Top-kriging with CK slightly improves the flood quantile predictions in ungauged sites. Moreover, results detected by the authors support the theory of other studies which have found that geostatistical methods outperform regression-based methods.

These applications of spatial interpolation techniques to regionalization of streamflow regime share a common background idea: both perform a smooth regionalization of streamflow indices seamlessly over the stream network (Top-kriging) or the Physiographical Space (PSBI) without identifying groups of hydrologically homogeneous regions.

Traditional methods for regional flood frequency analysis at ungauged sites are built upon the assumption that the hydrologic regime does not vary through time (i.e. stationary) at the ungauged site and at gauged sites. This assumption is questioned by several recent studies. Non-stationarity in the hydrologic regime can be induced by changes in the climatology but also in the drainage basin characteristics. In order to obtain accurate quantile estimates for hydraulic structure design or floodplain mapping, Leclerc and Ouarda (2007) presented a non-stationary regional approach,

whose results showed that a multiple regression model leads to quite efficient estimation of some non-stationarity regional flood quantiles. The authors investigate the use of CCA with the aim to measure similarity between ungauged sites and gauged basins and to delineate hydrological neighborhoods for regional transfer.

In a most recent work (Nezhad et al., 2010), a modified version of the original PSBI method, based on residual kriging (RK) in physiographical space, is proposed for regional flood frequency analysis. In this approach, in order to remove any possible spatial trends within the hydrological variables over the physiographical space, the trend is quantified and removed from the hydrological variable.

It is increasingly acknowledged that spatial proximity does not necessarily entail similarity in functional behaviour ( e.g. Ali et al., 2012), and that the efficiency of distance-based approaches can be considerably improved when applying some sort of hydrologically more meaningful distance measure (Bárdossy et al., 2005). For example, Merz et al. (2008) combined the Top-kriging method with catchment characteristics to enhance the predictive performance of the method. An alternative method to assess functional similarity was introduced by Archfield and Vogel (2010). Instead of using the spatially closest stream gauge as reference for transferring daily flow to an ungauged site, they proposed the kriging-based map-correlation method, which selects the reference stream gauge whose flows are most correlated to the ungauged site. Likewise, to define more significant metrics or dissimilarity measures for predicting flow, Samaniego et al. (2010) suggested the use of pair-wise empirical copula densities. The use of copulas in hydrology is quite recent, De Michele and Salvadori (2003) used them for a stochastic rainfall simulation whereas Favre et al. (2004) used copulas for flood frequency analysis. Bárdossy (2006) applied this formulation for finding better geostatistical models for groundwater quality parameters. Some recent advances in hydrological modelling that exploit copulas are reported in Salvadori and De Michele (2007). Recently, several efforts have been spent on the issues of multivariate design and quantiles (Chebana and Ouarda, 2011a; Salvadori et al., 2011); in Chebana and Ouarda (2011b) a new methodology based on a multivariate quantile version is proposed to identify multivariate extremes by using depth functions. Copulas have received increasing attention as a spatial analysis tool, as a better alternative to the traditional geostatistics for spatial modelling (Bárdossy and Li, 2008; Kazianka and Pilz, 2011) and for modelling dependence in space and time (Gräler and Pebesma, 2011).

One of the achievements of the PUB initiative of the IAHS was a synthesis of methods that before had been treated in a fragmented way (Blöschl et al., 2013). The synthesis proceeded along the dimensions of processes, places and scales. The synthesis across processes involves a consistent and coherent treatment of annual runoff, seasonal runoff, the flow duration curve, floods, low flows and entire hydrographs. The synthesis across places is built on the notion of similarity and draws together experience and data from numerous catchments in a region and from around the world. The synthesis across scales involves a balanced view of both

upscaling methods based on laboratory equations (such as distributed models) and lumped catchment scale models (such as regional statistical relationships).
The synthesis of results shows that most of the methods used for PUB in the past, simulate daily runoff by conceptual hydrologic models. These models need estimates of climate inputs and calibration against observed runoff which is not directly possible in ungauged basins. Hence for PUB, different methods for spatial interpolation of climate characteristics (Gaál et al., 2008; Szolgay et al., 2009) and transferring model parameters from gauged to ungauged basin has been evaluated (Parajka et al., 2013). The comparison of results of different transfer methods indicates that all of them show a similar predictive performance with considerable scatter within each method. Evaluation of studies applying large number of basins and dense stream gauge network shows that spatial proximity and geostatistical interpolation of model parameters perform better than other methods.
An alternative to hydrological modeling is direct interpolation of runoff values. The main advantage of direct interpolation is that it avoids the use of uncertain input variables such as precipitation and potential evaporation. The limitation is that this method is data intensive, i.e., it can only be applied in medium to densely gauged regions, and it is not applicable when one is interested in the causal relationship between precipitation and runoff (Blöschl et al., 2013).
The synthesis report of the initiative concluded with best practice recommendations for predicting runoff in ungauged basins (Blöschl, 2016).

## 2.2 Geostatistical spatial interpolation techniques

Specific techniques are necessary to regionalize the hydrological variables over the considered area. A particularly appealing set of approaches are geostatistics, which allow estimation of a variable including its uncertainty at locations where no measurements are available (Journel and Huijbregts, 1878).
Geostatistics adapt classic regression techniques to deal with spatially continuous or 'regionalized' variables - the values of which change with spatial location and the behavior of which is somewhere between a deterministic and a random variable (Bonham-Carter, 1994). It includes techniques to quantify spatial autocorrelation using variograms; to model parameter surfaces with or without dependent variables (kriging); to assess the variance of estimates.
A brief introduction to geostatistics is initially provided for reference before the description of the geostatistical interpolators. Most of the information about geostatistics in this section is from Bivand et al. (2013); Castrignanò (2010); Li and Heap (2008).
Although mining industry provided the impetus for geostatistics in the 1960s, geostatistics is can be traced back to the early 1910s in agronomy and 1930s in meteorology (Webster and Oliver, 2001). It was developed by Matheron (1963) with his theory of regionalized variables (known as geostatistics). Matheron's thesis

remains the theoretical basis of most present-day practice. The theory of regionalized variables forms the basis of procedures for analysis and estimation of spatially dependent variables. A key concept of this theory is that "When a variable is distributed in space, it is said to be regionalized" and "geostatistical theory is based on the observation that the variabilities of all regionalized variables have a particular structure" (Journel and Huijbregts, 1878). The theory essentially expresses the idea that values of a soil property at near places are likely to be similar, whereas those at places far from one another are not. It does so quantitatively and in a way that can be used for interpolation (Castrignanò, 2010).

Geostatistics assumes that a spatial variation of any variable can be expressed as the sum of three major components. These are:

1) a deterministic component associated with a constant mean value or a long–range trend;
2) a spatially correlated random component;
3) a white noise or residual error term that is spatially uncorrelated.

Thus, the spatial variable Z at the position x is given by:

$$Z(x) = m(x) + \varepsilon'(x) + \varepsilon'' \tag{2.1}$$

where $m(x)$ is a deterministic function describing the trend component of $Z$ at $x$; $\varepsilon'(x)$ is the term denoting the stochastic, locally varying spatially dependent residuals from $m(x)$ and $\varepsilon''$ is a residual, spatially independent noise term, having zero mean and variance $\sigma^2$.

Geostatistics is based on the concepts of:

- Regionalized variables;
- Random functions;
- Stationarity.

A random variable is any attribute that is expected to vary according to some probability distribution law. The random variable is characterized by the parameters of the distribution, such as mean and variance of the normal distribution. A regionalized variable $z(x)$ is a random variable varying in the space, the term regionalized specifies that its value depends on the spatial location, normally expressed by spatial coordinates. A regionalized variable $z(x)$ can be considered as a particular realization of a random variable $Z(x)$ for a fixed position $x$ within the area. If all values of $z(x)$ are considered at all locations within the area, $z(x)$ becomes a member of an infinite set of random variables, called a random function $Z(x)$. All the random variables of this set have the same probability distribution function $F(z)$, independent of $x$. Since $F(z)$ does not change when shifted in time and space, statistics such as mean and variance also do not change over time and space. Considering that most of the geostatistical operations only require knowledge of the

first two moments of the random function $Z(x)$, the property of stationarity should be referred to these.

In standard statistical problems, correlation can be estimated from a scatterplot, when several data pairs $\{x, y\}$ are available. The spatial correlation between two observations of a variable $z(x)$ at locations $x_1$ and $x_2$ cannot be estimated, as only a single pair is available (Bivand et al., 2013). To estimate spatial correlation from observational data, **stationarity assumptions** is needed.

A random function $Z(x)$ is said to be *first–order stationary* if its expected value (first moment) is the same at all locations:

$$E[Z(x)] = m \tag{2.2}$$

where $m$ is the mean of classic statistics and

$$E[Z(x) - Z(x + \boldsymbol{h})] = 0 \tag{2.3}$$

where $\boldsymbol{h}$ is the vector of separation between sample locations.

A random function $Z(x)$ is said to be second–order stationary if the spatial covariance $C(\boldsymbol{h})$ of each $z(x)$ and $z(x+\boldsymbol{h})$ pair is the same (independent of $x$) and depends on $\boldsymbol{h}$:

$$C(\boldsymbol{h}) = E[(Z(x) - m)(Z(x + \boldsymbol{h}) - m)] \tag{2.4}$$

where set $\boldsymbol{h} = 0$ the covariance equals the sample variance $C(0)$, therefore, the stationarity of $C(\boldsymbol{h})$ implies the stationarity of the sample variance.

Second–order stationarity does not apply if a finite variance or covariance cannot be defined, as in the case of trend phenomena: in this case a weaker form of stationarity, called the intrinsic hypothesis, must be assumed. This hypothesis requires that for all vectors $\boldsymbol{h}$, the variance of the increment $Z(x) - Z(x+\boldsymbol{h})$ be finite and independent of position, i.e. the semi-variance is defined as:

$$\gamma(\boldsymbol{h}) = \frac{1}{2}VAR[Z(x) - Z(x + \boldsymbol{h})] = \frac{1}{2}E\{[Z(x) - Z(x + \boldsymbol{h})]^2\} \tag{2.5}$$

Under this assumption, we basically state that the variance of $Z$ is constant, and that spatial correlation of $Z$ does not depend on location $x$, but only on separation distance $\boldsymbol{h}$. Then, we can form multiple pairs $\{z(x_i), z(x_j)\}$ that have (nearly) identical separation vectors $\boldsymbol{h} = x_i - x_j$ and estimate correlation from them. If we further assume *isotropy*, which is direction independence of semi-variance, we can replace the vector $\boldsymbol{h}$ with its length, $||h||$.

The concepts of regionalized variables and stationarity provide the theoretical basis for analysis of spatial dependence using semivariogram (commonly referred to as variogram). In geostatistics the spatial correlation is modelled by the variogram or semivariogram instead of a correlogram or covariogram. The variogram plots semi-variance $\gamma(\boldsymbol{h})$ between pairs of points as a function of distance $\boldsymbol{h}$ (Bivand et al., 2013).

The semi-variance $\gamma(\boldsymbol{h})$ describes the spatially dependent component of the random function $Z$. It is equal to the expected squared distance between sample values separated by given $\boldsymbol{h}$. The semi–variance between any two locations depends only on the distance and direction of separation between the two locations, but not on their geographic location. The semi–variance at a given $\boldsymbol{h}$ (called *lag*) is estimated as the average of the squared differences between all observations separated by the same *lag*:

$$\gamma(\boldsymbol{h}) = \frac{1}{2N(\boldsymbol{h})}\sum_{i=1}^{N(\boldsymbol{h})}[z(x_i) - z(x_i + \boldsymbol{h})]^2 \tag{2.6}$$

Where $N(\boldsymbol{h})$ is the number of pairs of observations separated by a given *lag* $\boldsymbol{h}$. This estimate is called the *sample* variogram.
The semi–variance can be defined in the terms of the variance $C(0)$ and spatial covariance $C(\boldsymbol{h})$ of $Z(x)$ when second–order stationarity applies (Figure 2.1), i.e.:

$$\gamma(\boldsymbol{h}) = C(0) - C(\boldsymbol{h}) \tag{2.7}$$

This equation shows that the variogram function is closely related to the covariance function, therefore it can be said that even $\gamma(\boldsymbol{h})$ is invariant by translation and it is indifferent to use the covariance or variogram as tool for the analysis of the spatial variability. Since $C(\boldsymbol{h}) \leq C(0)$ (the Cauchy–Schwarz inequality), in case of stationarity, the variogram is always limited, and the limit is represented by $C(0)$, that is the *sill*.
Experimental variograms are plots of the autocorrelation function at various *lag* distances for a given direction. They correspond to the sample covariance between the sample points separated by a fixed distance and describe the spatial correlation structure of the sampled data (Journel and Huijbregts, 1878). The experimental semi-variogram shows three important features (Figure 2.2).

- *Nugget* effect: the discontinuity at the origin, at $\boldsymbol{h}$ close to 0, due to short–scale variability or measurement errors;
- *Sill*: threshold value, limit of semi-variogram; The sill approximates the sample variance $\sigma^2$ for stationary data.
- *Range* of spatial dependence: separation distance; samples separated by distances larger than the range are spatially independent because the estimated semi-variance equals $\sigma^2$ implying random variation. On the contrary, samples within the range are spatially correlated, the range gives the meaning of influence of sample.

Semi–variances may also increase continuously without showing a definite range and sill, indicating the presence of trend effects and non–stationarity because the data still have a certain spatial dependence. It was stated above that two data points that are at a distance greater than the variogram range are not correlated, however

the variogram is not reliable for ***h*** greater than half the maximum size of the study area. The zone near origin in the variogram is of great importance in the estimation process, because the data closest to the location being estimated will receive greater weights (Castrignanò, 2010).

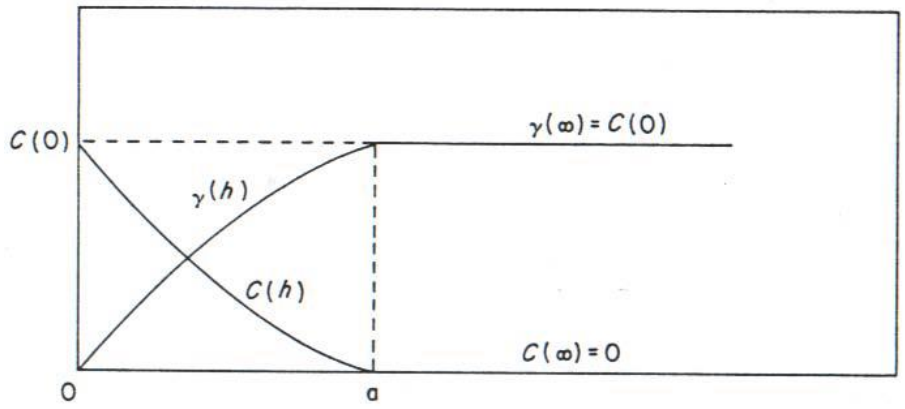


**Figure 2.1: Relationship between the spatial covariance *C(h)* and the semi–variance *γ(h)* (Journel and Huijbregts, 1878).**

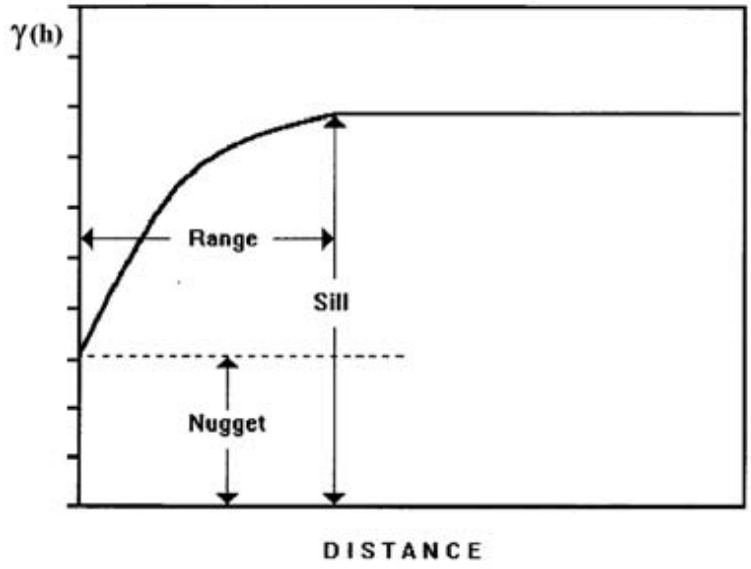


**Figure 2.2: Theoretical semi-variogram and its features (Castrignanò, 2010).**

In practice, the experimental variograms are approximated by theoretical variograms that guarantee to get a positive definite covariance matrix. A variogram model must fulfil the condition that no linear combination of variables can result in a negative variance of the derived variable. Such functions are called a *conditional negative semidefinite*. The most common variogram models ones are linear, spherical, exponential, Gaussian, power, periodic ones (Webster and Oliver, 2001). The choice of variogram model is crucial because it has a significant effect on the accuracy of kriging interpolation through the estimation of the interpolation weights $\lambda_i$. The shape of the experimental semi–variogram may take many forms, depending on the data and sampling interval used, thus the choice of variogram model is very important because each type yields quite different values for the nugget variance and

range, both of which are critical parameters for interpolation (Figure 2.3) (Castrignanò, 2010).

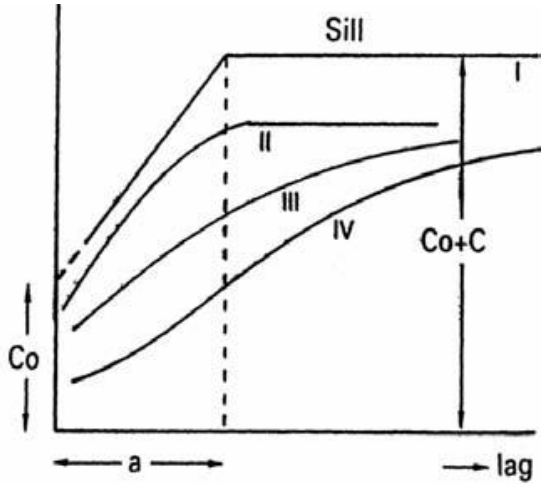


**Figure 2.3: Examples of semivariogram models (I linear; II spherical; III exponential; IV Gaussian) (Castrignanò, 2010).**

### 2.2.1 Kriging basics

Geostatistical theory provides a rigorous, spatially explicit set of methods to describe random variables and fields. The best-known geostatistical method, kriging, evolved from regression to consider spatial auto- and cross-correlations explicitly.
Geostatistics includes several methods that use kriging algorithms for estimating continuous attributes. Kriging is a generic name for a family of generalized least-squares regression algorithms, used in recognition of the pioneering work of Krige (1951).
The most basic form of kriging, among the Euclidian kriging methods, is the Ordinary kriging (OK). Here the predictions are based on the model:

$$Z(x) = m(x) + \varepsilon'(x) \tag{2.8}$$

in which the variable of interest is represented as a random field of values *z(x)*.
Almost all spatial interpolation methods (inverse distance squared, splines, radial basis functions, triangulation, etc.) estimate the value at a given location as weighted averages of sampled data at surrounding locations. They all share the same general estimation formula where the unknown value $z(x_0)$ of the variable to predict at position $x_0$ (i.e. the target position) can be estimated as a weighted average of the observations available $z(x_i), i = 1,2, \dots, N$ at the points $x_i$ in the neighborhood.

$$z(x_0) = \sum_{i=1}^{n} \lambda_i z(x_i) \tag{2.9}$$

$\lambda_i$ are the interpolation weights of the measurement at position $x_i$ and $n$ is the number of neighboring measurements used for interpolation. The difference among the spatial interpolation methods is in the assessment of the interpolation weights $\lambda_i$. Almost all assign weights according to functions that give a decreasing weight with

increasing separation distance. Kriging assigns weights according to a (moderately) data-driven weighting function, rather than an arbitrary function, but it is still just an interpolation algorithm and will give very similar results to others in many cases (Isaaks and Srivastava, 1989).

In the OK, the weights are chosen in such a way that the average estimation error is zero (unbiased) and the estimation has the smallest possible mean square error (best or minimum variance).

Ordinary kriging is often associated with the acronym BLUE for "Best Linear Unbiased Estimator" because it is an interpolation method where the expected bias is zero and the expected kriging error is minimized. Indeed, it is linear, because its estimates are weighted linear combinations of the sample values, unbiased because the estimated values are neither overestimated nor underestimated systematically. If we look at the whole surface, local over- and underestimations neutralize each other, and the average estimation error is equal to zero. It is best because it aims at minimizing the variance of the error for each interpolated point. In other words, it assigns optimal weights to each sample point considering not only the distance between the samples and the unknown point, but also the distances between the samples themselves. This allows to give less weight to clustered samples containing redundant information and to have the smallest variance among all unbiased linear estimators.

All kriging estimators are variants of the basic linear regression estimator $Z^*(x_0)$, which is a slight modification of equation (2.9), defined as follows:

$$Z^*(x_0) - \mu(x_0) = \sum_{i=1}^{n} \lambda_i [Z(x_i) - \mu(x_i)] \tag{2.10}$$

with

$x_0$, $x_i$ : location vectors for estimation point and one of the neighboring data points, indexed by $i$

$n$: the number of sampled points in local neighborhood used for the estimation of $Z^*(x_0)$

$\mu(x_0), \mu(x_i)$ : expected values (means) of $Z(x_0), Z(x_i)$

$\lambda_i$ : kriging weight assigned to datum $z(x_i)$ for estimation location $x_i$; same datum will receive different weight for different estimation location.

The three main kriging variants, Simple (SK), Ordinary (OK), and Universal (kriging with a trend UK), differ in their treatments of the trend component, $\mu(x_0)$. For simple kriging, we assume that the trend component is a constant and known stationary mean, $\mu(x_0) = m$. For ordinary kriging, rather than assuming that the mean is constant over the entire domain, we assume that it is constant in the local neighborhood of each estimation point, that is $\mu(x_i) = \mu(x_0)$ for each nearby data value $Z(x_i)$ that we are using to estimate $Z(x_0)$ and we force for the bias condition that $[1 - \sum_{i=1}^{n} \lambda_i] = 0$ that is $\sum_{i=1}^{n} \lambda_i = 1$. OK estimates the local constant mean, then performs SK on the corresponding residuals, and only requires the stationary mean

of the local search window (Goovaerts, 1997). Universal kriging is much like ordinary kriging, except that instead of fitting just a local mean in the neighborhood of the estimation point, we fit a linear or higher-order trend in the *(x,y)* coordinates of the data points. A local linear trend model would be given by $\mu(x_0) = m(x,y) = a_0 + a_1 x + a_2 y$. UK estimates the trend components within each search neighborhood window and then performs SK on the corresponding residuals.

The goal in the OK is to determine weights $\lambda_i$ that minimize the variance of the estimator

$$\sigma_E^2(x_0) = Var\{Z^*(x_0) - Z(x_0)\} \tag{2.11}$$

Under the unbiasedness constraint

$$E\{Z^*(x_0) - Z(x_0)\} = 0 \tag{2.12}$$

Using a Lagrangian multiplier $\mu$, minimization of the estimation variance under the constraint of unbiasedness yields a set of $n+1$ linear equations and the weights $\lambda_i$ can be found by solving the kriging system:

$$\begin{cases} \sum_{j=1}^{n} \lambda_j \gamma_{ij} + \mu = \gamma_{0i}\,, & i = 1, \dots, n \\ \sum_{j=1}^{n} \lambda_j = 1 \end{cases} \tag{2.13}$$

$\gamma_{ij}$ and $\gamma_{0i}$ refers to the semivariances between the observed locations $x_i$ and $x_j$ and between the observed location $x_i$ and the interpolated location $x_0$, respectively.
The estimation variance $\sigma_i^2$ that represents possible measurement error or uncertainty in the prediction in $x_0$ is then given by:

$$\sigma^2(x_0) = \mu + \sum_{i=1}^{n} \lambda_i \gamma_{0i} \tag{2.14}$$

In the case of spatial dependence, it is worth noting that semi-variance tends to increase with the distance between the observations, therefore errors decrease with the density of data and not just with their total number, as in the case of traditional models of classification (Castrignanò, 2010).
As so far said about the kriging method and its optimal and unbiased characteristics is all true, but on the condition that the model is correct. However, the choice of the model affects only partially the predictions, and this is one of the strengths of kriging. Error variances, instead, can be seriously affected by the model.
The main properties that characterize the kriging are:

- Starting from the data available, the interpolated value is the most accurate;
- During the estimation, an error term is calculated so that the interpolated value can be used with a good degree of confidence;

- The observed values do not affect the estimation variance. It depends only on the semivariogram model and on the location of the data in relation to the interpolated points;
- Kriging is an exact interpolator. In fact, when a kriged location coincides with a sample location, the estimated values are equal to those observed. When this happens, the weights within the neighborhood are all zero and the estimation variance is equal to the nugget variance of the semivariogram model;
- The kriged location affects only the nearest few samples. These are spatially correlated with the initial location and they are most weighted. So, the variogram needs to be accurate only on the first few legs, and this is an important advantage.

Different procedures are necessary in the case of randomly sparse sampling. Distant points must be included owing to the scarcity of samples and estimation variance could be large, requiring additional sampling. These considerations allow to research the optimal number and the optimal localization of samples.
Moreover, if there are enough samples at short lags, computer times and costs are reduced, the optimal number of neighbor samples depends on the configuration of the points to the kriged location and on the degree of variation and anisotropy (Castrignanò, 2010).
Its simplicity of computations makes the Ordinary kriging a widely used method, but some drawbacks must be highlighted. The first is that some local discontinuities could be produced where interpolated points coincide with observations. This means that the particular places where the samples were collected significantly affect these discontinuities. Finally, results obtained by the kriging depend on the sampling methodology.
The last aspect to point out is that estimates carried out with the Ordinary kriging are different from the Top-kriging ones. The main difference is that the estimates are similar along Euclidian distance in space and not along the stream network, as it happens in the case of Top-kriging.

### 2.2.2 Top-kriging method

Top-kriging or topological kriging, is a kriging interpolation procedure proposed by Skøien et al. (2006) that takes into account the geometric organization and structure of hydrographic network, the catchment area and the nested nature of catchments. Top-kriging method is a Best Linear Unbiased Estimator (BLUE) particularly useful when streamflow-related variables have to be found in ungauged catchments. It can be used for the spatial interpolation of streamflow-related variables like mean annual discharge, flood characteristics, low flows and so on.
Being a linear estimator, Top-kriging assumes linear aggregation: this means that the method only applies to variables that are mass conserving over the catchments. The

authors suggest that the method can also be profitably used, as an approximation, for variables that do not aggregate linearly but show a degree of averaging. The assumption is that the observed variable of interest can be seen as a linear aggregate of a conservative point process in space and/or time. The aggregated observed values can then in most cases be seen as the linear average of the process within the support we are interested in, such as runoff per unit area for runoff (specific runoff). The assumption about a point process can in many cases be hypothetical (such as the point runoff) and can in general be somewhat relaxed in the sense that the process needs to aggregate linearly within the range of supports of the observations and prediction locations (Skøien et al., 2014). The example application of Top-kriging to the specific 100-year flood shown in their study, suggests that even if the streamflow-related variable is not mass conserving, the Top-kriging estimates are much better than the Ordinary Kriging ones. In fact, although Top-kriging is based on linear aggregation it does not necessarily reproduce the mass-balance of the variable of interest (Sauquet et al., 2000).

The method is also based on the general stationarity assumption for geostatistical methods, i.e., that the expected variance between measurements of the point process is a function of separation distance. The implementation of the method does not take non-stationarity of the mean into account, usually done through universal kriging approach, although it is possible to add an external drift, but this is commonly solved by local kriging approach using for interpolation only the closest stations with the highest modelled correlation. The method will still produce satisfying result even when this assumption is violated to some degree, like ordinary kriging. The examples shown in (Skøien et al., 2008) indicate that predictions can be relatively good despite violations of the stationarity assumptions, whereas estimates of prediction uncertainty may be less reliable.

In Top-kriging the basin runoff is represented as a spatially continuous process that exists at any point in the area and stream flow is the integral of the local runoff over the catchment. At the base of the method there is the concept that stream-flow is controlled by two groups of variables. In the first group are included rainfall, evapotranspiration and soil characteristics, i.e. variables that are continuous in space and directly related to the local runoff generation. These kinds of variables could be characterized by the Euclidian distances. The second group of variables is related to runoff aggregation and routing along the stream network. Mean annual discharges, flood characteristics, low flows and stream temperature, for example, are included in this group: they are defined for points on the stream network so they cannot be represented by Euclidian distances. The Top-kriging method combines these two groups of variables in a geostatistical framework.

In Top-kriging, the measurements are not point values but are defined over a catchment area A. If a non-zero support A is accounted for, the gamma values, founded from a theoretical semivariogram model, need to be obtained by regularization considering the catchments area. Considering the existence of a point

variogram $\gamma_p$, the gamma value or the expected semivariance between two measurements with catchment areas $A_1$ and $A_2$ is:

$$\gamma_{12} = 0.5 \cdot Var\big(z(A_1) - z(A_2)\big) =$$

$$= \frac{1}{A_1 A_2}\int_{A_1}\int_{A_2}\gamma_p(|x_1 - x_2|)\,dx_1 dx_2 - 0.5 \times [\frac{1}{A_1^2}\int_{A_1}\int_{A_1}\gamma_p(|x_1 - x_2|)\,dx_1 dx_2$$

$$+\frac{1}{A_2^2}\int_{A_2}\int_{A_2}\gamma_p(|x_1 - x_2|)\,dx_1 dx_2] \qquad (2.15)$$

$x_1$ and $x_2$ are position vectors within each catchment used for the integration. The first part of this expression integrates all the variance between the two catchments, while the second part subtracts the averaged variance within the catchments. The second part is the smoothing effect of the support, which indicates that the variance of the averaged variable decreases as the support area increases. Eq. (2.15) can be used to estimate the variogram of the averaged variable from the point variogram, this procedure is termed regularization. Once the gamma values are obtained, these are inserted into the kriging matrix (Eq. (2.13)) to calculate the weights $\lambda_i$ for the interpolation scheme. It is important to highlight that in Top-kriging the integration is performed over the catchment area that drains to the outlet of the target catchment. The complexity and sometimes the impossibility to carry out analytically the integration in Eq. (2.15), makes it necessary to replace the integrals in sums and to discretize the catchment area by a grid. Figure 2.4 shows a schematic of two nested catchments, their discretization by a square grid, and the distances between the discretized points within the catchments.

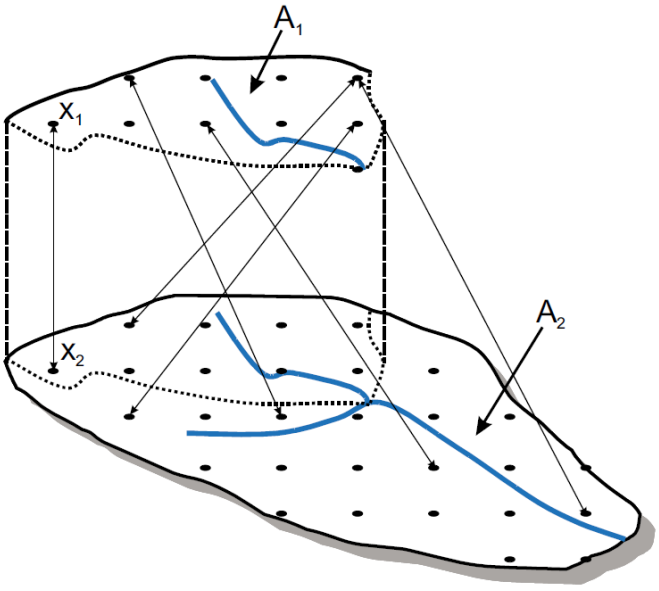


**Figure 2.4: Schematic stream network and catchment boundaries with point pairs shown (Skøien et al., 2006).**

Compared to other interpolation methods, one of the advantages of kriging is that it provides an evaluation of the kriging variance of the estimate at any location. The uncertainty of the estimates is represented by the variance $\sigma_R^2$ and is given by Eq. 2.14 where $\gamma_{0i}$ is the gamma value between the target catchment and the neighboring catchments.

It is important to highlight that in Ordinary kriging the same weights $\lambda_i$ are assigned to all the neighbouring catchments, while in Top-kriging the weights are different. In particular, the larger basins have the highest weight: in fact, these are regarded as the most certain or those which have at least partial measurement than the mean.

Also the uncertainty patterns estimated by Top-kriging differ substantially from those of Ordinary kriging. The latter only depend on the centroid distances of gauged and ungauged catchments, while the Top-kriging uncertainties take into account the nested nature of the basins. Overall, the Ordinary kriging uncertainties are a consequence of the use of the Euclidian distances because these do not reflect the intuitive distribution of the estimation errors. Indeed, the uncertainties are too uniform within the region, demonstrating that they do not consider the information provided by gauged and ungauged catchments. Instead the advantage of the Top-kriging procedure is that it is able to capture exactly this kind of information.

# Chapter 3

# Application of Top-kriging method

## 3.1 Motivation

Direct interpolation of runoff observations to ungauged sites is an alternative to hydrological model regionalization. Most of the methods used for PUB in the past, simulate runoff values by conceptual hydrologic models. These models need estimates of climate inputs and calibration against observed runoff which is not directly possible in ungauged basins. Take into account spatial proximity for geostatistical interpolation of streamflow related variables could be better than the application of other methods.

The main advantage of direct interpolation is that it avoids the use of uncertain input variables such as precipitation and potential evaporation. The limitation is that this method is data intensive, i.e., it can only be applied in medium to densely gauged regions. The estimation is particularly important in small headwater basins characterized by sparse hydrological and climate observations, but often large spatial variability. The main objective of this part of dissertation is to evaluate Top-kriging interpolation accuracy for predicting specific *n*-year flood quantiles in Tuscany Region. The idea is to assess the capability of Top-kriging model to predict flood quantiles in ungauged sites and to model through Top-kriging the spatial correlation structure, or the spatial variability, of the design flood over the study region. In conclusion, the accuracy and reliability of predictions in ungauged catchments by Top-kriging procedure is investigated, underlying the strengths and weaknesses of the method in the final comparison to the predictions resulting from traditional at-site flood frequency analysis approach and hydrologic simulations.

## 3.2 Study area and dataset

The analysis is carried out on the annual maximum streamflow time series with more than 10 years of observations recorded from 1924 to 2011 (Figure 3.3) by 26 runoff gauges located in the Arno river basin (Figure 3.1). The Arno River is almost entirely situated within Tuscany, Central Italy, its basin occupies about one third of Tuscany's surface. The river is about 241 km long while the mean elevation is of 353 m a.s.l.. Station density exceeds approximately 3 stations per 1000 km$^2$, it is estimated by dividing number of stations by the catchment area (about 8830 km$^2$).
The polygon shapefiles of 26 watersheds in the Arno river basin are identified and approximately 100 watersheds to be used for predictions have been defined (Figure 3.2).

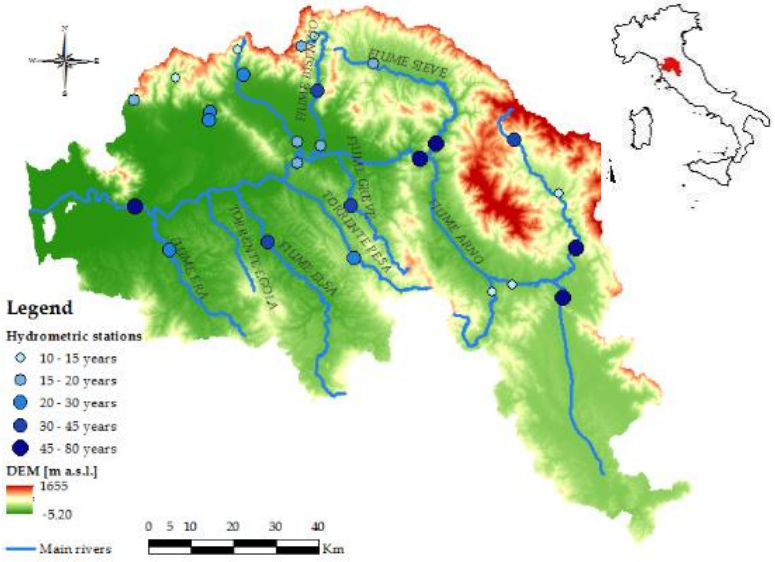


**Figure 3.1: DEM of the study area with 26 hydrometric stations. The sizes of the dots are relative to the time series length.**

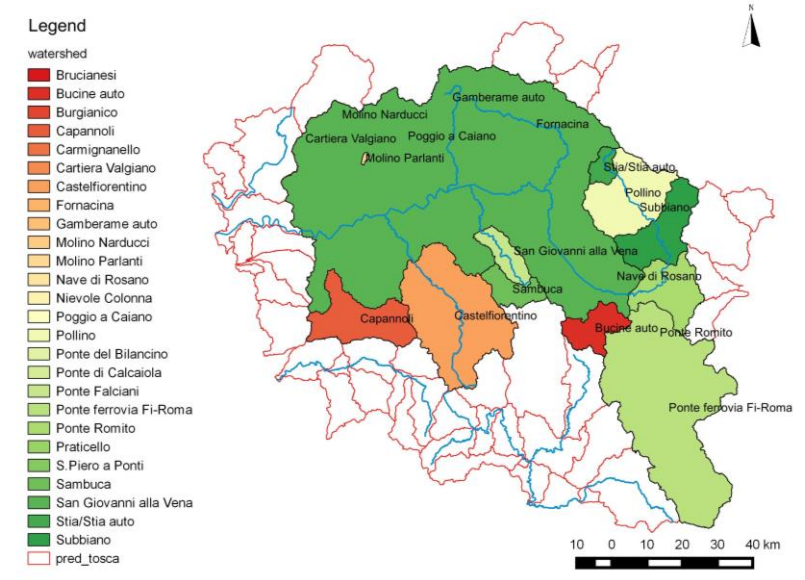


**Figure 3.2: Arno river watersheds and watersheds for prediction for Top-kriging analysis.**

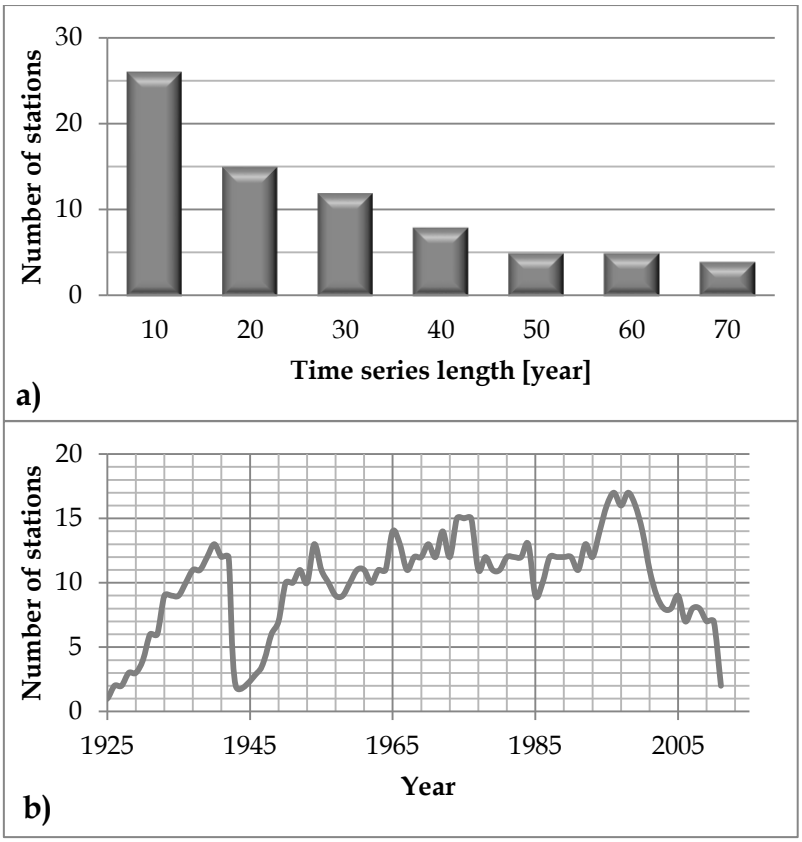


**Figure 3.3: Annual maximum stream flows in the study area. a) Distribution of the stations based on the length of the available series. b) Evolution of the monitoring network in the years between 1924 and 2011.**

A specific runoff is needed as input in Top-kriging. Flood quantiles corresponding to several return periods, particularly 10, 50, 100, 200, 500-year $T_r$ standardized by the basin area to an exponent of 0.65 (the factor $A^{0.65}$), in order to account for the scale effect (Archfield et al., 2013), are considered as specific runoffs. It is worth remanding that flood quantile of a given $T_r$ is the design flood used for planning and floodplain management investigations defined by its probability of occurrence. Table 3.1 presents some basic statistics on flood quantiles, we can also note extra information in Appendix A1.

An at-site flood frequency analysis is carried out at each station of the dataset. Empirical estimates of flood quantiles were determined by fitting appropriate probability distributions to the discharge data by means of the R function `MSClaio2008`, part of the package `nsRFA`. Frequently, the choice of the probabilistic model to be used for the frequency analysis of hydrological extremes is based on subjective criteria, or it is the result of the application of several statistical hypotheses tests. Here, an application of the Model Selection Criteria (`MSClaio2008` R function) is provided by use of specific tools for model selection, like the well-known Akaike Information Criterion (AIC) and Bayesian Information Criterion (BIC). An additional model selection criterion, based on the Anderson-Darling goodness-of-fit test statistic is applied. The information on the Model Selection Criteria are reported in Laio et al. (2009), see the paper for more details and references. In the figures below (Figure 3.4 and 3.5) are presented the time series of two stream gauges. In Figure 3.4 it is

possible to note the example of the application of `MSClaio2008` R function where the several candidate distributions as well as the distribution selected by one criterion are plotted in a log-normal probability plot.

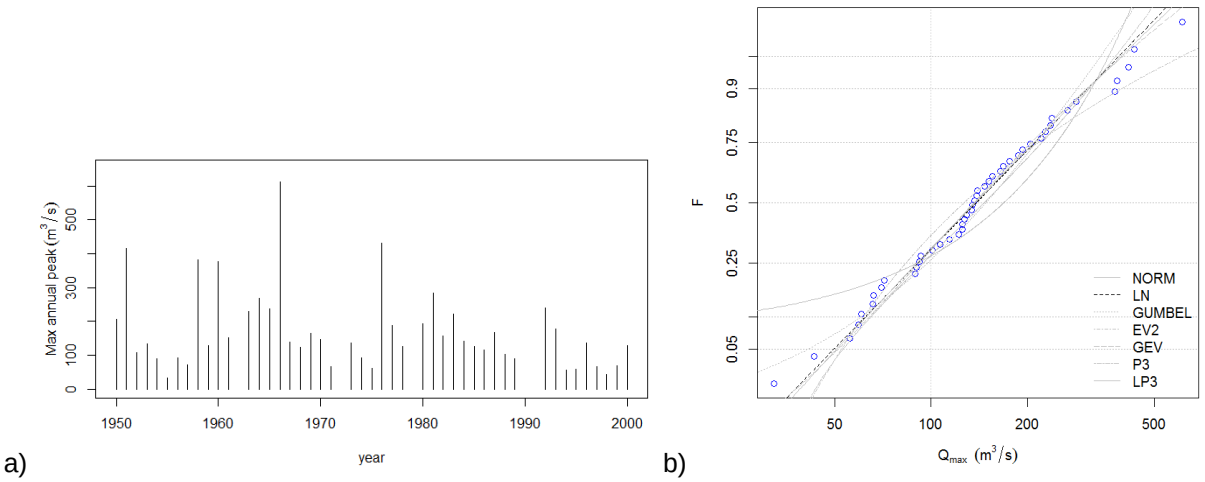


**Figure 3.4: a) Time series of annual maximum peak flows registered from Castelfiorentino stream gauge b) The observed data by Weibull plotting position (blue dots), the several candidate distributions (grey lines), the distribution selected by one criterion (black line - LOGNORMAL) in a log-normal probability plot.**

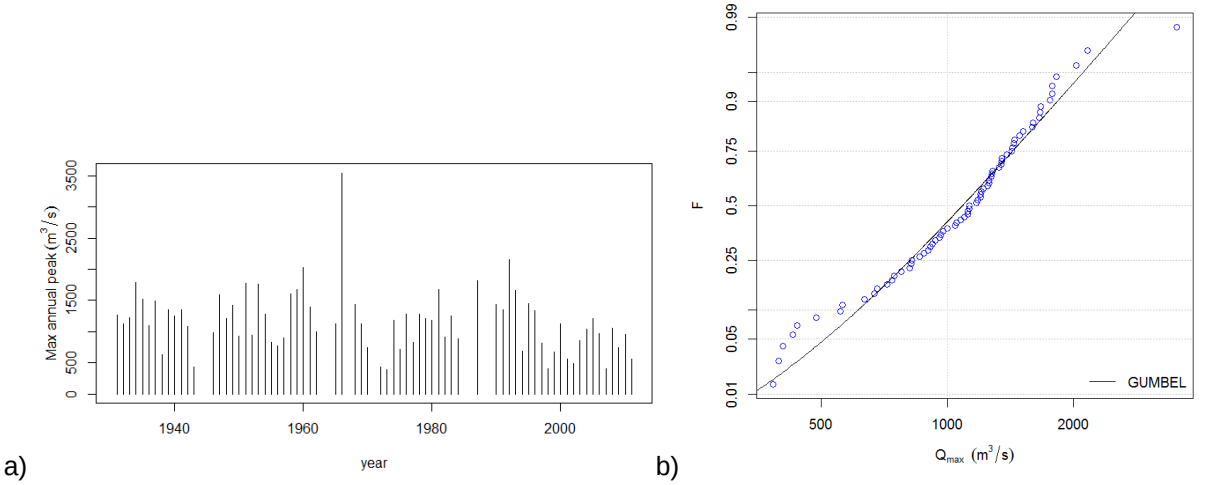


**Figure 3.5: a) Time series of annual maximum peak flows registered from Nave di Rosano stream gauge b) The observed data by Weibull plotting position (blue dots), the distribution selected by one criterion (black line - GUMBEL) in a log-normal probability plot.**

**Table 3.1: Statistics on flood quantiles corresponding to 10, 50, 100, 200, 500 years return periods.**

| Flood quantile | Minimum [$m^3/s$] | Median [$m^3/s$] | Maximum [$m^3/s$] |
|---|---|---|---|
| **10 yr** | 2.1 | 245.2 | 1941.4 |
| **50 yr** | 3.1 | 373.5 | 2611.3 |
| **100 yr** | 3.5 | 395.8 | 2879.7 |
| **200 yr** | 3.9 | 434.1 | 3140.2 |
| **500 yr** | 4.5 | 537.0 | 3475.3 |

## 3.3 Implementation on the Arno river basin

The application of the Top-kriging is based on the `rtop` R-package almost entirely implemented in the statistical environment R (R Core Team, 2013). Inputs of TK method is the specific runoff ($m^3/s/km^2$).

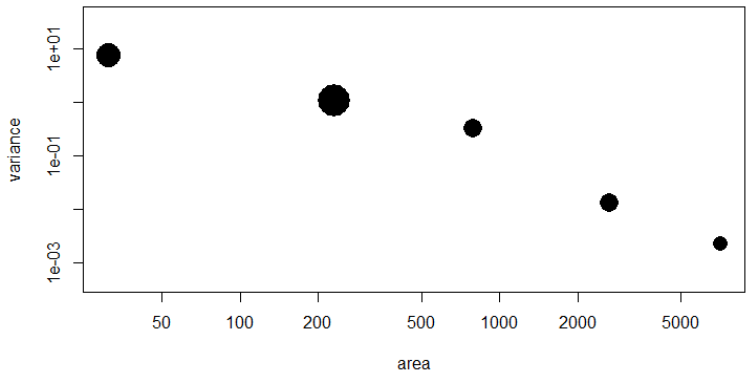


**Figure 3.6: the relationship between area and variance. The sizes of the dots are relative to the number of observations in each area class.**

One of the assumptions in Top-kriging is that the variance decays with increasing area.

The sample variogram is estimated as a binned variogram. A number of variograms have been tested and the exponential variogram model is chosen for its well fit to runoff time series.

Parameters of `rtop` have been set (for a complete explanation of the parameter see Skøien et al. (2014), particularly:

**Table 3.2: Parameters of rtop chosen for variogram fitting in Top-kriging method.**

| Parameters of rtop | Description | Value |
|---|---|---|
| model | Variogram model type | Exp |
| gDist | Ghosh-distance | TRUE |
| rresol | Minimum number of discretization points in each element | 50 |
| hresol | Number of discretization points in one direction for elements in binned variograms | 5 |
| nmax | Number of nearest observations to be used for kriging prediction | 5 |
| amul | Number of areal bins within one order of magnitude | 2 |
| dmul | Number of distance bins within one order of magnitude | 2 |

A sensitivity analysis of the parameter for variogram model assessment is carried out. Nevertheless, we did not fully explore all possible parameter settings of the `rtop` package, so that is possible that better results could be obtained with further investigations. The theoretical exponential variogram model is fitted to the estimated binned variogram through an automatic procedure. It is possible to visualize the goodness of fit of the variogram as well as doing an exploratory analysis for screening the data before variogram fitting and interpolation.

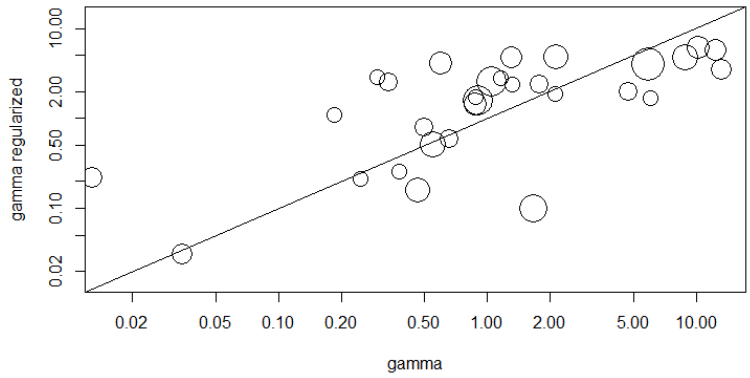


**Figure 3.7: The difference between the sample semivariances and the regularized semivariances.**

## 3.4 Analysis and control of the results

In order to compare the flood quantiles predicted by Top-kriging a leave-one-out cross-validation approach is applied in the `rtop` R-package. In this validation approach, each of the 26 study stream gauge is subsequently removed from the data set, and the top-kriging method is then applied to estimate the flood quantiles at the removed stream gauge from the remaining 25 stream gauges.

Figure 3.8 shows the scatter plots of observed and predicted flood quantiles corresponding to 10, 50, 100, 200, 500-year $T_r$ and the confidence intervals computed with linear regression approach. Figure 3.9 shows in the left panel the residuals, i.e. the errors between the observed and predicted flood quantile plotted versus the 26 study stream gauges recognizable by the code of the station, in the right panel the histograms of z-score computed as ratio between residuals and kriging standard deviation. This z-score should ideally have a $N(0,1)$ distribution, the method does not give a z-score with a perfect normal distribution but the skewness is very small. It is possible to note that some pairs of catchments exhibit quite large semivariances also for small distances, this can particularly be the case for combinations of small and large catchments. Some trials on the possibility to exclude these catchments from the study have been carried out, however we decided to continue using them for reporting the weaknesses of the method. In particular, the residuals are higher for Ponte del Bilancino (4610) and Ponte di Calcaiola (4820) catchments for lower $T_r$, maybe it gives too large weights to these small catchments. Moreover, the comparison with the empirical estimates obtained in the at-site flood frequency analysis for Capannoli (5130) and Pollino (4400) catchments shows that Top-kriging is not able to do predictions correctly. The reason depends on the complexity to obtain good estimation by means of a frequency analysis in catchments characterized by very short time series (The time series length for Pollino stream gauge, that is no longer in service since 1942, is 10 years) or by outliers in the series (Capannoli is a sub-basin of 334 km$^2$ wherein very high observations in the first years of service have been registered).

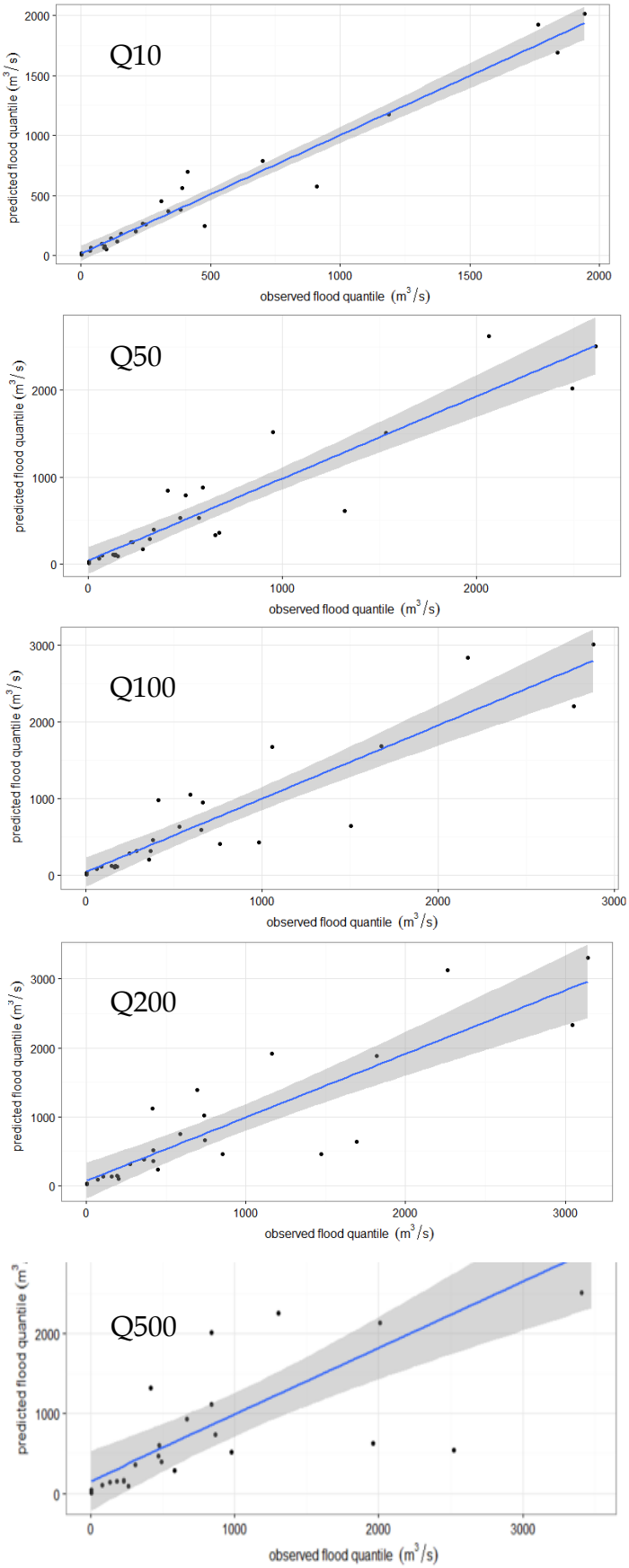


**Figure 3.8: Scatter plots of observed and predicted flood quantile.**

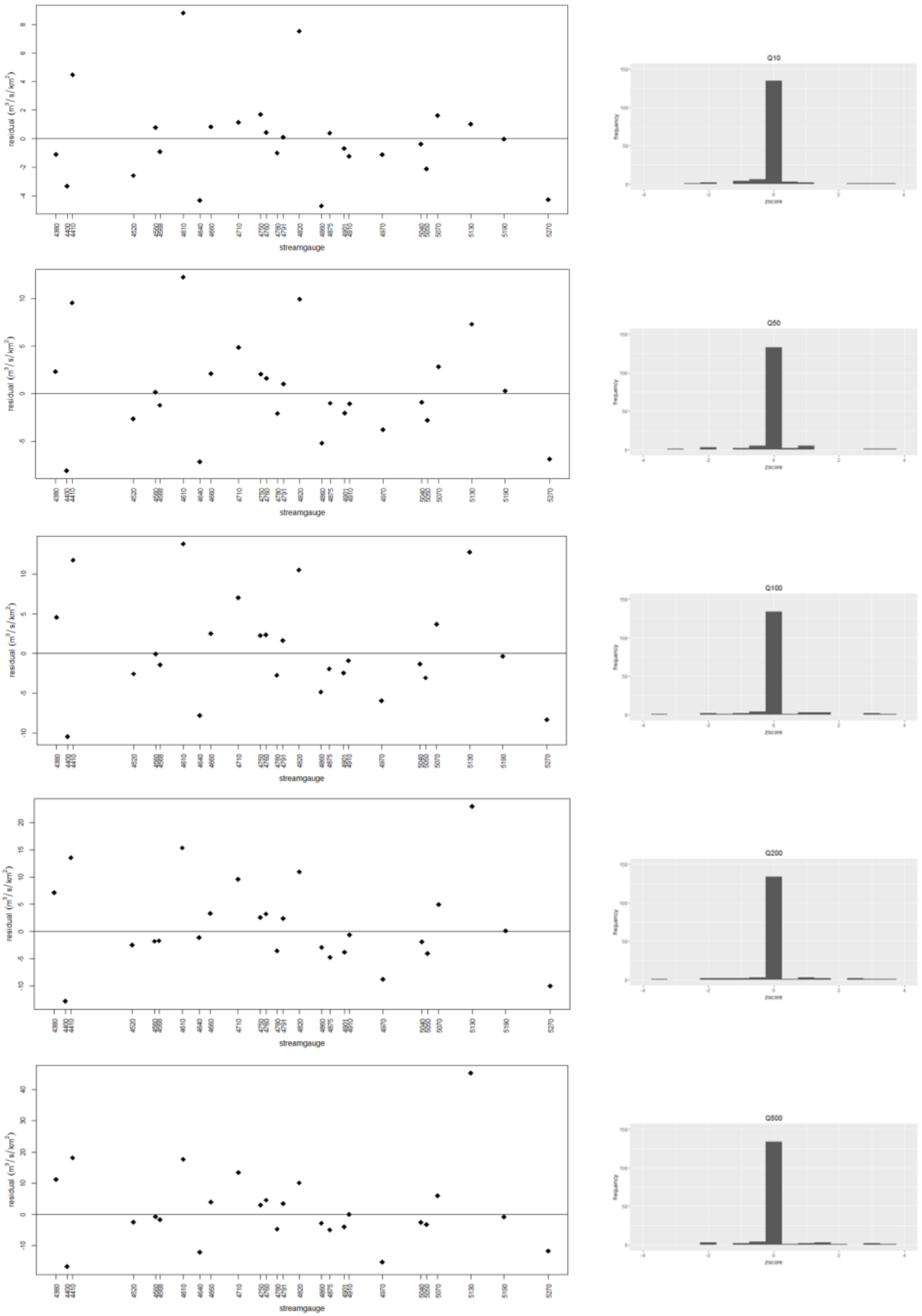


**Figure 3.9: (left panel) the residuals, i.e. the errors between the observed and predicted flood quantile by study stream gauge; (right panel) histograms of z-score (residuals/kriging standard error).**

**Table 3.3: The goodness of fit of the TK: performance indices computed from a leave-one-out cross-validation approach.**

| Performance indices (cross validation mode) | | | | | |
|---|---|---|---|---|---|
| | Q10 [m³/s] | Q50 [m³/s] | Q100 [m³/s] | Q200 [m³/s] | Q500 [m³/s] |
| **μ (obs)** | 469.3 | 650.4 | 734.7 | 826.6 | 966.1 |
| **ME** | 9.5 | 4.1 | 8.5 | 3.3 | -8.4 |
| **MAE** | 75.7 | 178.9 | 225.1 | 297.3 | 417.6 |
| **RMSE** | 118.6 | 274.2 | 340.8 | 453.9 | 663.7 |
| **$R^2$** | 0.96 | 0.87 | 0.84 | 0.76 | 0.63 |
| **NSE** | **0.96** | **0.86** | **0.82** | **0.73** | **0.56** |
| **PBIAS (%)** | 2.0 | 0.60 | 1.20 | 0.40 | -0.90 |
| **d** | 0.99 | 0.96 | 0.96 | 0.93 | 0.89 |
| **$d_1$** | 0.91 | 0.84 | 0.82 | 0.79 | 0.74 |
| **r** | 0.98 | 0.93 | 0.91 | 0.87 | 0.79 |

The results are compared through different error measurement methods (Table 3.3). The Mean Error (ME), Mean Absolute Error (MAE) as well as the Root Mean Squared Error (RMSE) are in the same units of observations. RMSE gives the standard deviation of the model prediction error, a smaller value indicates better model performance. Percent bias (PBIAS) measures the average tendency of the simulated values to be larger or smaller than their observed ones, the optimal value of PBIAS is 0.0, with low-magnitude values indicating accurate model simulation. Positive values indicate overestimation bias, whereas negative values indicate model underestimation bias. The Nash-Sutcliffe Efficiency (NSE) values gives an idea of the predictive power of the models. It should be note that the efficiency coefficient is sensitive to extreme values and might yield fairly good results when the dataset contains large outliers. In fact, the NSE strongly decrease with the increase of return periods.

The performance indices used for evaluating hydrological models are generally of the quadratic type (RMSE, Pearson correlation coefficient r, NSE, etc.), this is appropriate when, like in many streamflow forecasting applications, the focus is on the ability to reproduce potentially dangerous flood events (Lombardi et al., 2012). However, the use of squares implies a greater influence on the index of the larger flow values. Legates and McCabe Jr. (1999) suggested for a complete assessment of model performance to take into account relative error measure (like the modified index of agreement $d_1$) as well as absolute error measure (e.g. MAE), that provides an evaluation of the error in the units of the variable. MAE and RMSE are here reported in order to avoid to present only indices more sensitivity to the larger values. The Index of Agreement (d) developed by Willmott (1981) is a standardized measure of the degree of model prediction error and varies between 0 and 1, a value of 1

indicates a perfect match, and 0 indicates no agreement at all. The index of agreement can detect additive and proportional differences in the observed and simulated means and variances; however, it is overly sensitive to extreme values due to the squared differences (Legates and McCabe Jr., 1999). Krause et al. (2005) recommend the use of a modification of the index of agreement for increasing the sensitivity for lower values, j = 1 may be used, so that the errors are given their appropriate weighting, resulting in a more overall sensitivity measure for the quality of the model results.

## 3.5 Modelling uncertainty

Top-kriging method estimates kriging standard errors in order to give an estimation of the prediction uncertainty in addition to the prediction itself. The results can be visualized in Figure 3.10 and Figure 3.11. First, we can notice that the CV is slightly higher for the small catchments, the larger catchments have smaller CV. We can also note that the CV is consistently higher in the Capannoli watershed, a watershed characterized by very high observations, and the smallest Molino Parlanti and Cartiera Valgiano watersheds.

On the other hand, in the northern part of the figures, where prediction values are higher, CV is very low, maybe it comes from the nested structure of the catchments in this region, they are all watersheds along the Arno river main stream.

In conclusion, Top-kriging seems to perform better in nested catchments and larger scale catchments but no for headwater or where there is a high spatial variability. In fact, Top-kriging explicitly takes the nested structure of the catchments into account and it will therefore give better predictions for highly nested catchments. A limitation of this model errors assessment procedure is that "observations" are indeed the result of the at-site flood frequency analysis carried out even in watershed characterized by short time series (Pollino stream gauge). Therefore, the observations are affected by uncertainty too. On the other hand, Top-kriging is not likely to perform well for the not nested Capannoli, Cartiera Valgiano and Fornacina sub-basins especially for high return period. In fact, a simulation for 500-years return period flood quantile Q500 without these catchments increase consistently the Nash-Sutcliffe Efficiency up to 0.87 value allowing to obtain a median NSE of 0.85.

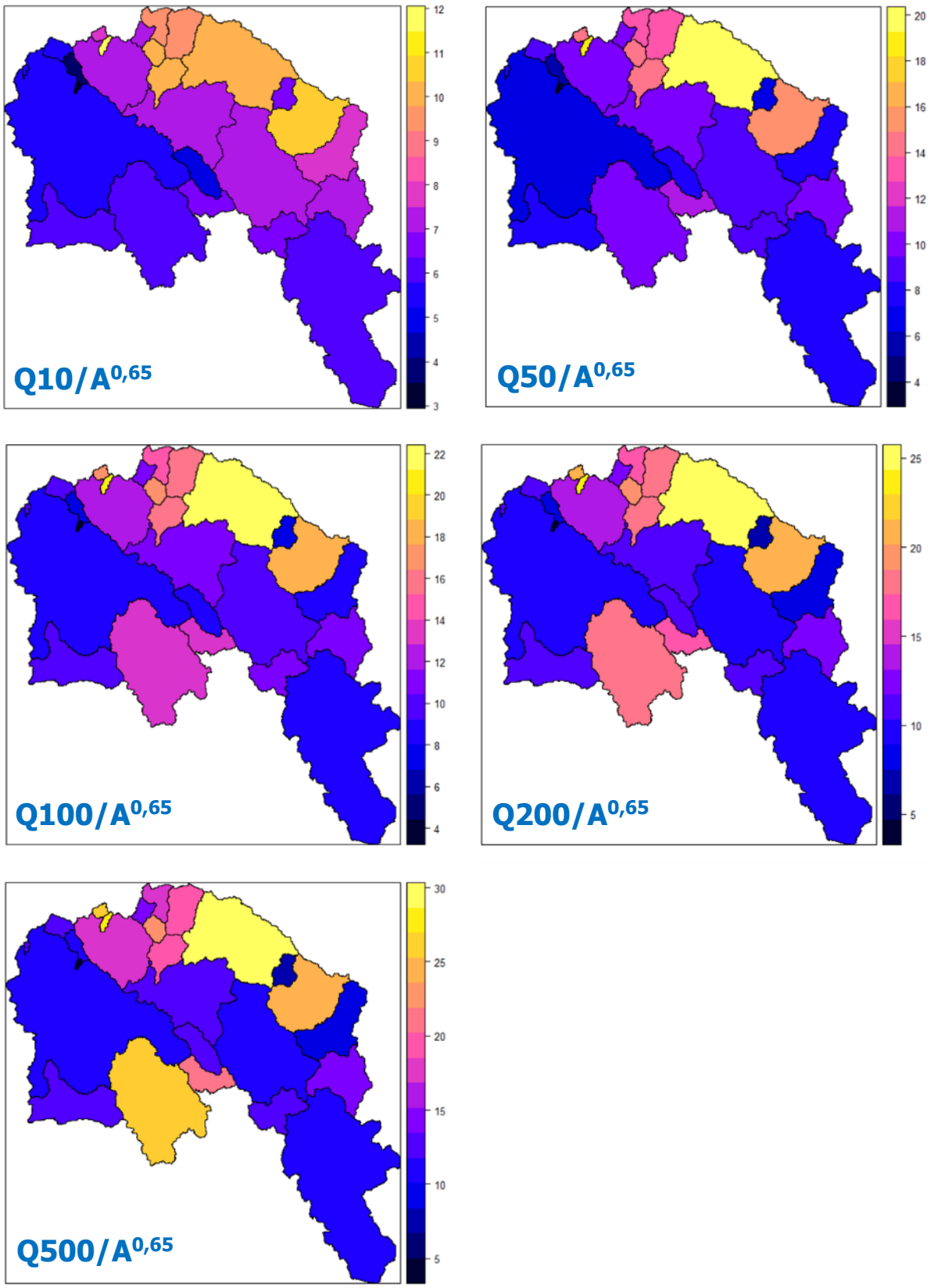


**Figure 3.10: Predictions of specific runoff $QT_T/A^{0.65}$ ($m^3/s/km^2$) plotted on the watersheds.**

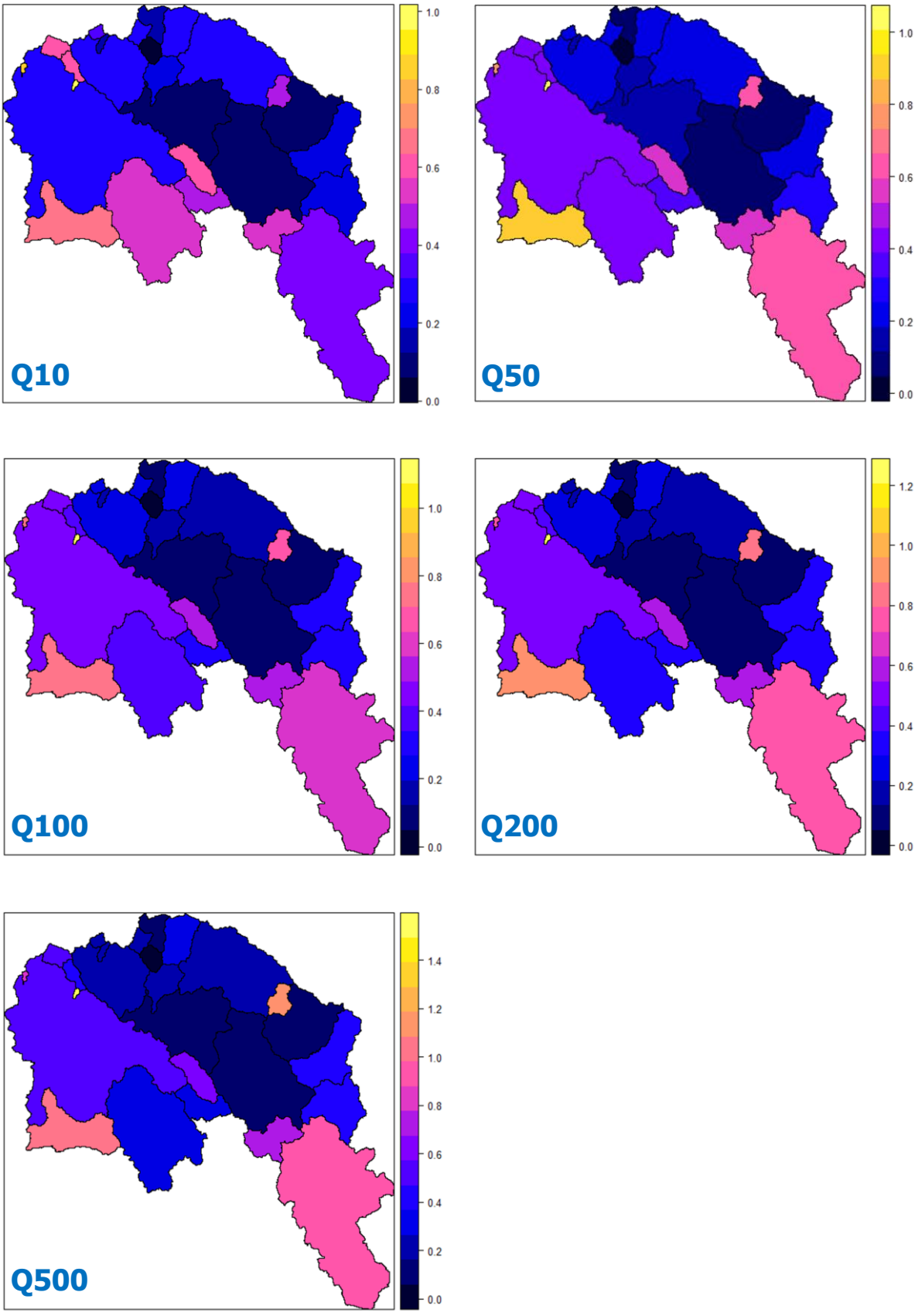


**Figure 3.11: Estimated uncertainty presented as a coefficient of variation (kriging standard deviation divided by the prediction itself) for the predictions of Q10, Q50, Q100, Q200, Q500 flood quantiles.**

# Chapter 4

# Uncertainty Quantification in the context of hydrology

## 4.1 Definitions in the context of hydrology

**Probability**

The probability of an event occurring in a particular trial is the frequency with which it occurs in a long sequence of similar trials. In a Bayesian view, the probability of an event is dependent upon the state of information available and this information can include expert opinion. Probability theory forms the basis of classical statistics, which has estimators based on a likelihood function that represents how likely an observed data sample is for a given model and parameter set.

**Randomness**

In statistics, and hydrology as well, a random process is such that its outcome cannot be predicted deterministically. Randomness does not imply lack of knowledge about the process dynamics or impossibility to set up a deterministic model for it. However, if a deterministic model can be set up for a process, randomness implies that such a model cannot perfectly predict the process outcome.

**Random Variable**

A random variable maps all possible outcomes from a random event into the real numbers. As such, it is affected by uncertainty and cannot be deterministically predicted. Random variables can assume discrete and continuous values.

**Stochastic Process**

A stochastic process can be defined as a collection of random variables. The output of a stochastic process is affected by some uncertainty that is described by the corresponding probability distributions. This means that there are many possible paths for the evolution of the process, with some of them being more likely and others less. A stochastic process can assume discrete or continuous values. Although the random variables of a stochastic process may be independent, in most commonly considered situations in hydrology, they exhibit statistical correlations. A stochastic process can include a deterministic representation but always includes a random component which makes its output uncertain.

**Stationarity**

A stochastic process is strictly stationary when the joint probability distribution of an arbitrary number of its random variables does not change when shifted in time or space. As a result, parameters such as the statistics of the process also do not change over time or position. Stationarity is a property of the mathematical representation of the system, or an ensemble of outcomes from a repeatable experiment, and therefore

does not constitute an actual property of the natural process itself. Recently, the scientific literature presented contributions stating that stationarity is dead because of hydrological change and climate change (Milly et al., 2008). Actually, stationarity is an assumption and therefore can hardly be dead.

**Ergodicity**

A stochastic process is said to be ergodic if its statistical properties can be deduced from a single, sufficiently long sample (realization) of the process.

**Uncertainty**

In the context of hydrology, uncertainty is generally meant to be a quantitative indication of reliability for a given hydrological quantity, either observed or inferred by using models. The indication of reliability can be provided by estimating the error affecting the quantity or the expected range of variability (due to uncertainty) for the quantity itself. Uncertainty can be broadly grouped into two major categories, namely, aleatory and epistemic uncertainty, and can be inferred by using probabilistic or nonprobabilistic methods.

**Deterministic versus Stochastic**

Stochastic methods incorporate the concept of randomness and provide both estimations (i.e., deterministic part) and associated errors (stochastic part, i.e., uncertainties represented as estimated variances). All other methods are deterministic because they do not incorporate such errors and only produce the estimations. In other words, deterministic methods have no assessment of errors with the predicted values, while stochastic methods provide an assessment of the errors associated with the predicted values. In UQ, the most dominant approach is to treat data uncertainty as random variables and recast the original deterministic systems as stochastic modeling systems.

**Uncertainty Assessment – Uncertainty Quantification – Uncertainty Estimation**

It is a quantitative evaluation of uncertainty affecting a hydrological variable, parameter, or model. Uncertainty estimation and uncertainty quantification will be considered synonymous with uncertainty assessment (UA), which is different from uncertainty analysis and uncertainty modeling. The former is a preliminary step of uncertainty assessment aimed at identifying the reasons for the presence of uncertainty and the nature of uncertainty itself, while the latter term refers to the tools that are used for UA.

**Confidence bands – Confidence Intervals**

A range around an estimated quantity that encompasses the true value with a probability $1-\alpha$, where $\alpha$ is the significance level and $1-\alpha$ is the confidence level. It is worth pointing out that the terminology is sometimes ambiguous. Some authors use the term confidence band or confidence interval when referring to the distribution of estimates that cannot be observed (e.g., a model parameter), while the term prediction interval is used when referring to the distribution of future values. Moreover, some authors indicate with the term tolerance interval a range in the observations that encompasses a $1-\alpha$ proportion of the population of the related

random variable. Confidence bands are usually computed with linear regression approach and the meta-Gaussian approach (Montanari and Brath, 2004). Moreover, Locally Weighted Least Squares Regression 'loess' and Generalized Additive Model 'gam' smoothing methods can be also applied.

## 4.2 Classification of Uncertainty

There have been many attempts presented in the literature to classify uncertainty in hydrology. It is generally agreed that uncertainties can be grouped into two major categories: (1) natural variability (also called structural uncertainty, aleatory, external, objective, inherent, random, irreducible, or stochastic uncertainty) and (2) knowledge uncertainty (also called epistemic, functional, internal, reducible, or subjective uncertainty (Hall and Solomatine, 2008; Koutsoyiannis et al., 2009; Table 1 in NRC, 2000). A systematic UQ effort aims to estimate the effects of structural uncertainty (uncertainty about the validity of a particular mathematical model) and parametric uncertainty (uncertainty about parameters and driving forces in a particular model) on predictive uncertainty. These two sources of uncertainty are sometimes referred to as epistemic uncertainty, since they arise from incomplete knowledge and can be reduced by collecting more data. Other classifications were proposed. According to the causes for the presence of uncertainty in hydrology, the following main sources of error might be identified:

- inherent randomness: reflects the intrinsic behavior of hydrological processes, the geometry of the control volumes, the meteorology, the variability of the surface and subsurface flow paths, etc.;
- model structural uncertainty: reflects the inability of the hydrological model to represent precisely the true behavior of hydrological systems;
- model parameter uncertainty: reflects the lack of a sufficiently extended database of good quality, or the inefficiency of the optimization algorithm and/or the related objective function used to calibrate the model parameters to observed data;
- data uncertainty: emerges from limitation of the monitoring techniques (instrumentation error, rating curve approximations, etc.) or variability of the spatial and temporal distribution of the observed hydrological variables (spatial variability of rainfall, time variability of streamflow, etc.);
- operation uncertainties: represents an emerging awareness among hydrological modelers and end-users when using models to make engineering or management decisions in real time applications.

In some hydrological applications, uncertainty is assessed in an aggregated solution, therefore quantifying global uncertainty without separate different sources of error. Assessment of the global uncertainty of the model output is by far the application

that is most frequently presented by the hydrological literature (Ajami et al., 2007; Beven and Binley, 1992; Hoeting et al., 1999; Krzysztofowicz, 2002; Montanari and Brath, 2004; Shrestha et al., 2009), as a means for quantifying model reliability and providing end-users with operational indications.

## 4.3 The topic of uncertainty quantification in hydrology

Some authors considered that uncertainty in hydrology is epistemic and therefore can be in principle eliminated through a more accurate representation of the related processes (Sivapalan et al., 2003). However, others authors suggested that uncertainty is unavoidable in hydrology, so it is impossible to develop a fully deterministic model that is able to remove uncertainty because it is originated from natural variability and related to inherent unpredictability in deterministic terms, which is typically referred to as randomness (Montanari et al., 2009; Montanari and Koutsoyiannis, 2012). It is generally agreed that uncertainty in hydrology cannot be eliminated, no matter if it is epistemic in nature or induced by inherent randomness. In particular, the paper of Montanari et al. (2009) is the introduction to *Water Resources Research* special section on Uncertainty Assessment (UA) in surface and subsurface hydrology, which represents a reference for anyone dealing with uncertainty in hydrology. An overview of probabilistic and nonprobabilistic approaches to uncertainty analysis, of issues and challenges is here reported. In scientific literature, procedures where deterministic hydrological modeling was efficiently coupled with UA were proposed, several methods are available, ranging from statistically based to subjective approaches. Kavetski et al. (2006) introduced the Bayesian Total Error Analysis (BATEA), a method for explicitly accounting for measurement uncertainty in both input (precipitation) and output data (river flows). Uncertainty in precipitation and river flow is often considered to be dominant, because of the spatial variability of rainfall and snowfall on the one hand, and the errors in the determination of the rating curve on the other. Relevant examples for the assessment of parameter uncertainty are the Shuffled Complex Evolution Metropolis University of Arizona algorithm (SCEM-UA), the MultiObjective Shuffled Complex Evolution University of Arizona (MOSCEM-UA), the Multialgorithm Genetically Adaptive Method for Multiobjective Optimization (AMALGAM) methods (Vrugt et al., 2003a, 2003b; Vrugt and Robinson, 2007). Within the method for the assessment of the global uncertainty of the model output, see, for instance, the Generalized Likelihood Uncertainty Estimation (GLUE) methodology of Beven and Binley (1992), the Bayesian Forecasting System (BFS) proposed by Krzysztofowicz (2002), the Bayesian Model Averaging (BMA) proposed by Hoeting et al. (1999). BMA tends to be computationally demanding and relies heavily on prior information about models. The Maximum Likelihood version of BMA (MLBMA, see Neuman, 2003; Ye et al., 2008) makes it computationally feasible. BMA is also used within the Integrated Bayesian Uncertainty Estimator (IBUNE) proposed by Ajami et al. (2007).

Finally, the Machine Learning Techniques (Shrestha et al., 2009; Shrestha and Solomatine, 2008). In order to combine parameter estimation with sensitivity analysis and model diagnostic, (Wagener et al., 2003) proposed the DYNamic Identifiability Analysis (DYNIA). Likelihood computation might be avoided by using data assimilation methods, for which a comprehensive review was presented by Liu and Gupta (2007), or the Bayesian uncertainty assessment method developed by Bulygina and Gupta (2009) or the approach presented by Götzinger and Bárdossy (2008). Finally, a methodological scheme for estimating the probability distribution of the output from a process-based (deterministic) hydrological model, thereby integrating hydrological modeling and UA, is proposed by Montanari and Koutsoyiannis (2012).
An attempt of classification of the most-used approaches to uncertainty assessment is presented in Table 4.1 (Montanari, 2011).

**Table 4.1: Most used uncertainty assessment methods in hydrology and their classification (Montanari, 2011).**

| *Assessment method* | *Classification* | *Type of uncertainty estimated* |
|---|---|---|
| AMALGAM | Nonprobabilistic, parameter estimation | Parameter |
| BATEA | Probabilistic, parameter estimation, uncertainty assessment, sensitivity analysis | Precipitation induced |
| BFS | Probabilistic, Bayesian | Global |
| BMA | Probabilistic, multimodel | Global |
| DYNIA | Nonprobabilistic, identifiability analysis | Parameter |
| GLUE | Nonprobabilistic (when an informal likelihood is used), parameter estimation, uncertainty assessment, sensitivity analysis | Global, parameter, data, structural |
| IBUNE | Probabilistic, parameter estimation, uncertainty assessment, sensitivity analysis | Global, precipitation induced, model structure induced |
| Machine learning | Nonprobabilistic | Usually global, in principle all |
| Meta-Gaussian | Probabilistic, data analysis | Global |
| MOSCEM-UA | Nonprobabilistic, parameter estimation, sensitivity analysis | Parameter |
| SCE-UA | Probabilistic, parameter estimation | Parameter |

The author points out that classification is ambiguous in some cases because he distinguishes between probabilistic and nonprobabilistic methods, as well as among the seven categories introduced by Matott et al. (2009), but it is an hard task to classify an approach as either probabilistic or not. The decision to use probabilistic or nonprobabilistic methods is currently the most controversial issue in hydrologic uncertainty analysis. However, there are methods based on probability theory, but in real-word applications simplifying assumptions are often introduced which finally lead to a nonprobabilistic estimation of the likelihood of a given scenario. Such assumptions are introduced to overcome operational problems, for instance, due to lack of enough data to support a statistical application. Regarding Parameter uncertainty quantification, methods based on importance sampling aim to identify a set of behavioral model parameter configurations according to a selected objective function. Then, parameter distributions are estimated using a weighted combination of the behavioral parameter sets. GLUE is perhaps the most-used method based on importance sampling (Montanari, 2011).
Analysis of the range of GLUE applications shows that the majority of the applications refer to rainfall-runoff modelling (as in the case of study of Beven and

Binley (1992)) but there are also significant number of applications in flood frequency estimation, urban hydrology, soil and hydraulic modelling and so on.
The main assumption underlying the methodology is that different set of model parameters or structures may be equally likely as simulators of the real system, so it rejects the concept of an optimum model and parameter set. The acceptance of the existence of multiple likely models has been called equifinality (Beven, 1993): it means that this should be considered and accepted as a generic problem in hydrological modelling rather than simply reflecting the problem of identifying the true model in the face of uncertainty.
The first step in the application of the GLUE method is the selection of different modeling options (different hydrological model and different parameters). These choices should be done trying to limit the dimension of the sample space of the parameters and of the models: in this way, the computational requirements of the procedure can be reduced. The second step involves the generation of a high number of simulation by sampling the model and parameter spaces, in accordance with a prior probability distribution. It is worth noting that if previous knowledge is not available, uniform sampling can be used. The probability of trying all the most relevant solutions increases if in turn increases the number of simulation. Finally, the different models are run for each set of parameters to compare the model outputs to observed data. Formal or informal likelihood measures are then used to evaluate the performance of each test: if some parameter sets are deemed non-behavioral can be rejected. If instead, the set of parameters leads to obtain an efficiency above the threshold set, these parameters are retained. Likelihood measures need to set weighted uncertainty bounds and these are calculated depending on the likelihood (Freer et al., 1996). If the likelihood measures or the procedure uses to compute the rescale weights are informal, the results computed with GLUE do not possess the classical meaning in term of probability and for this reason many authors classify GLUE as a non-probabilistic approach. On the contrary, if formal statistical procedures are used, GLUE behaves as a probabilistic methodology.
One of the advantages of the GLUE approach is that, in principle, it could be applied even if observed historical data are not available: this refers to those real-world applications in which the expert knowledge is at the basis of the estimation of the likelihood measure. The downside is that GLUE, from a computational point of view, is highly demanding, especially when the number of significant model parameters is high. Because of this limit, when dealing with complex models, the choice of the GLUE is not the most recommended.
The GLUE method is a global method that in most application treats characteristics of the complex errors associated with each behavioral parameter set implicitly. Moreover, it can be generalized in the sense of using a range of potential likelihood measures and a range of ways of combining likelihood measures. But the modelling process is characterized by multiple sources of uncertainty, so there is not a unique solution to their estimation, highlight the authors themselves 20 years on (Beven and

Binley, 2014). The first criticism of the method arises from the use of the term "likelihood". In the original paper by Beven and Binley (1992) the authors refers to the likelihood in a very general sense, and not in the restricted sense of maximum likelihood theory which is developed under specific assumptions. More recent applications to hydrological modelling have been based on the use of formal likelihood functions, but this requires a definition of a formal model of the characteristics of the model residuals. In practice, real applications may involve significant errors that result from a lack of knowledge rather than simple random variability, so failures in the results might be not caused by the model structure, but because input and evaluation data are inconsistent in some intervals of the record. The principal consequence of treating errors as aleatory, when really they are epistemic, is that the information of the calibration data is overestimated. The choice of a likelihood measure must be made in explicit way in any application, even if it remains difficult to define a measure that actually reflects the information content in applications subject to epistemic errors.

It is worth noting that the bounds of the prediction are always conditioned by the assumptions that underlie the estimate: in particular, the prior distribution of models run and the choice of likelihood measure. These assumptions should be more or less objective, but they must be explicit. Then, if they are inappropriate to statistical error assumptions, they can be reviewed and modified. This kind of review should be an important part of the modelling process, but it is often neglected.

Computer constraints are another limit for the application of the GLUE methodology because it is a model particularly slow to run, it is still not possible to sample sufficient realizations or deal with high number of parameter dimensions. Anyway, the computer power available will continue to increase and this will allow the application of GLUE method to a wider range of problems in the future.

Predict runoff in ungauged river basins is notoriously a difficult task because the tremendous spatio-temporal heterogeneity of climatic and landscape properties, involve significant unknowns and uncertainties. Flood risk assessments are associated by considerable uncertainty, which needs to be evaluated and clearly communicated to decision makers. As reported by Viglione et al. (2013), these uncertainties are due to many reasons. Hydrological processes have enormous spatiotemporal variability, which is difficult to capture (Grayson and Blöschl, 2000). Any stream gauge may be far from the ungauged basin of interest and there may be uncertainties in the collected data (Montanari, 2007). Moreover, predictive errors of methods arise from input data uncertainties, model parameter uncertainties and model structure uncertainties, where the latter involves all sources of uncertainty that previously are not considered explicitly (Montanari, 2011). The data and the parametric uncertainties can be defined by estimating the probability distributions of the input data and parameters, that means model them as random variables rather than deterministic. Model structure uncertainty is estimated by analyzing the model error in the simulation of data observed, assuming that this error is independent

from the data and parametric uncertainties. The integration of the three sources of uncertainty above mentioned is carried out within the modeling framework proposed by Montanari and Koutsoyiannis (2012). This probability based theoretical scheme was implemented for the Italian National Research Project ''Uncertainty estimation for precipitation and river discharge data. Effects on water resources planning and flood risk management'' in 2008, providing very satisfactory results, leading to a statistically significant estimate of the probability distribution of the simulated variables.

Major sources of uncertainty include the statistical analysis of extreme events from short time series with inherent measurement errors, the spatial extrapolation of data, the process models (that are not a perfect representation of reality) and parameterization and calibration, data used for calibration of models, scarce data for model validation, and the flood damage estimation often based on data from limited numbers of events (Aronica et al., 2013). There are still some important open issues that need further research, such as the identification of information required for reducing uncertainty as well as the identification of new parameter calibration and model validation strategies.

The new Scientific Decade 2013–2022 of IAHS, entitled "Panta Rhei—Everything Flows", is dedicated to research activities on change in hydrology and society and their interaction (Montanari et al., 2013). Hydrology should be effectively combined with "water security", including policy development and implementation. Water security, in its wider meaning, is a defining challenge for society in the 21st century, it includes water resources management as well as flood risk monitoring and mitigation.

The study of change in hydrological systems and society implies fundamental science questions (Montanari et al., 2013). Among these, the science question 4 is: "How can we use improved knowledge of coupled hydrological–social systems to improve model predictions, including estimation of predictive uncertainty and assessment of predictability?" Science question 4 concentrates on the improvement of hydrological predictions, by gaining a better understanding of the related processes with a particular focus on indeterminacy, namely, the occurrence of randomness that prevents the implementation of a fully deterministic description. Randomness may be an intrinsic property of hydrological processes, however, a random description may be an alternative to a deterministic one, even in the presence of epistemic uncertainty (which is related to a lack of knowledge or limited computational capacity or monitoring means).

Activities may include:

- development of theoretical schemes for the integrated modelling of hydrological knowledge and hydrological uncertainty (Beven, 2009a);
- setting up strategies for estimating and communicating uncertainty, and solutions for reducing decision-making and operational uncertainty;
- use of advanced monitoring techniques for reducing data errors;

• development of advanced prediction methods in the presence of indeterminacy.

Since epistemic uncertainties are important in hydrological modelling, we should try to account for such errors in model evaluations even though it will be difficult to quantify.

In principle, assessing the measurement uncertainties associated with both input and evaluation data independently of any simulation model structure should be possible. In practice, two difficulties arise, both associated with epistemic issues (Beven and Binley, 2014). The first is connected to the limitations of the available measurement techniques or number of measurements or an evaluation variable that is commensurable with a model predicted variable.

Examples are the uncertainties associated with rainfall: Interpolation of rain gauge observations requires a model, estimation of rainfall intensities from radar reflectivity requires a model. Both of these models might require different parameters for different events, which may themselves be subject to epistemic uncertainties, especially when limited data are available to estimate the interpolation characteristics (Mcmillan et al., 2012). Furthermore, the estimation of high values of discharge is obtained through the extrapolation of flood levels beyond the range of the rating curve measurements, it might involve epistemic uncertainty too. There are also commensurability issues about relating point measurements of soil water to model predicted variables at catchment scale.

The second difficulty is that even when we could make some sort of assessment of input errors, the impact of those errors on prediction uncertainties depends on processing through a particular model structure and parameter set (Beven and Binley, 2014). The inverse of this problem is seen in some recent studies that try to identify input errors as part of a Bayesian identification methodology (e.g. the BATEA studies of Thyer et al., 2009 and the DREAM studies of Vrugt et al., 2009 but see also Beven, 2009b in respect of the latter). Given an independent estimate of input error, we can then use a forward propagation of that error through any given combination of model structure and parameter set for comparison with any evaluation data. However, even assuming that input uncertainties can be defined before running any of the models, a full evaluation of the effects will then require many realizations to be run with each model parameter set greatly increasing the computational burden. How important this is will depend on how sensitive are the results to input uncertainty relative to other uncertainties, often input uncertainties cannot be considered negligible (Beven and Binley, 2014).

As a matter of fact, uncertainty estimation of Hydrological Predictions is today one of the most important topics of hydrology, according to the numerous contributions in recent scientific literature.

# Chapter 5

# Inverse problem theory and methods for model parameter identification

In the last two decades, the field of inverse problems has certainly been one of the fastest growing areas in applied mathematics. The inverse problem consists of using the actual result of some measurements to infer the values of the parameters that characterize the system (Tarantola, 2004). Inverse problems typically lead to mathematical models that are not well-posed in the sense of Hadamard, i.e., to ill posed problems. This means especially that their solution is unstable under data perturbations. Numerical methods that can cope with this problem are the so-called regularization methods. For linear problems, this theory can be considered to be relatively complete, for nonlinear problems, the theory is so far developed to a lesser extent (Engl et al., 1996).

The Parameter identification can be described through observations or measurement of the response of the system. Parameter identification approaches start from the idea that the choice of parameters should be such as to minimize a certain functional error.

The classical optimization approach leads to regularization procedures wherein the difference between observed and predicted system output is measured and parameters that minimised this difference are found. In the Bayesian update approach, the unknown parameter is modelled as a random variable (RV), called the *prior* model, so the unknown quantity is embedded in a probability distribution, where the spread of the probability distribution reflects the uncertainty about that quantity. Additional information on the system through measurement or observation changes the probabilistic description to the so-called *posterior* model. From a Bayesian point of view, many regularization techniques correspond to introducing additional information, imposing certain prior distributions on model parameters. In a Bayesian manner the task of determining the parameters in a computational model, is simplified to just computing the conditional expectation, see (Jaynes, 2003; Stuart, 2010; Tarantola, 2004). The problem now is well-posed, but at the price of 'only' obtaining probability distributions on the possible values of the uncertain parameters, which now are modelled as random variable.

On the other hand, one naturally also obtains information about the remaining uncertainty. Predicting what the measurement should be from some assumed parameters is computing the forward problem. The inverse problem is approached by comparing the forecast from the forward problem with the actual information.

In applications, it is frequently of interest to solve inverse problems: to find $q$, an input to a mathematical model, given $y$ an observation of the solution of the model. We have an equation of the form

$$y = \mathcal{G}(q) \tag{5.1}$$

In summary, the probabilistic concept transforms the prior expert-based probability description to a posterior via the incorporation of observations. From a Bayesian point of view this further means that the unknown parameters are taken to be uncertain and are modelled with the help of random variables (RVs)/fields (RFs), whose probability descriptions are coming from expert knowledge.
This prior knowledge is then updated to a posterior distribution via Bayes's rule given in terms of conditional probabilities. In this regard, the process of assimilating more information obtained via experiments becomes well-posed. As a final outcome, the posterior distribution summarizes all available information about the model parameters such as the mean value, variance, probability of occurrence etc. (Rosić et al., 2014).

## 5.1 Bayesian solution of inverse problem: numerical approaches

For a review of the existing algorithmic tools which are used when adopting the Bayesian approach to inverse problems see (Stuart, 2010). These include MCMC methods for sampling the posterior distribution, variational methods and filtering methods.
Bayes's theorem is commonly accepted as a consistent way to incorporate new knowledge into a probabilistic description. The elementary textbook statement of the theorem is about conditional probabilities

$$\mathbb{P}(I_q|M_z) = \frac{\mathbb{P}(M_z|I_q)}{\mathbb{P}(M_z)}\mathbb{P}(I_q) \tag{5.2}$$

where $I_q$ is some subset of possible parameters q's, and $M_z$ is the information provided by the measurement. This becomes problematic when the set $M_z$ has vanishing probability measure, but if all measures involved have probability density functions (pdfs) it may be formulated as

$$\pi_q(q|z) = \frac{p(z|q)}{P_n}p_q(q) \tag{5.3}$$

where $p_q$ is the pdf of q, $p(z\,|\,q)$ is the likelihood of $z = \tilde{y} + \varepsilon$ given q, as a function of q sometimes denoted by L(q), and $P_n$ is a normalizing factor such that the conditional density $\pi_q(.\,|\,z)$ integrates to unity. These terms are in direct correspondence with those in Eq. (5.2). Please observe that the model for the RV representing the error $\varepsilon(\omega)$ determines the likelihood functions $\mathbb{P}(M_z|I_q)$ resp. $p(z|q)$.

There are two equivalent approaches to Bayesian update (BU): one where it is expressed by conditional probabilities and one where it is a conditional expectation (Rosić et al., 2013). The easiest point of departure for conditional expectation is to define it not just for one piece of measurement $M_z$ but for sub-σ algebras. The linear Bayesian update as conditional expectation may be seen as find $K \in L(\mathcal{Y}, \mathcal{Q})$ such that:

$$K = arg_{H \in \mathcal{L}(\mathcal{Y},\mathcal{Q})} \min \| q - H(Y(q)) \|_Q^2 \tag{5.4}$$

And we set $\mathbb{E}(q|\sigma(Y))_l$ := K(Y(q)), a linear in Y approximation to $\mathbb{E}(q|\sigma(Y))$.
From either computation we get

$$K = C_{q,z} C_z^{-1} = C_{q,z}(C_y + C_\varepsilon)^{-1} \tag{5.5}$$

Where $C_\varepsilon$ for the error RV, $C_y$ for the measurement prediction, and $C_z$ for the measurement itself. Here the operator K is also known as the Kalman gain, which obviously depends on $C_\varepsilon$ the covariance of $\epsilon$. In case $C_y + C_\varepsilon$ is not invertible or close to singularity, its inverse in Eq. (5.5) should be replaced by the Moore–Penrose pseudo-inverse; but usually $C_\varepsilon$ is non-singular, assuring the existence of the inverse in Eq.(5.5).
In the case of prior information represented by the forecast RV $q_f$, which results in the measurement forecast $y_f = Y(q_f)$, the projection uses K from Eq. (5.5), and is adjusted by

$$q_a = q_f + K(z - y_f) \tag{5.6}$$

We point out that $q_a, q_f, y_f$ are RVs and observe that $z = \hat{y} + \varepsilon$ where also the error term is a RV, hence the quantity z is a RV and Eq. (5.6) is an equation between RVs.
It is worth to point out the representation of the Bayesian approach to identification (Figure 5.1). We assume our prior knowledge to be in an a priori distribution with corresponding RV $q_f(\omega)$. $q_f(\omega)$ is then propagated through the model $S$ and the measurement operator $Y$ to the forecasted (predicted) measurement $y(\omega)$. This is our proxy model. The prediction is then compared to noisy data $z(\omega)$ coming from real measurements, and the resulting difference is forwarded to the Bayes filter, which further gives the posterior distribution $q_a(\omega)$, that is also the updated value of $q_f(\omega)$. This is the Bayesian update expressed in terms of RVs instead of measures. It is the estimate of the unknown parameters $q$ after the measurement has been performed.

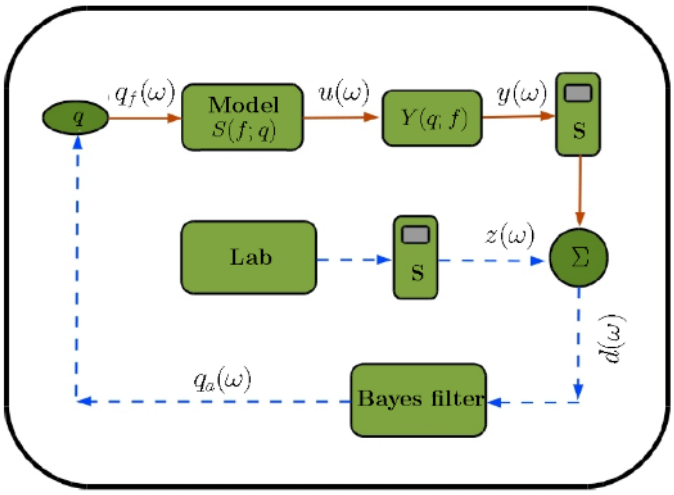


**Figure 5.1: Schematic representation of Bayesian approach to identification (Rosić et al., 2014).**

One of the most commonly used methods for solving practical systems with random inputs is Monte Carlo sampling (MCS) or one of its variants. It is well known that Monte Carlo simulations imply representation by random samples and they represent the most expensive methods but they allow to obtain reference results and to control other approximation methods. In MCS, one generates (independent) realizations of random inputs based on their prescribed probability distribution. For each realization, the data are fixed and the problem becomes deterministic. Upon solving the deterministic realizations of the problem, one collects an ensemble of solutions, i.e., realizations of the random solutions. From this ensemble, statistical information can be extracted, e.g., mean and variance. Although MCS is straightforward to apply as it only requires repetitive executions of deterministic simulations, typically a large number of executions are needed, for the solution statistics converge relatively slowly. The need for a large number of realizations for accurate results can incur an excessive computational burden, especially for systems that are already computationally intensive in their deterministic settings. Techniques have been developed to accelerate convergence of the MCS, e.g., Latin hypercube sampling and quasi Monte Carlo sampling, to name a few (Xiu, 2010). We usually see the results of MC simulations depending on the number of realizations.

Before to any simulation, the key step is to properly characterize the random inputs. More specifically, the goal is to reduce the infinite-dimensional probability space to a finite-dimensional space that is amenable to computing. This is accomplished by parameterizing the probability space by a set of a finite number of random variables, preferably mutually independent (Xiu, 2010). To summarize, the probability space defined by the random inputs should be properly characterize by a set of a finite number of mutually independent random variables. Another important aspect to take into account is the type of the pseudo-random numbers generator. Generation of points is at the root of MCS, it is indispensable for the creation of random variable outcomes obeying a given distribution.

### 5.1.1 Ensemble Kalman filter (EnKF) method

The simplest way to numerically estimate $q_a$ is to sample the equation (5.6) in a MC fashion. The procedure starts by building ensembles of prior samples and arranging the samples in a matrix $Q_f := [q_f(w_1);\ldots; q_f(w_Z)]$, similarly the forecasts $Y_f := [y_f(w_1);\ldots; y_f(w_Z)]$ and measurements $Z$, such that Eq. (5.6) can be formulated in a matrix notation as

$$Q_a = Q_f + K\,(Z - Y_f\,) \tag{5.7}$$

in which K takes the form $K = C_{qf,yf}(C_{yf} + C_\varepsilon)^{-1}$ as in Eq. (5.5). The covariances needed to compute K have to be estimated from the sample. This simply takes the form

$$C_{qf,yf} \approx \frac{1}{Z-1}\, Q_f Y_f^T \text{ and } C_{yf} \approx \frac{1}{Z-1}\, Y_f Y_f^T \tag{5.8}$$

This method is a Monte Carlo method, hence it also suffers from the slow convergence with increasing Z. On the other hand, it is fairly simple to implement: all it needs are random samples. In practice the number of samples is often low, and then special care is needed when computing the covariances and the Kalman gain K. To reduce the computation time, one may use the proxy model instead of a forward simulator. In this manner, only the update formula in Eq. (5.6) is sampled.

### 5.1.2 Markov chain Monte Carlo (MCMC) method

The Markov chain Monte Carlo (MCMC) method (Gamerman and Lopes, 2006) is one of the most commonly used techniques for this kind of parameter estimation. In MCMC methods, the Markov chain is constructed such that the asymptotic distribution of the chain is the Bayesian posterior distribution. The posterior is sampled by letting the Markov chain run for a sufficiently long time. With the intention of accelerating the MCMC method some authors (Bazargan et al., 2013; Kučerová et al., 2012; Marzouk and Xiu, 2009; Marzouk et al., 2007) have introduced stochastic spectral methods into the computation. Expanding the prior random process into a polynomial chaos (PCE) or a Karhunen-Loève expansion (KLE), the inverse problem becomes an inference on the weights of the KLE or PCE coefficients. Another solution is to combine polynomial chaos theory with the maximum likelihood estimation and to calculate the parameter estimates in a recursive manner or to apply a local linearization of the forward model to improve the acceptance probability of proposed moves.
However, the previously mentioned methods are all based on pure sampling procedures, or a combination of spectral approximations and MCMC. Therefore, they are slowly convergent and often computationally infeasible especially when one deals with large-scale problems.

### 5.1.3 Wiener's Polynomial Chaos Expansion (PCE) based method

Update method based on Wiener's Polynomial Chaos represents an innovative approach in the BU methods. Stochastic solutions are expressed as orthogonal polynomials of the input random parameters, and different types of orthogonal polynomials can be chosen to achieve better convergence.
To avoid the sampling procedure presented previously in a form of the ensemble Kalman filter (EnKF) algorithm, one may use the opportunity to functionally approximate the random variables (fields) in Eq. (5.6). In this light the linear Bayesian procedure can be reduced to a simple algebraic method. Starting from the functional representation of the prior

$$\hat{q}f = \sum_a q_f^{(a)} H_a(\omega) \tag{5.9}$$

And the proxy model for the forecasted measurement

$$\hat{y}_f(\omega) = \sum_{\mathcal{F}} y_f^{(\alpha)} H_\alpha(\omega) \tag{5.10}$$

One may discretize Eq. (5.6) as

$$\hat{q}a = \hat{q}f + K(\hat{z} - \hat{y}f) \tag{5.11}$$

where $\hat{z} \in \mathbb{R}^{L\,X\,Z}$ is the PCE of the measurement. Here, K in Eq. (5.11) is the Kalman gain evaluated in an algebraic way knowing that

$$C_{qf,yf} = \sum_{a>0} a!\; q_f^{(a)} (y_f^{(a)})^T \tag{5.12}$$

Note that in the numerical computation $\hat{q}_\mathrm{a} \in \mathbb{R}^Z$ , $\hat{q}_\mathrm{f} \in \mathbb{R}^Z$ , $\hat{y}_\mathrm{f} \in \mathbb{R}^{L\,x\,Z}$ and $\hat{z} \in \mathbb{R}^{L\,x\,Z}$ are PCEs with cardinality Z determined by (L+1) RVs and polynomial order p. Here, the number (L+1) subsumes all the RVs describing the prior and the RVs $\{\theta_i\}_{i=1}^{L}$ used to model the measurement error $\epsilon$.
It is essentially a spectral representation in random space and exhibits fast convergence when the solution depends smoothly on the random parameters. Frequently, methods based on sampling procedures like MCMC method are slowly convergent and often required expensive computational cost, therefore, the research group of the Institute of Scientific Computing of the Technische Universität Braunschweig constructed a more efficient approach based on conditional expectation to considerably speed up the computation, which is an equivalent way to formulate BU. The conditional expectation has significant computational advantages and a very direct geometrical interpretation as an orthogonal projection, it can be approximated by linear or higher order maps, which should be found during the updating. In this way BU is an algebraic formula, which can be computed in a purely analytical way as indicated in (Pajonk et al., 2013, 2012, Rosić et al., 2013, 2012). In (Saad and Ghanem, 2009) it appears as a variant of the Kalman filter.

RVs could be discretized trough their samples as well as by functional approximations (Xiu, 2010). This means that all RVs, are described as functions of known RVs. Many different systems of functions can be used, classical choices are multivariate polynomials, standard Hermite polynomials in independent Gaussian RVs, i.e. Wiener's polynomial chaos (Wiener, 1938), as well as trigonometric functions, kernel functions as in kriging, radial basis functions, sigmoidal functions as in artificial neural networks (ANNs), or functions derived from fuzzy sets.
The main idea in the publications (Pajonk et al., 2013, 2012, Rosić et al., 2013, 2012) is to do the Bayesian update directly on the Wiener's Polynomial Chaos Expansion (PCE) without any sampling. The authors have developed a method which combines BU with the representation of random variables by PCE. The resulting update equation is fully deterministic and thus does not involve any sampling error, as opposed to Monte Carlo methods. The original Kalman filter has been shown to be a low order special case of the new method. The method has shown some appealing mathematical properties, as well as experimental capabilities. It is a promising combination of Bayesian inversion and uncertainty quantification techniques based on the PCE (Pajonk et al., 2012).

# Chapter 6

# MOBIDIC modelling of the Arno river basin

## 6.1 MOBIDIC hydrological model description

The hydrological model MOBIDIC (MOdello di Bilancio Idrologico DIstribuito e Continuo) is developed by the Department of Civil and Environmental Engineering of the University of Florence. More details about MOBIDIC can be found in (Campo et al., 2006; Castelli et al., 2009; Castillo et al., 2014; Yang et al., 2014), see the papers for more information and the hydrological balance equations.
The operational framework of MOBIDIC model is the real-time for water balance evaluation and hydrological forecast in the major river basins of Tuscany region.
The Regional Hydrologic Service of Tuscany (SIR) employs MOBIDIC model to perform water balance simulations at river basin scale as well as to simulate and predict possible scenarios of hydrogeological and hydraulic hazards as decision support system (DSS) for planning and prevention activities for the purposes of Regional Functional Centre (CFR). The developed modeling system in real time forecasting mode uses hydro-meteorological data of regional monitoring network, and the quantitative predictions of atmospheric precipitation computed by means of different numerical models by the LaMMa Consortium. MOBIDIC outputs in terms of runoff discharges along the hydrographic network, represent also input data for the hydraulic model QRF (Quantity Risk Forecast), developed by the Arno river basin Authority as Centre of Competence of the Italian Department of Civil Protection, as DSS for the civil protection management during extreme events. The centre of competence collaborates on a functional and operative level within the national alert system, which include the network of functional centers and the regional structures, and it is managed by the Department of Civil Protection and by the Regional Governments. They particularly contribute in collecting information useful for predicting, monitoring and supervising the various types of phenomena.
The selected hydrological model MOBIDIC is a distributed and conceptual model with continuous temporal representation for coupled energy and mass balance solving, the monitoring of the water content in the soil, and the forecasting of floods.
The outputs of MOBIDIC are estimated and predicted soil water content (in “large” and “small” pores), hydrological and energy balance components (evapotranspiration, soil temperature) and discharge in each branch of the river network, including minor branches.

It is a raster based model, it performs the rainfall-runoff simulation based on a small-scale discretization of the soil and sub-soil processes that contributed to the total runoff. The spatial domain for the computation of the hydrological processes is represented by a horizontal discretization of the basin in square cells and a vertical separation into five layers: (1) vegetation, (2) surface reservoirs (rivers and basins), (3) gravitational soil, (4) capillary soil, (5) groundwater (Castelli et al., 2009).
Within each grid cell the soil and sub-soil processes are simulated according to conceptual schemes based on linear and nonlinear reservoirs:

- Surface energy balance (soil-vegetation-atmosphere system, Evapotranspiration phenomena);
- Hydrologic soil balance (Infiltration, Adsorption, Interflow phenomena in capillary and gravitational reservoirs);
- River and reservoir routing (Surface runoff);
- Groundwater balance (Percolation phenomena in Groundwater storage).

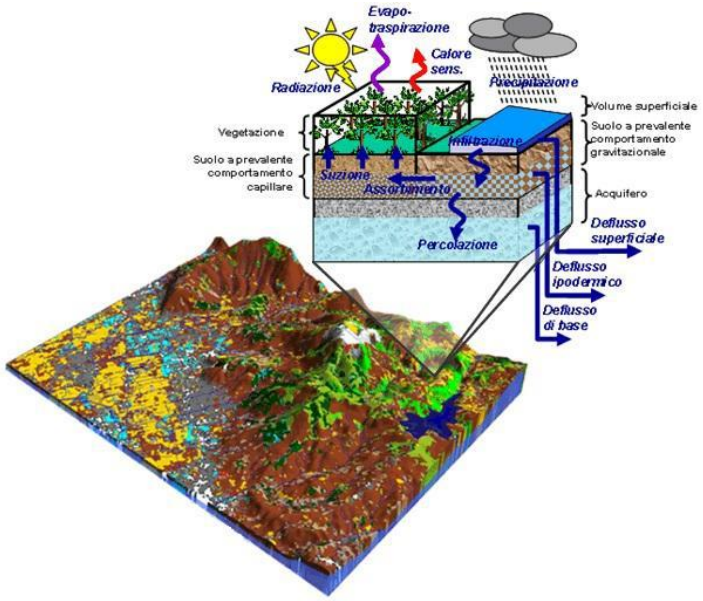


**Figure 6.1: Discretization of the soil and sub-soil processes in hydrological model MOBIDIC (Vanni, 2015).**

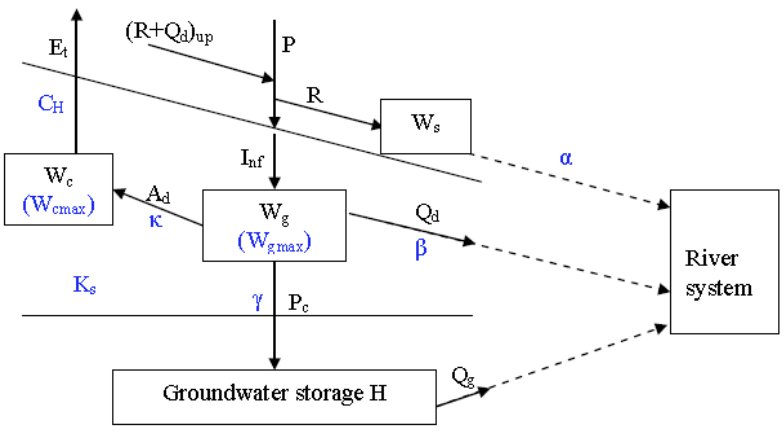


**Figure 6.2: Schematic representation of MOBIDIC model (Yang et al., 2014).**

In Figure 6.2 the boxes are the water storages (gravitational storage *Wg*, capillary storage *Wc*, groundwater storage *H*, surface storage *Ws*, and the river system) while the arrows represent the hydrological fluxes (evaporation $E_t$, precipitation *P*, infiltration $I_{inf}$, adsorption $A_d$, percolation $P_c$, surface runoff *R*, interflow $Q_d$, groundwater discharge $Q_g$, and surface runoff and interflow from upper cells $(R+Q_d)_{up}$). In blue characters the major model parameters are highlighted. We can observe the link between some parameters and the physical phenomena to be considered in the water balance.
The MOBIDIC simulations are driven by a number of calculation control parameters for setting numerical and data flow schemes.
Among the following possibilities, it is possible to choose:

- The type of conceptual scheme for the hydrologic soil balance:

  Bucket – Double-bucket gravitational and capillary (it is the one we use);
  CN – Soil Conservation Service-Curve Number.

- The type of conceptual scheme for the river flow routing:

  Lag – Fixed lag;
  Linear – Linear reservoir (it is the default scheme, the one we use);
  Musk –Muskingam;
  MuskCun - Muskingam-Cunge.

- The type of the scheme for the surface energy balance:

  2L – 2 Layers scheme (it is the default scheme, the one we use);
  1L – 1 Layer scheme;
  Snow – 4 Layers forward scheme (2 layers for soil and 2 layers for snowpack);
  None – the surface energy balance is deactivated (it is the one we use for design hydrograph).

- The type of the scheme for the aquifer modelling (it has been neglected because the schematization requires additional information, in many cases not available or available on limited areas):

  Linear – Conceptual linear reservoir (it is the default scheme);
  Dupuit – Dupuit approximation for phreatic aquifer.
  ModFlow – Link with MODFLOW groundwater model.

## 6.2 Recent flood events in the Arno river basin

In this dissertation, MOBIDIC model is used both for long term hydrologic simulations (Chapter 7) and computations of the design hydrographs (Chapter 8). Therefore, as shown in section 6.4.2, the hydrometeorological data required for the numerical examples of parameter identification procedure are those for long-term hydrologic simulation, while those for design hydrographs consist basically of

design rainfall. Since the main goal of later sections is to show how the Bayesian update works, the methodology is here presented first for a synthetic numerical example, then for a specific flood event occurred on 28.11.2012 in the Arno river sub-basins. However, for practical utilization, a complete procedure of identification should be described with the help of more measurements of flood events, that is expensive in terms of computation time and memory and that might be addressed in future studies. Even so, we identified in the Arno river basin recent heavy storm events, in order to detected recent floods in this last decade. The Arno river basin authority provides data for 11 extreme events. Discharge data collected by 37 stream gauges are analyzed and 11 stream gauges are neglected (4 out of Arno river basin, 7 characterized by No Data for at least one event). Finally, 9 flood events in the period 2012-2014 have been selected (Table 6.1). For this recent hydro-meteorological extreme events occurred in the Arno river basin, the input meteorological data for MOBIDIC model and the flow data for model validation are collected.

**Table 6.1: Recent flood events identified in the Arno river basin.**

| **Flood event date** | **Stream gages with highest stage $H_{max}$ (m szi) recorded during the flood event** | **River Sub-basins** |
|---|---|---|
| 28.11.2012 | Ponte alle Mosse (FI), S. Giovanni alla Vena (PI) (**4.09**), Poggio a Caiano (PO) (**4.71**) | Mugnone, Arno, Ombrone PT |
| 04.12.2012 | Pisa a Sostegno | Arno |
| 18.03.2013 | Vaiano Gamberame (PO), Prato, S. Piero a Ponti (FI), Pontelungo (PT), Poggio a Caiano (**6.36**) | Bisenzio Ombrone PT |
| 29.03.2013 | Vaiano Gamberame, Prato, S. Piero a Ponti, Pontelungo, Poggio a Caiano | Bisenzio Ombrone PT |
| 22.10.2013 | Greve (FI), Vaiano Gamberame, Molino d'Era (PI), Case Grisella (PI) | Greve, Bisenzio, Era, Sterza |
| 05.01.2014 | Vaiano Gamberame, S. Piero a Ponti, Pontelungo, Poggio a Caiano | Bisenzio Ombrone PT |
| 19.01.2014 | Vaiano Gamberame, S. Piero a Ponti Pontelungo, Poggio a Caiano | Bisenzio Ombrone PT |
| 31.01.2014 | Belvedere (PI), S. Giovanni alla Vena (**6.20**), Pisa | Era, Arno |
| 10.02.2014 | Nave di Rosano (FI), Montelupo (FI), Pontedera (PI), Fornacina (FI), S. Piero a Ponti, Poggio a Caiano, Belvedere, S. Giovanni alla Vena (**6.07**), Pisa | Arno, Sieve, Bisenzio, Ombrone PT, Era |

According to the hydro-meteorological event reports by SIR, this events should be considered as extreme and rare events: for one event, occurred in Florence in 2012, the cumulative rainfall depth in 24 hours registered by Firenze Università rain gauge

has been estimated as the rainfall depth of 40 years $T_r$ (Figure 6.3) Another selected hydro-meteorological extreme event occurred in October of 2013: Volterra rain gauge registered around 100 mm in 2 hours (Figure 6.4).

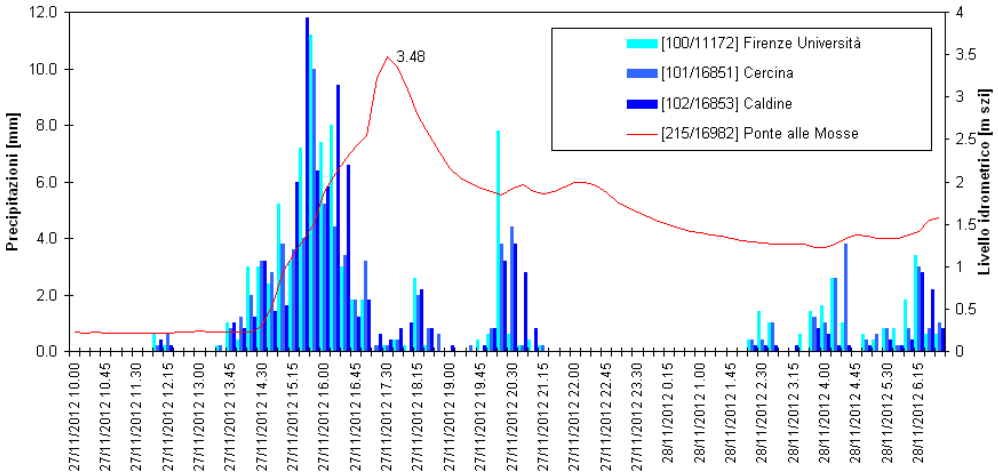


**Figure 6.3: Histogram of 15' rainfall recorded the 27-28.11.2012 in Firenze Università, Cercina, Caldine rain gauges and water level recorded in Ponte alle mosse strem gauge (Mugnone river flood) (source: www.adbarno.it).**

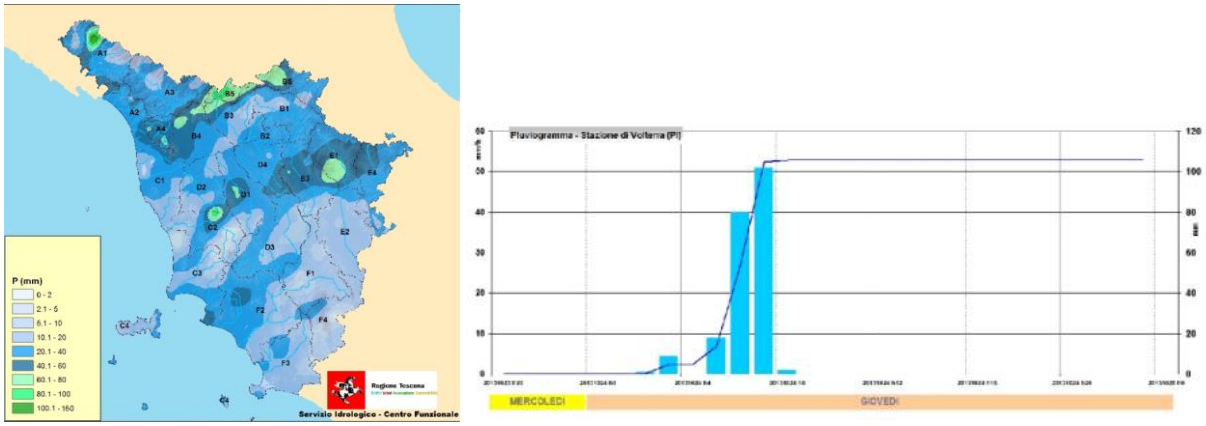


**Figure 6.4: Spatial distribution of the cumulative rainfall recorded from 23.10.2013, h:20:00 to 24.10.2013, h:24:00 (left panel) and the histogram of hourly rainfall and CDF recorded in Volterra rain gauge (right panel) (CFR, 2013).**

How and when can we say if hydrological event has been an extreme event?
The concept of extreme event is not univocal and easily definable, because it strongly depends on the morphological and climatic features of the concerned areas. In fact, rainfalls and floods may last minutes, hours or even weeks, depending on the area considered and on the length of the main stream. Moreover, a huge rainfall (an intense precipitation) may represent a standard situation in humid areas, whereas in arid areas may be qualified as a very extreme event. For this reasons the definition of extreme event cannot have a quantitative boundary, but must be seen in a probabilistic view, it is strictly related to the definition of return period (recurrence interval). The return period is an estimate of the likelihood of an event to occur. It is a statistical measurement typically based on historic data denoting the average

recurrence interval over an extended period of time, and is usually used for risk analysis.

Extreme event is generally defined as the occurrence of a value of a weather or climate variable above (or below) a threshold value near the upper (or lower) ends of the range of observed values of the variable (IPCC, 2012). Extreme events have extreme values of certain important meteorological variables. Damage is often caused by extreme values of certain meteorological variables, such as large amounts of precipitation (e.g., floods), high wind speeds (e.g., cyclones), high temperatures (e.g., heat waves), etc. Extreme is generally defined as either taking maximum values or exceedance above pre-existing high thresholds (Stephenson, 2008).

## 6.3 MOBIDIC model input

The dataset used in the MOBIDIC model includes:

- The geographic data;
- The hydrometeorological data.

All the information about the data location, parameters and computation options, i.e. everything that defines the contents and modes of a given case study, are managed through the records of a configuration file. The configuration file is a text file whose name is given by the user and must have extension *.cfm* (e.g. *Arno_Basin.cfm*) and must be stored in the main MOBIDIC folder.

```
196 ####### GIS PROCESSING AND SIMULATION CONTROLS
197
198    #REQUIRED# Option to wait for new data at end of computation (realtime mode)
199                      # [integer number, 0=NO, 1=YES]
200 realtime             0
201
202    #REQUIRED# Degradation factor from grid data space resolution to model space resolution, non dimensional
203                      # [positive integer number]
204 degradfac            10
205
206    #REQUIRED# Data and model time step, in seconds
207                      # [positive number in float or exp notation, eg: 86400 for daily data]
208 basestep             900
209
210    #REQUIRED# Consolidated dataset to be created by GIS preprocessing
211                      # [full pathname to .mat file, eg: \blue_nile\geodat\gisdata.mat]
212 gisdatapath          C:\mobidic\Arno_basin\gisdata\gisdata.mat
213
214    #REQUIRED# Directory where the model states will be stored
215                      # [directory path including terminal \, eg: \blue_nile\states\]
216 statespath           C:\mobidic\Arno_basin\design200\
217
218    #REQUIRED# Type of channel routing scheme
219                      # [one amnog the following options 'Musk', 'MuskCun', 'Lag', 'Linear']
220 routtype             Linear
221
222    #REQUIRED# Type of soil hydrology scheme
223                      # [one amnog the following options 'BUCKET', 'CN']
224 bilatype             BUCKET
225 enertype    None
226
227 ####### GROUND STATIONS AND TIME SERIES
228
```

**Figure 6.5: Example of a configuration file.**

The various information that need to be specified in a configuration file may be logically subdivided in the following categories:

- General identification parameters;
- Calculation control parameters;

- Global hydrologic parameters;
- Information about geographic data in raster format;
- Information about geographic data in vector format;
- Information about hydrometeorologic data.

### 6.3.1 The geographic data

In MOBIDIC the river basin is represented as a rectangular grid with an arbitrary spatial discretization sets regarding digital elevation model (DEM) spatial resolution. In details, for the watershed identification and the hydrological characterization, these geographic data are used:

- DEM with 500m square cells adopted as the model computational grid size;
- Flow direction: direction of maximum ground slope;
- Flow accumulation: extension of the superficial contributing watershed;
- River network.

The Flow direction and accumulation grids are automatically derivable from DEM by employing one of the several specific GIS procedures (Hydrology Toolbox in ArcGIS).

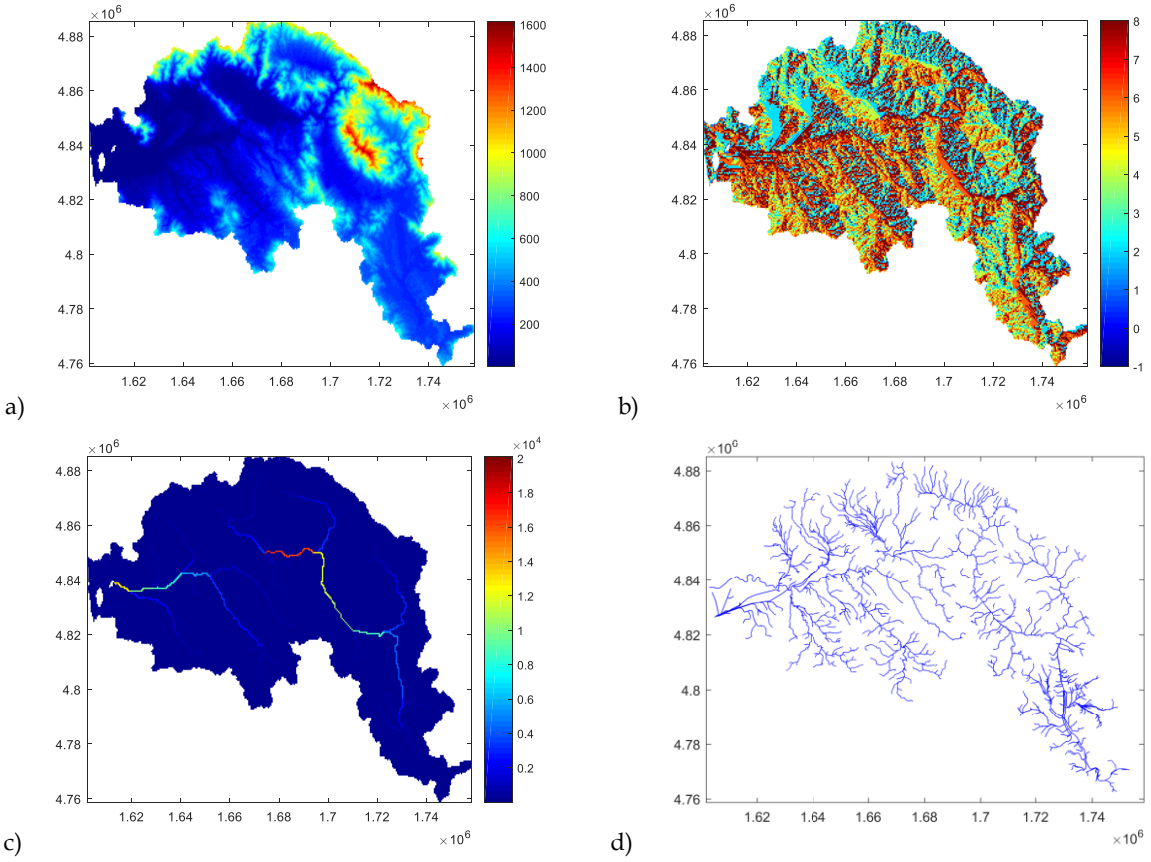


**Figure 6.6: Geographic data for the hydrological characterization in raster format a) DEM (m a.s.l.), b) Flow direction, c) Flow accumulation and in vector format d) river network.**

Others required geographic data in raster format describes the main soil and surface land parameters. They are:

- *Wgmax*: Maximum water holding capacity (volume per area unit, units in *mm*) of the gravitational reservoir;
- *Wcmax*: Maximum water holding capacity of the capillary reservoir;
- *Ks*: Saturated hydraulic conductivity (units in *mm/hour*) of the soil superficial layer;
- *Kf*: Hydraulic conductivity (units in *m/s*) of the soil deep layer (or of the aquifer), i.e. Groundwater reservoir coefficient set equal to 1e-07;
- *Alb*: Albedo coefficient of land surface set equal to 0.2;
- *CH*: Heat turbulent exchange coefficient between land surface and atmosphere.

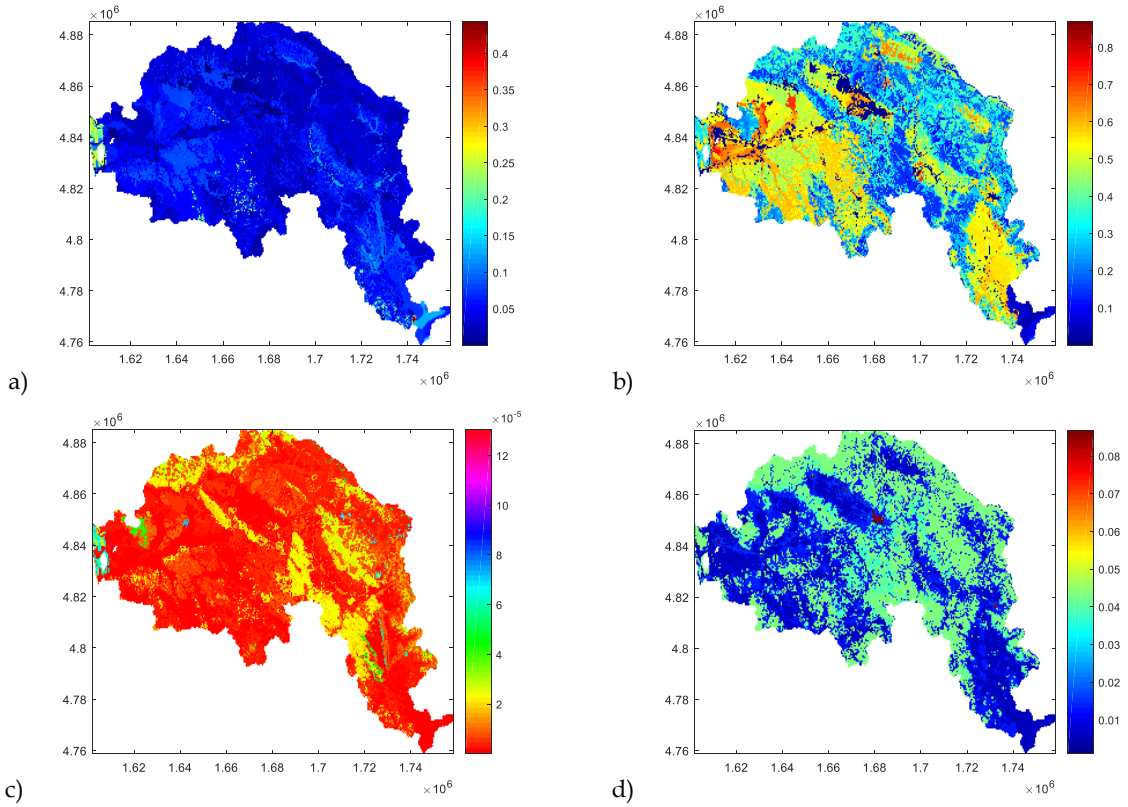


**Figure 6.7: Example of optional raster data for soil and vegetation a) Wgmax - gravitational capacity, b) Wcmax - capillary capacity, c) Ks - soil hydraulic conductivity, d) CH - heat turbulent exchange coefficient between land surface and atmosphere.**

In the frame of a scientific collaboration project between the Department of Civil and Environmental Engineering of the University of Florence and the Tuscany Region, Unit for Prevention of Hydrogeological and Hydraulic Risks for research activity on flood risk mitigation, the MOBIDIC model was updated (Castelli, 2014). As a result of this study, a new evaluation of soil hydraulic parameters such as *Wgmax*, *Wcmax*, *Ks*, the so called "new type of soil" for the Tuscany region territory have been performed. Since a lack of direct measurements, the physical-hydrological behavior of soil is described using the so-called Pedo Transfer Functions (PTF). By means of

some standardization operations of the Tuscany regional soil database and of measured data relating to the characteristics of the soil horizons such as soil texture, structure, content of organic matter, the water retention curve for each soil texture class and the hydraulic conductivity have been estimated.
In order to obtain gravitational and capillary water values spatially distributed as required by the MOBIDIC model, starting from the individual water retention curves calculated for each soil horizon and using new criteria of aggregation, a unique value of the hydrological parameters estimated is obtained for each cell of the rasters.
The storage capacities *Wgmax* and *Wcmax* may be respectively defined as the maximum water content above the field capacity and the maximum water content between the field capacity and the wilting point.
The field capacity and the wilting point are two important moisture characteristics of soils. The moisture in soils includes all forms of water that enter the soil system and it is derived mainly from precipitation or may be supplied by the lateral movement of water over the surface or within the body of the soil itself. Underground water may also contribute, though flooding by rivers provides the greater part of the soil moisture. The total volume is determined by the intensity of rainfall, vegetation cover, infiltration capacity, permeability and slope, speed of snow melting and original moisture content of the soil. The state and movement of water in soils is very complex, water is held with varying degrees of tension or suction within the soil, commonly expressed in bars. After the soil has been saturated and the excess water drained away, the soil is said to be at field capacity and the water is held a tension of about 0.05 bars (i.e. 5kPa, 60μm dimension pores). Providing more detail about soil water limits in the study of Castelli, 2014, the gravitational water content is held a tension of about 0.1 bars (i.e. 30μm dimension pores). If plants are growing on the soil they will extract moisture until they cannot extract any more, then they will wilt and eventually they will die if the soil is not rewetted. The point at which permanent wilting starts is known as the wilting point where water is held at about 15 bars, but this value does differ slightly from soil to soil and plant to plant. Thus water held between field capacity and wilting point is the water available to plants. As water content decreases, tension on the water becomes greater or soil water potential becomes less. The amount varies from soil to soil being greatest in silty soils and least in sands as shown in Figure 6.8 (a). In this figure, it is possible to note that the wilting point increases as the texture become finer and the field capacity increases up to silt loam then levels off.
Regarding water state in soil, the classical method is to classify soil water into gravitational, capillary and hygroscopic (Figure 6.8 (b)). The gravitational water flows freely downwards through the soil and is held at a tension of about <0.1bar. Capillary water is held in the pores and on the surfaces of the particles at 0.1 to 31 bars and moves in any direction in response to a moisture gradient (FitzPatrick, 1980).

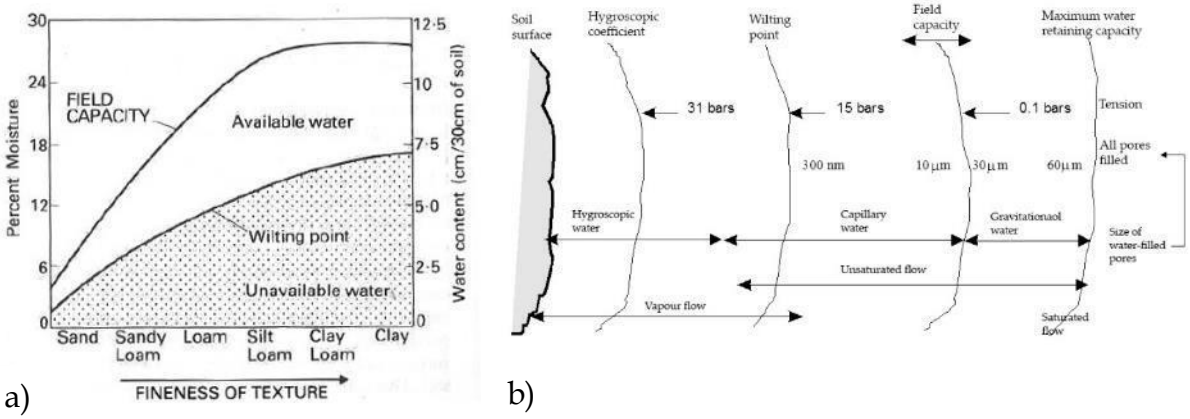


**Figure 6.8: a) General relationship between soil moisture characteristics and soil texture b) Relationship between the types of the water, types of flow and suction (FitzPatrick, 1980).**

The Gis data in raster format as well as in vector format should be pre-processing before the calculations execution of the hydrologic balance. The execution of the module of geographical data pre-processing can be started by command line on Windows system:

```
buildgis_mysql_include GOLOCAL MOBIDIC case_study.cfm
```

Since the case study is always the same, geographic data modifications are not required for the several necessary simulations. It means that it is possible to run the pre-processing module once, and use the file *gisdata.mat* created in the last step for all the simulations. In effect, the file *gisdata.mat* has been provided by the Department of Civil and Environmental Engineering of the University of Florence and it is the same used by Regional Hydrologic Service of Tuscany and Arno River Basin Authority.

### 6.3.2 The hydrometeorological data

Since MOBIDIC model can be used for various applications, the hydrometeorological data has some differences between runs for long term hydrologic simulations, runs for real time forecasting and computations of the design hydrographs (see Section 6.3.3).

The climatic input required for the numerical examples of parameter identification procedure described in the next paragraph are those for long-term hydrologic simulation. The hydrometeorological data are provided to MOBIDIC model by means of the *meteodata.mat* that should be organized in 6 structure arrays as much as climatic input, where each element represents a measurement station (either real or virtual).

Therefore, continuous time series of precipitation (mm), air maximum temperature (°C), air minimum temperature (°C), air humidity (%), solar radiation ($Wm^{-2}$), wind speed ($ms^{-1}$) measured at the gauges inside the sub-basin for the above mentioned (Table 6.1) hydro-meteorological extreme events occurred in the Arno river basin have been collected.

The simulated time is given by the length of time series (6 days) as well as the calculating step of the model should be consistent with the temporal step of the time series (15 min time resolution). In particular, for the studied flood event occurred on 28.11.2012, the following figures show the input climatic time series registered in

- 106 pluviometric stations;
- 36 thermometer stations;
- 17 hygrometer stations;
- 4 radiometer stations;
- 8 anemometer stations.

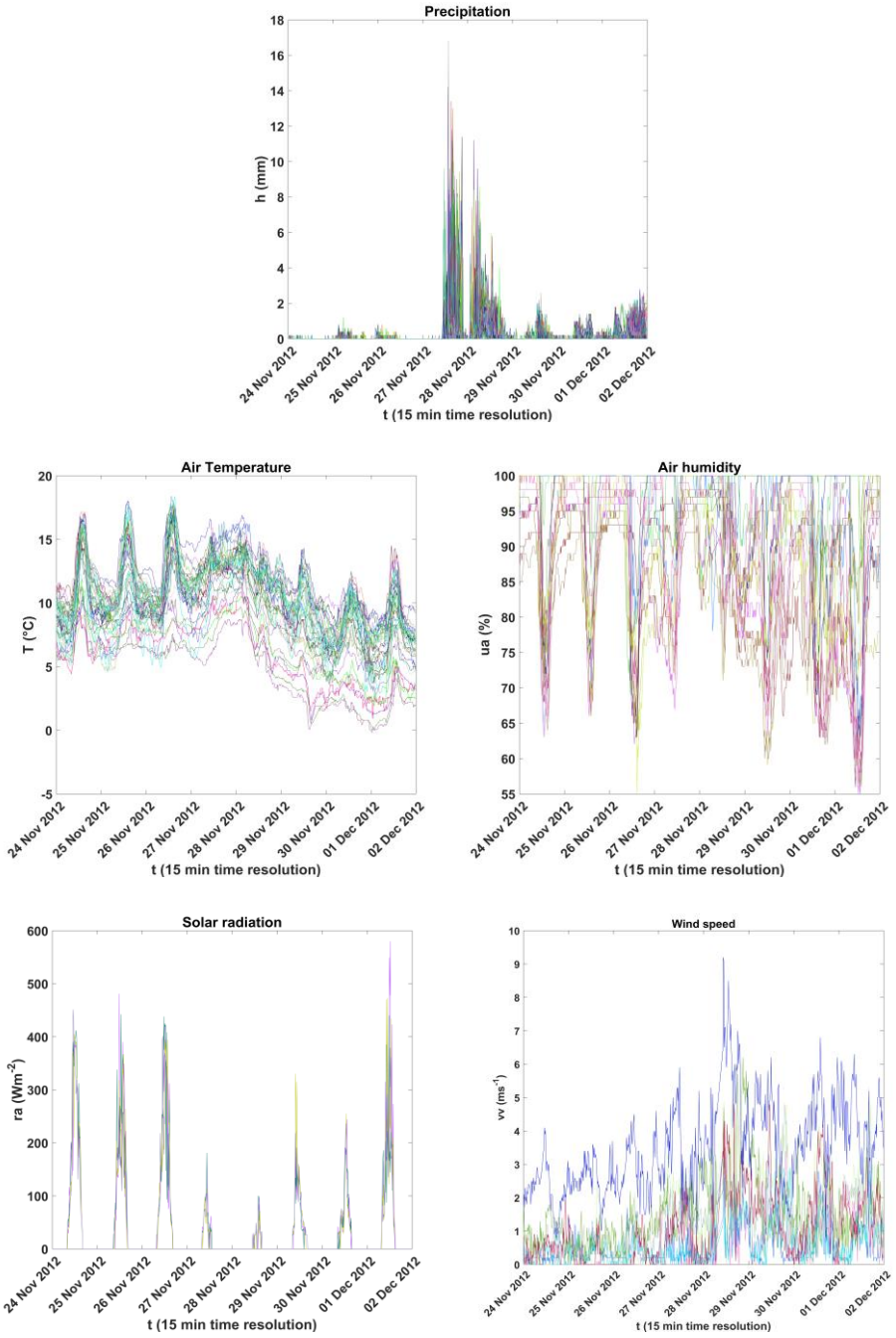


**Figure 6.9: Climatic time series of precipitation (mm), air maximum temperature (°C), air minimum temperature (°C), air humidity (%), solar radiation ($Wm^{-2}$), wind speed ($ms^{-1}$) measured at the gauges inside the Arno river sub-basin for the 28.11.2012 flood event.**

Moreover, discharge data for the 9 flood events above mentioned to be use as measurements in the Bayesian update and to assess model performance are collected (Table 6.2).

**Table 6.2: 25 Maxima values of discharges recorded by 25 stream gauges in the Arno river sub-basin during the selected 9 flood events. The selected stream gauges are ordered from upstream to downstream, along the course of the Arno river and its tributaries.**

| Stream gauges | | | Flood events (YYYYMMDD) | | | | | | | | |
|---|---|---|---|---|---|---|---|---|---|---|---|
| | | | 20121128 | 20121204 | 20130318 | 20130329 | 20131022 | 20140105 | 20140119 | 20140131 | 20140210 |
| CODE | Basin | NAME | $Q_{max}$ [$m^3/s$] | $Q_{max}$ [$m^3/s$] | $Q_{max}$ [$m^3/s$] | $Q_{max}$ [$m^3/s$] | $Q_{max}$ [$m^3/s$] | $Q_{max}$ [$m^3/s$] | $Q_{max}$ [$m^3/s$] | $Q_{max}$ [$m^3/s$] | $Q_{max}$ [$m^3/s$] |
| 4379 | Arno | Stia | 26.0 | 5.9 | 12.7 | 5.6 | 25.0 | 5.0 | 4.6 | 24.0 | 18.0 |
| 4411 | Arno | Subbiano | 447.6 | 83.7 | 571.8 | 266.0 | 466.4 | 81.0 | 115.7 | 511.6 | 591.2 |
| 4571 | Arno | Montevarchi | 684.3 | 196.7 | 743.4 | 346.7 | 899.6 | 74.4 | 85.1 | 840.0 | 901.5 |
| 4591 | Arno | Incisa Valle | 692.3 | 252.3 | 754.1 | 416.9 | 817.3 | 107.8 | 124.2 | 898.5 | 995.3 |
| 4659 | Arno | Nave di Rosano | 851.0 | 302.8 | 1063.0 | 505.9 | 839.0 | 191.4 | 372.7 | 1162.0 | 1657.0 |
| 4679 | Arno | Firenze Uffizi | 826.0 | 255.3 | 1097.2 | 527.6 | 856.6 | 174.4 | 386.4 | 1222.6 | 1691.8 |
| 4811 | Arno | Ponte a Signa | 1154.8 | 503.2 | 1353.5 | 625.8 | 942.2 | 489.2 | 705.4 | 1655.7 | 1929.6 |
| 4901 | Arno | Montelupo | 1219.3 | 565.6 | 1435.9 | 697.0 | 955.3 | 562.8 | 776.1 | 1673.3 | 1954.0 |
| 5001 | Arno | Fucecchio valle | 1491.5 | 609.4 | 1383.3 | 696.7 | 1190.4 | 591.3 | 824.6 | 1978.6 | 1982.9 |
| 5181 | Arno | Pontedera | 1694.7 | 604.3 | 1462.8 | 644.9 | 1167.5 | 554.7 | 790.1 | 2191.3 | 2176.6 |
| 5191 | Arno | S.Giovanni alla Vena | 1820.1 | 615.3 | 1489.8 | 717.7 | 1241.3 | 626.9 | 824.7 | 1931.6 | 1924.5 |
| 4521 | Canale della Chiana | Ponte Ferrovia FI_Roma | 129.3 | 117.6 | 52.1 | 58.2 | 118.7 | 4.8 | 26.9 | 173.8 | 155.3 |
| 4568 | Ambra | Bucine | 71.0 | 20.0 | 36.0 | 28.0 | 109.0 | 4.1 | 9.2 | 66.0 | 47.0 |
| 4731 | Greve | Scandicci | 140.0 | 48.0 | 27.9 | 13.1 | 165.6 | 2.7 | 16.1 | 98.4 | 174.3 |
| 4921 | Pesa | Turbone | 122.0 | 49.4 | 35.9 | 19.0 | 148.0 | 5.1 | 32.2 | 130.0 | 132.0 |
| 4971 | Elsa | Castelfiorentino | 181.2 | 87.9 | 87.9 | 21.6 | 218.7 | 11.5 | 41.1 | 266.3 | 182.9 |
| 4981 | Elsa | Ponte a Elsa | 250.4 | 131.9 | 150.0 | 17.2 | 274.0 | 13.1 | 34.9 | 355.9 | 262.0 |
| 5005 | Egola | Fornacino | 51.2 | 52.3 | 21.0 | 13.6 | 55.8 | 6.3 | 13.3 | 57.7 | 26.9 |
| 5115 | Era | Molino di Era | 58.4 | 61.2 | 14.4 | 6.8 | 331.0 | 1.7 | 5.5 | 80.4 | 38.4 |
| 5131 | Era | Capannoli | 84.0 | 95.0 | 70.0 | 31.7 | 89.0 | 16.6 | 34.4 | 120.0 | 76.0 |
| 4623 | Sieve | S.Piero a Sieve-Carza | 67.1 | 77.8 | 55.4 | 29.9 | 60.6 | 24.2 | 95.1 | 82.2 | 97.5 |
| 4641 | Sieve | Fornacina | 390.7 | 231.2 | 307.8 | 120.1 | 266.2 | 78.5 | 289.6 | 330.9 | 485.5 |
| 4782 | Bisenzio | Prato | 101.6 | 35.2 | 232.0 | 147.8 | 291.8 | 183.0 | 112.8 | 167.4 | 181.6 |
| 4791 | Bisenzio | S.Piero a Ponti | 114.9 | 80.8 | 248.8 | 155.3 | 236.1 | 194.6 | 152.6 | 197.0 | 250.5 |
| 4875 | Ombrone Pistoiese | Poggio a Caiano | 136.4 | 133.8 | 234.1 | 151.5 | 218.4 | 213.3 | 165.9 | 234.8 | 225.3 |

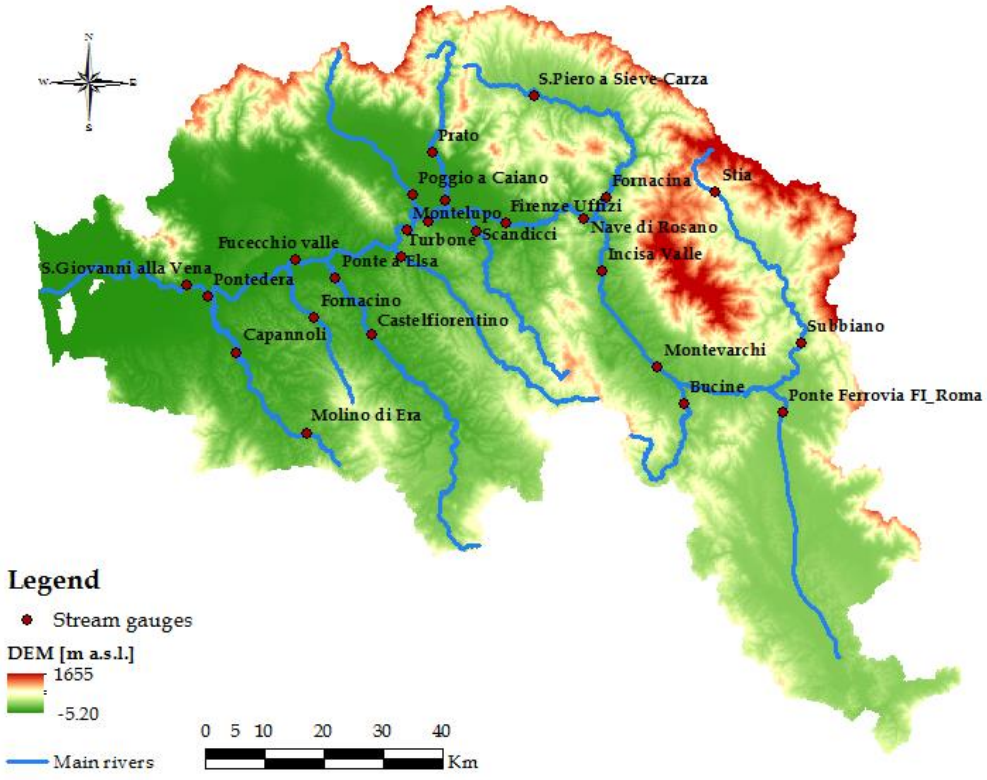


**Figure 6.10: DEM of the study area with 25 hydrometric stations used for MOBIDIC long term simulations.**

As a matter of fact, input meteorological data registered by regional hydro meteorological monitoring network and discharge data obtained by applying the stage-discharge relation are affected by uncertainties. However, since we don't know the accuracy, precision and sensitivity of sensors of the monitoring network and the accuracy of the rating curve in use to the Arno river basin authority and Regional Hydrologic Service of Tuscany, this sources of uncertainty are take into account in the simulations assuming a 2% of measurement errors. At the same time, we collected from the CFR some information regarding the number and the sampling time of discharge measurements for rating curves assessment in the stream gauges of Arno hydrographic network. Finally, 25 stream gauges were selected for their geographical position as well as for the reliability of the rating curve (Figure 6.10).
It is worth remanding, that the stream gauges record a "water surface level" that, by means of the rating curve, allow to trace back to the stream flow rates associated to that level. The rating curve, or stage-discharge relation, is identified for a given cross-section by interpolating measured discharges and concurrent observations of water depths. Since rating curves are normally used to convert river stage observations into discharge values, uncertainty on these curves results in errors in streamflow hydrographs. The curve is generally calibrated over a series of water level measured at a certain time and the concurrent river discharge, which is often estimated trough the velocity-area method (Fenton and Keller, 2001; Herschy, 1999). Even though discharge values are not direct measurements, but rather estimates of the real and unknown discharge values, they are seldom associated with a statement of their uncertainty in practical applications (Herschy, 2002). A recent study proposed by Domeneghetti et al. (2012) considers the overall uncertainty affecting river flow measurements and proposes a framework for analyzing the uncertainty of rating-curves and its effects on the calibration of numerical hydraulic models. Results of this study highlight the significant role of extrapolation errors and how rating-curve uncertainty may be responsible for estimating unrealistic roughness coefficients.
Figure 6.11 shows the cross section and the rating curve for few stream gauges considered in this analysis, in the caption is also reported the latest and the highest measurements performed by SIR-CFR where available.

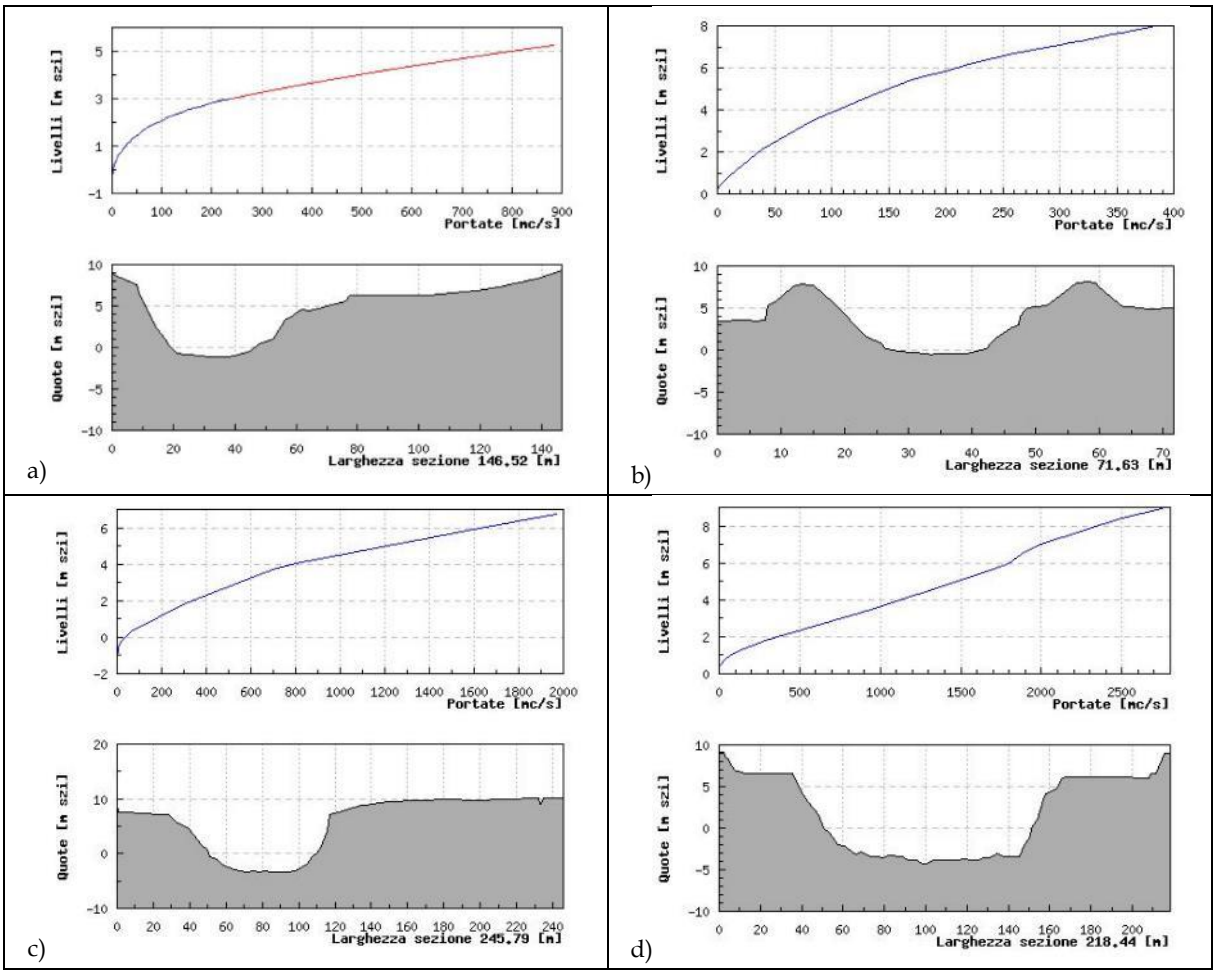


**Figure 6.11: Cross section and rating curve (blue line values in the range of measurement, red line extrapolation) a) Fornacina, latest measurement: 20.05.2016, b) Poggio a Caiano, latest measurement: 16.10.2015, highest measurement: 09.12.2006 (y=5.4 m szi, Q=168 m³/s) c) Nave di Rosano, latest measurement: 20.05.2016 (y=0.3 m szi, Q=63.8 m³/s), highest measurement: 07.12.2010 (y=1.42 m szi, Q=232 m³/s) d) S. Giovanni alla Vena, latest measurement: 02.10.2012 (y=0.75 m szi, Q=40.54 m³/s), highest measurement: 22.11.2000 (y=3.56 m szi, Q=929 m³/s) (Source: www.sir.toscana.it)**

The development of an accurate stage-discharge relation requires numerous discharge measurements at all ranges of stage and streamflow. These relations must be continually checked against on-going discharge measurements because stream channels are constantly changing, just think about the continuous morphological evolution in stream channels. New discharge measurements plotted on an existing stage-discharge relation graph would show this, and the rating could be adjusted to allow the correct discharge to be estimated for the measured stage. Frequently, the estimation of high values of discharge is obtained through the extrapolation of the higher water levels values beyond the range of the rating curve measurements. In this case, prediction errors can be very high and this should be taken into account. It is crucial to consider, for a correct assessment of the measure, that the uncertainty of the estimation of discharge is gradually increasing with the increase of water level (Claps et al., 2003). The high uncertainty in the estimation of the flood values does not seem to be erasable, while the problem of the stability of the rating curve can be studied in a simpler way: in fact, only focusing on flood events, the rating curve can be considered as not very variable for high values of discharge. It is fair to assume

that the rating curve for high flows would remain almost constant over time, and so it is possible to determine a scale of flow rates with limited validity to flood events. Moreover, the error due to rating curve approximation is smaller than the discharge values range recorded during flood events. Besides, research activity is ongoing for assessing data uncertainty related to the rating curve determination and extrapolation.

### 6.3.3 Rainfall design

The hydrometeorological data for the computation of design hydrographs must be given in the form of parameters of the rainfall Intensity-Duration Frequency (IDF) curve at one or more stations and for one or more design recurrence intervals.
In the same collaboration project of Department of Civil and Environmental Engineering and Tuscany Region for research activity on flood risk mitigation, a Regional frequency analysis of extreme rainfall was carried out (Caporali et al., 2014). The regional frequency analysis is the most robust and more used method in the scientific and technical field to estimating extreme events, such as the annual maximum of rainfall height $h_d$ of duration $d$, in ungauged basins. The choice of this approach allows using the pluviometric information available for different rain gauges in the study area, thus reducing the uncertainties associated with the lack of homogeneity of the historical series observed in the different measurement sites. In the regional analysis, data recorded in different sites belonging to the same hydrologically homogeneous region are considered as a unique sample (Caporali et al., 2008).
Among the different methods of regional frequency analysis, the index variable method introduced by (Dalrymple, 1960) is the most widely used. It requires a two-step procedure. The first step is the division of the study area into regions or zones which have the same probability distribution. Initially, the regions were mainly based on existing geographical or administrative boundaries. Later, tests for regional homogeneity were introduced (Wiltshire, 1986) and the importance of identifying homogeneous regions was demonstrated (Hosking et al., 2009). The second step provides a scale factor represented by the index variable. The criteria of homogeneity can be defined considering both hydrological condition and statistical parameters. The extreme value of the hydrological variable, with an assigned return period $T_r$ and relative to the selected site is expressed, in fact, as the product of two terms: the scale factor of the examined site (the index variable) and the dimensionless growth factor, which has regional validity. The methodology deal with the delineation of homogeneous regions, the identification of a robust regional frequency distribution and the assessment of the scale factor or the index rainfall.

### 6.3.3.1 Study area and dataset

The investigated area includes the main river basins of Tuscany region, the Arno river itself, but also Serchio and Ombrone Grossetano rivers, the small river basins of the Tuscany coast, the Magra river basin, and some subbasins of Tevere and Fiora rivers (Figure 6.12). The dataset includes the annual maxima of daily rainfall, the annual rainfall maxima for different durations 1, 3, 6, 12 and 24 hours and 15, 20, 30 and 45 minutes, recorded and validated by Regional Hydrologic Service of Tuscany in the period 1916-2012. Stations are selected on the basis of the completeness of records and they are chosen only when at least 30 years of records are available, and finally the time series are validated.

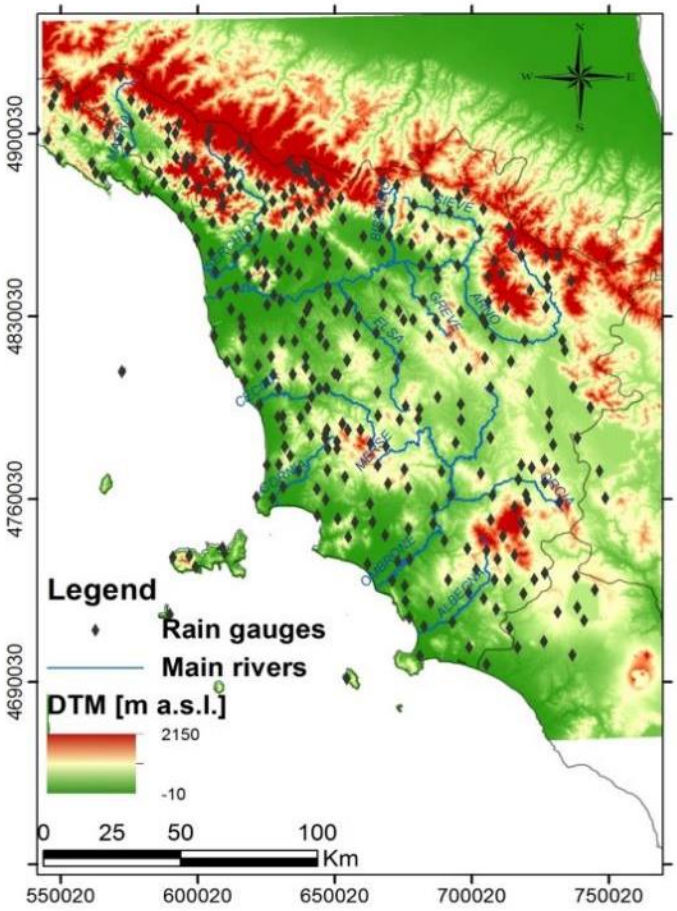


**Figure 6.12: Rain gauges stations, with more than 30 years of daily precipitation data, on the DTM (Digital Terrain Model) of the investigated area with a resolution of 70 meters.**

Table 6.3 shows the length of the time series, the number of the rain gauges and the number of data available both for daily and hourly rainfall. The dataset of daily rainfall covers the period 1916-2012, while the one related to hourly rainfall covers the period 1928-2012. Statistics about the number of precipitation data are obtained by combining the time series of traditional analogue stations with the automatic ones, placed in the same position, thus ensuring the continuity of the series.

**Table 6.3: Consistency of dataset of annual maxima of daily and hourly rainfall.**

| Years | Annual maxima of daily rainfall | | | Annual maxima of hourly rainfall | | |
|---|---|---|---|---|---|---|
| | Number of Gauges | Number of Data | on average | Number of Gauges | Number of Data | on average |
| N ≥ 10 | 622 | 24026 | 38,63 | 404 | 12327 | 30,51 |
| N ≥ 15 | 509 | 22688 | 44,57 | 317 | 11294 | 35,63 |
| N ≥ 20 | 427 | 21327 | 49,95 | 225 | 9743 | 43,30 |
| N ≥ 25 | 379 | 20287 | 53,53 | 174 | 8634 | 49,62 |
| **N ≥ 30** | **351** | **19528** | **55,64** | **152** | **8040** | **52,89** |
| N ≥ 35 | 315 | 18371 | 58,32 | 137 | 7558 | 55,17 |
| N ≥ 40 | 279 | 17040 | 61,08 | 117 | 6818 | 58,27 |
| N ≥ 45 | 241 | 15444 | 64,08 | 100 | 6117 | 61,17 |
| N ≥ 50 | 214 | 14183 | 66,28 | 85 | 5412 | 63,67 |
| ***Total*** | ***795*** | ***24902*** | ***31,32*** | ***540*** | ***12880*** | ***23,85*** |

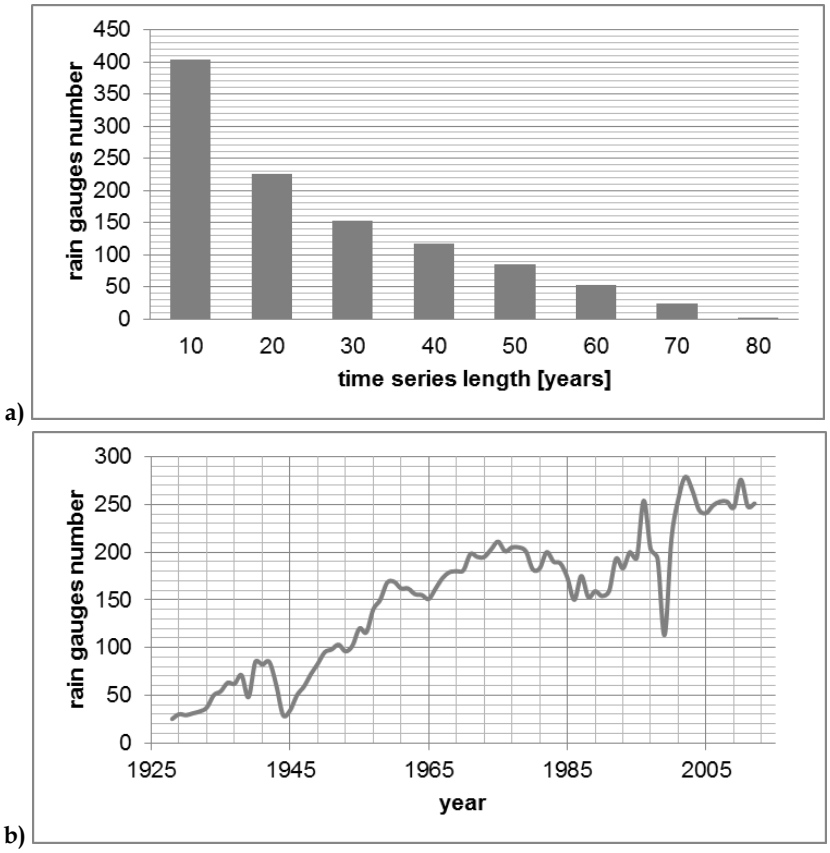


**Figure 6.13: Annual maximum of hourly rainfall in the study area. a) Distribution of the stations based on the length of the available series. b) Evolution of the monitoring network in the years between 1928 and 2012.**

The study area has an extension of about 23.000 km$^2$: in the case of daily values, the area is covered by 795 stations, with an average density of one station every 30 km$^2$. In the case of hourly data, the stations are 540, with an average density of one station every 43 km$^2$.

The dataset of precipitation extremes was created starting from the data stored in a database used for previously studies by the research group of Hydrology of the Department of Civil and Environmental Engineering of the University of Florence until 2000. The dataset was integrated with the data given by the Regional Hydrologic Service of Tuscany (SIR) for the period 2001-2012.

During the data validation procedure, some singularities in the year 1938 were found. The entire series of the daily maximum values of that year has been reconstructed for all the stations, consulting and transcribing the official data published in the Hydrologic Annals of year 1938. Moreover, some values recorded at the end of 1990s have been deemed non plausible and then deleted because extracted from series characterized by an excessive number of missing data.
The available maximum annual rainfall series have been obtained after a phase of selection, processing and validation of data. First, the conformity among data from different sources has been verified. Where significant differences have been detected, a new quality control has been carried out, according to two methods:

- Cross-check of the official data published in the Hydrological Annals until 1996 with those published on the SIR website;
- Research of errors through a comparison with the maximum rainfall data recorded on the same day in neighboring sites.

#### 6.3.3.2 Methodology: definition of homogeneous regions

Several studies show that the traditional two parameters probability distributions are not able to fit correctly the observations characterized by more intense and rare events, i.e. they are not able to adequately model the upper tail of extreme rainfall events (Rossi et al., 1984). Distributions with more than two parameters can better represent extreme hydrological events, but a larger amount of data is necessary. For this reason, the frequency analysis in hydrology is often carried out on a regional basis (see Section 2.1) that allows using a higher number of time series, recorded at different gauge sites, belonging to the same homogenous zone.
The investigation described here uses the probability distribution TCEV - Two Component Extreme Value (Rossi et al., 1984) to describe the annual maximum of rainfall height $h_d$ of duration d. The TCEV probability distribution is a distribution of four parameters. The parameters estimation is based on a three levels hierarchical approach (Fiorentino et al., 1987).
For each regionalization level, the assumed hypothesis, i.e. the ability to reproduce the statistical characteristics of the observed time series in the region, is verified. The statistical behaviour of the regional model is tested by comparing the theoretical regional distribution with the observed regional distribution of the considered statistics (skewness G, coefficient of variation Cv). An alternative system to describe the form of probability distributions is the use of the L-moments, introduced by (Hosking and Wallis, 1997).
The various hypothesis of subdivision analyzed are based on the analysis of the four maps shown in Figure 6.14.

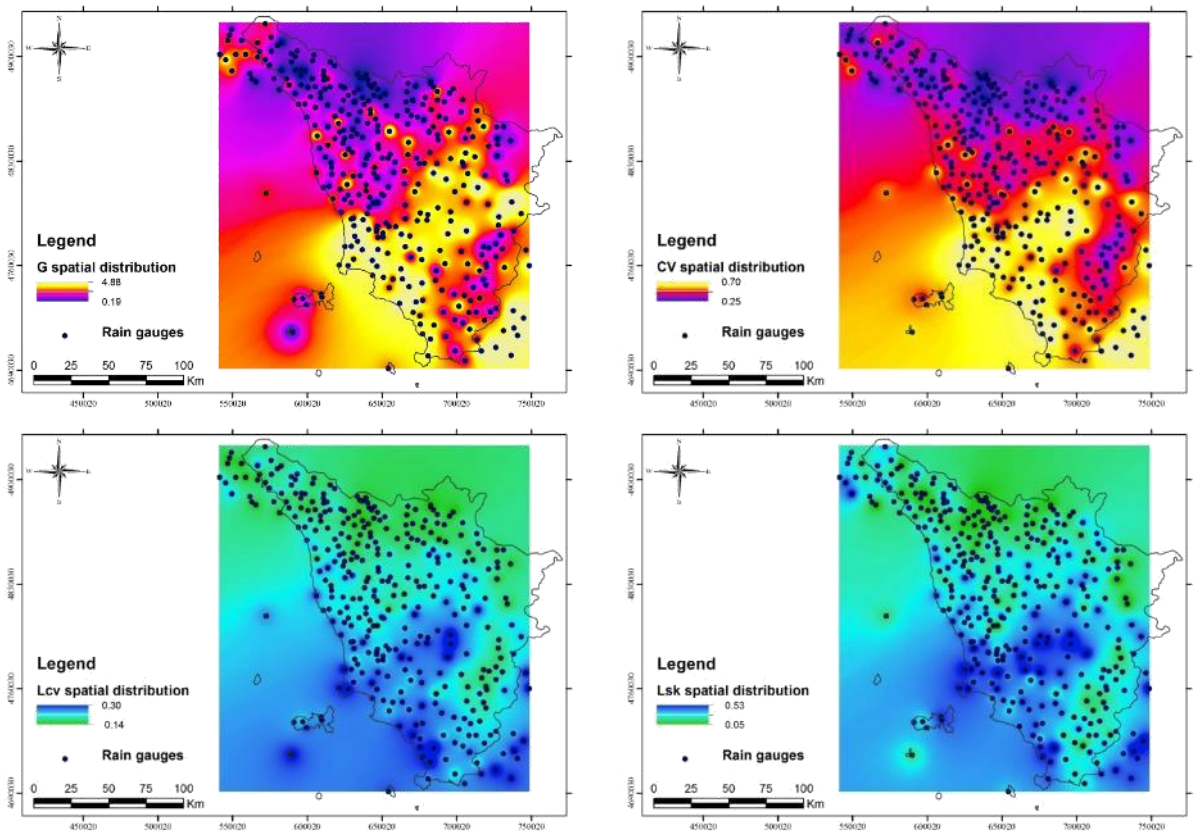


**Figure 6.14 - Spatial distribution of sample coefficients of Skewness G and Variation Cv and estimated with L-moments: Lsk e Lcv (Hosking e Wallis, 1997).**

The analysis of the spatial distribution of the sample asymmetry coefficients G and Lsk, suggests hypothesizing a subdivision of the study area into more regions, already for the first level of the estimation procedure. In fact, their spatial variability is relatively small on the side of the Apennines, while there is a more pronounced variability on the Tyrrhenian side.

For all the hypothesis of subdivision, the TCEV distribution parameters, at the 1° and 2° level, have been estimated according of a jointed procedure, based on the Maximum Likelihood (ML) method (Gabriele and Iiritano, 1994).

In order to verify the accuracy of homogeneity hypothesis of the territorial subdivision, the study introduces a comparison between the observed cdf of coefficients G (Lsk) e Cv (Lcv) and the theoretical ones obtained with a Monte Carlo techniques as:

- Graphically
- Difference between $\mu(x)obs - \mu(x)th$ and $\sigma(x)obs - \sigma(x)th$
- t Student test for the mean, Wilcoxon test for the mean, the $\chi^2$ test
- Discordancy D and Heterogeneity H test (Hosking and Wallis, 1997)
- Gumbel probability plot test of the observed and the theoretical of the TCEV model growth curves.

The Tuscany region has been examined according to 4 different hypotheses of subdivision in homogeneous regions and subregions, with a gradually increasing of number of regions. The best final subdivision of the investigated area in homogeneous regions is shown in Figure 6.15.

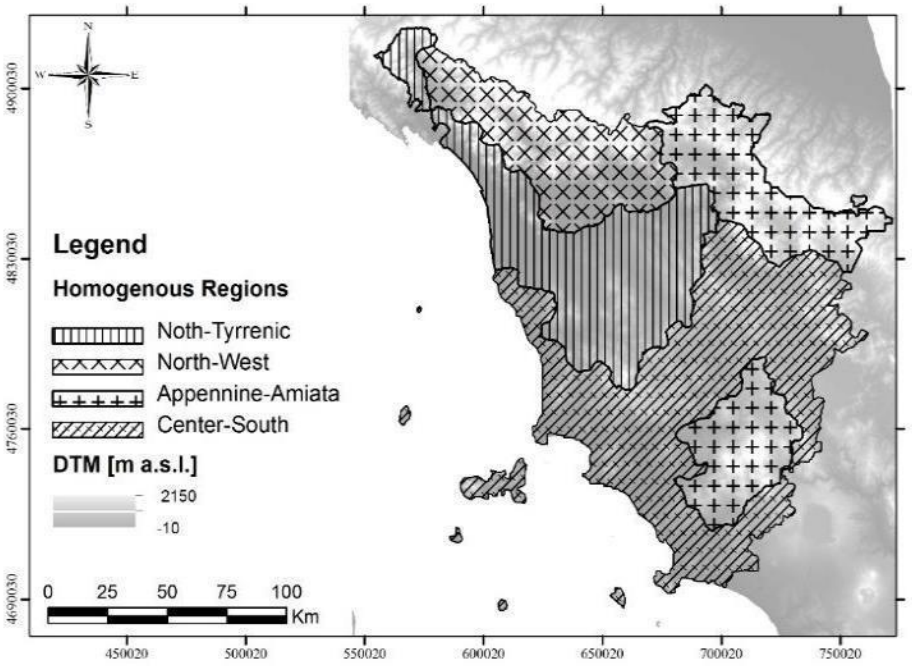


**Figure 6.15: Subdivision of the study area in four regions statistically homogeneous. In the background the Digital Terrain Model of the area is represented**

### 6.3.3.3 Methodology: growth factor assessment

In the study by (Caporali et al., 2014), the Two Component Extreme Value – TCEV distribution characterized by four parameters has been chosen.

The TCEV distribution was introduced for flood frequency analysis, in order to estimate the *T*-year flood at any river location in a given region (ungauged river basin sites) and to improve at site estimations, usually based on limited dataset (number of available time series and time series length). In the TCEV distribution two components are distinguishable (eq. 6.1): the first component, the basic one, describes the most frequent events characterized by a low magnitude; the second component describes the outliers, characterized by more intense and rare events. The cumulative distribution function of the TCEV distribution $F(x)$ is the following:

$$F_X(x) = exp\left\{-\Lambda_1 exp\left(-\frac{x}{\theta_1}\right) - \Lambda_2 exp\left(-\frac{x}{\theta_2}\right)\right\} \quad (6.1)$$

Where $\Lambda_1, \Lambda_2$ are the shape parameters and $\theta_1, \theta_2$ are the scale parameters, respectively of the basic (subscript 1) and the outlying (subscript 2) components. Since $\Lambda_i$ $(i = 1,2)$ is the mean number of events (maximum rainfall depth), which belong to each component $i$, and $\theta_i (i = 1, 2)$ represents the at-site central value of the hydrological variable, then $\Lambda_1 \gg \Lambda_2$ and $\theta_1 \ll \theta_2$.

Together with the TCEV distribution, a hierarchical three level regionalization procedure has been proposed in an Italian research project on floods, called VaPI - Valutazione delle Piene in Italia (*Floods Evaluation in Italy*) (Fiorentino et al., 1987), developed within the research activity of the "*National Group for Prevention from Hydrogeological Disasters*" (GNDCI) of the Italian National Research Council.

With reference to the TCEV model, using the dimensionless variable $X' = \frac{X}{\mu}$, where $\mu$ refers to the mean of the chosen statistical distribution, it is possible to obtain the growth curve of the dimensionless variable $X'$. The curve is characterized by the three parameters $\Lambda^*, \theta^*, \Lambda_1$.

$$F_{X'}(x') = exp\left[-\Lambda_1 \exp(-\eta x') - \Lambda^* \Lambda_1^{\frac{1}{\theta^*}} \exp(-\frac{\eta x'}{\theta^*})\right] \quad (6.2)$$

where $\theta^* = \theta_2/\theta_1$ and $\Lambda^* = \Lambda_2/\Lambda_1^{\frac{1}{\theta^*}}$. The spatial homogeneity hypothesis for the TCEV parameters $\theta^*$and $\Lambda^*$ also implies the hypothesis of statistical constancy of the theoretical coefficient of skewness (Beran et al., 1986).

For each region the daily rainfall growth curve has been defined. The direct estimation of the growth curve for a given duration has been carried out if the daily rainfall growth curve was not considered valid for the experimental cumulative distribution function of hourly rainfall maxima. The comparison between the theoretical growth curve of the TCEV model for hourly duration and the recorded rainfall of 30 minutes duration of time series longer than 30 years has demonstrated the possibility to represent the sub-hourly values with the theoretical growth curve of the TCEV model for 1 hour storm duration. The parameters of TCEV distribution and simplified expression of the growth factor $K_{Tr}$ for different durations are reported in Table 6.4.

**Table 6.4: Parameters of the TCEV distribution and simplified expression of the growth factor $K_T$ for different durations.**

| Regions | θ* | Λ* | $\Lambda_1$ | η | $K_{Tr}$ | validity |
|---|---|---|---|---|---|---|
| **North-Tyrrenian** | 1,533<br>2,634 | 0,075<br>0,438 | 10,840<br>31,195 | 3,061<br>4,937 | -0.5217+0.501·Ln Tr<br>0.2558+0.533·Ln Tr | 1 hour duration d<br>d ≥ 3 h and 1 day |
| **North-West** | 2,347<br>2,600<br>2,129 | 0,077<br>0,176<br>0,129 | 15,956<br>22,755<br>19,232 | 3,503<br>4,091<br>3,769 | -0.9315+0.670·Ln Tr<br>-0.3397+0.636·Ln Tr<br>-0.3705+0.565·Ln Tr | 1 hour duration d<br>3 h ≤ d ≤ 24 h<br>daily rainfall |
| **Appennine-Amiata** | 1,010<br>2,456 | 0,027<br>0,127 | 22,078<br>33,292 | 3,698<br>4,350 | -0.1529+0.273·Ln Tr<br>-0.3605+0.565·Ln Tr | 1 hour ≤ d ≤ 12 h<br>d = 24 h and 1 day |
| **Center-South** | 1,844<br>2,481<br>3,381 | 0,100<br>0,718<br>0,206 | 13,686<br>24,020<br>28,325 | 3,342<br>5,086<br>4,516 | -0.4901+0.552·Ln Tr<br>0.4634+0.488·Ln Tr<br>-0.4421+0.749·Ln Tr | 1 hour duration<br>3 h duration<br>d ≥ 6 h and 1 day |

Table 6.5 shows the values of the dimensionless growth factor $K_{Tr}$, for the final subdivision into 4 regions, relative to some fixed return periods and valid for the daily rainfall heights.

**Table 6.5: Values of the growth factor $K_{Tr}$ for daily rainfall data and for different return periods.**

| Tr | 2 | 5 | 10 | 20 | 30 | 50 | 100 | 150 | 200 | 500 |
|---|---|---|---|---|---|---|---|---|---|---|
| **North-Tyrrhenian** | 0,89 | 1,25 | 1,54 | 1,88 | 2,08 | 2,35 | 2,71 | 2,93 | 3,08 | 3,57 |
| **North-West** | 0,93 | 1,26 | 1,50 | 1,74 | 1,89 | 2,09 | 2,39 | 2,57 | 2,71 | 3,18 |
| **Appennine-Amiata** | 0,93 | 1,23 | 1,44 | 1,67 | 1,81 | 2,02 | 2,32 | 2,52 | 2,67 | 3,16 |
| **Center-South** | 0,89 | 1,22 | 1,51 | 1,88 | 2,14 | 2,50 | 3,01 | 3,31 | 3,53 | 4,21 |

### 6.3.3.4 Methodology: assessment of the index rainfall

The hypothesis that the estimated Generalized Extreme Value (GEV) at the gauge sites corresponds to the estimated extreme value of the regional frequency analysis, underlies the following processing.

The index rainfall at the gauge sites can be therefore assumed as the ratio of the GEV distribution estimated rainfall $X_{Tr}$ and the probabilistic growth factor (Eq.6.3) (Caporali et al., 2008):

$$\mu(X_{Tr}) = \frac{X_{Tr}}{K_{Tr}} \tag{6.3}$$

where $\mu(X_{Tr})$ is the index rainfall at the gauge site; $X_{Tr}$ the local estimation of rainfall depth at return period $T_r$ and $K_{Tr}$ is the regional probabilistic growth factor at return period $T_r$ valid for the homogeneous regions.

For all the rain gauges stations with more than 20 years of annual rainfall maxima of duration 1, 3, 6, 12 and 24 hours, the estimates of the rainfall heights, for different durations and different return periods, have been carried out using the GEV distribution: finally 219 rain gauges with 43 years of data on average have been used.

The GEV distribution is chosen because it is the most appropriate for a local analysis: it is a reliable distribution for sample series with more than ten data and it describes the trend of extreme hydrological variables at different durations through the shape factor. Moreover, it is the most widespread probabilistic distribution in the literature for the local analysis of extreme rainfall (Katz et al., 2002).

The index rainfall has been defined (third level of regionalization) for each homogenous region, for each rainfall duration $d$ through a multivariate model of climatic and geo-morphological characteristics introduced by (Caporali et al., 2008).

$$\mu = a_0 + a_1 \cdot \ln(MAP) + a_2 \cdot z + a_3 \cdot \left[ \sin\left( \frac{Asp}{2} - \frac{\pi}{2} \right) + \pi \right] \cdot \left| Asp \right| + a_4 \cdot hm \tag{6.4}$$

where $\mu$ is the index rainfall in the location; $a_i$ the parameters of the model; $MAP$ the mean annual precipitation value; $z$ the elevation; $Asp$ the terrain aspects; and $hm$ is the sample average of extreme time series at gauge sites.

The rainfall value, distributed over the whole region with a discretization of 1 km cells, has been used for the construction of the Mean Annual Precipitation (MAP). The values of the annual average rainfall have been calculated and the spatial distribution of the precipitation over the study area has been obtained using the Inverse Distance Weighted (IDW) method. The minimum value of the MAP is about

600 mm in the south area of the region while the maximum value exceeds 2600 mm in the northern Apennine area (Figure 6.16.a).
The Digital Terrain Model (DTM) shown in Figure 6.16.b has been constructed starting from the regional technical maps 1:10.000 of the Tuscany region and it is composed by cells of 10x10 meters. Also the values of the terrain aspect (Figure 6.16.c) has been detected using a GIS software starting from the DTM.

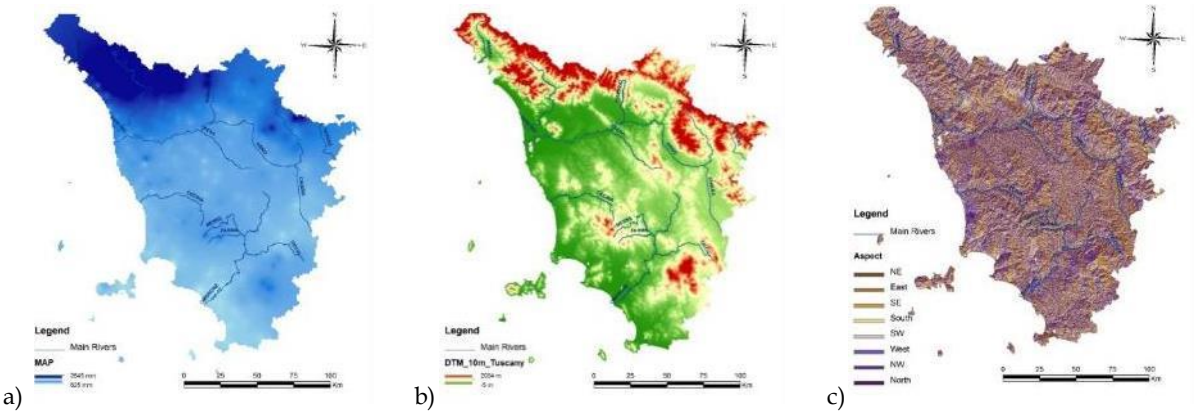


a) b) c)

**Figure 6.16: a) Mean Annual Precipitation (MAP) of the Tuscany region for the period 1916-2003; b) DTM (Digital Terrain Model) of the Tuscany region with a resolution of 10 meters; c) Terrain aspects calculated from the DTM 10x10m.**

The sample average of extreme time series *hm*, for the five storm durations analyzed (1 hour, 3, 6, 12 and 24 hours), have been calculated from the data recorded in each station with a sample mean.
For extending the values of *hm* to the whole region, an interpolation by Ordinary Kriging has been used. Kriging is a geostatistical spatial interpolation technique that allows to interpolate the value of a variable considering the values that it takes in neighboring points.
The values of the sample mean of the rainfall height time series, with assigned duration, interpolated over the whole region, are shown in Figure 6.17.

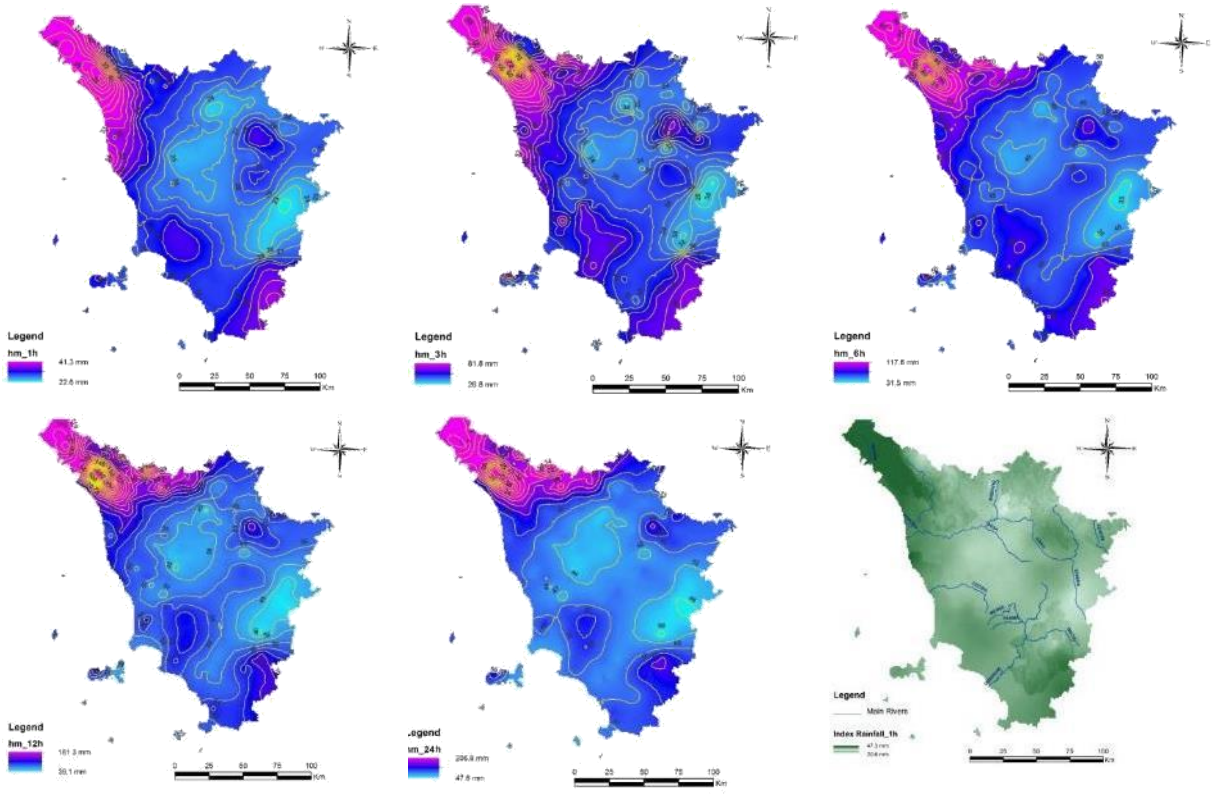


**Figure 6.17: The mean values of the time series of Annual Maximum of Rainfall Depth with storm durations: 1 hour, 3, 6, 12, 24 hours, interpolated by Ordinary Kriging. Example of 1 hour duration spatial distribution of index rainfall (low right panel).**

Finally, for each of the 4 regions it is possible to estimate the hydrological extreme value with assigned return period through:

$$x(F) = \mu \cdot x'(F) = \mu \cdot x'(F = 1 - \frac{1}{T_r}) \quad (6.5)$$

$$h = \mu_d \cdot K_{Tr} \quad (6.6)$$

where $h$ are the rainfall with duration $d$ of 1 hour, 3, 6, 12, 24 hours, and return period $T_r$ assumed equal to 2, 5, 10, 20, 30, 50, 100, 150, 200, 500 years, $\mu_d$ is the index rainfall for rainfall durations $d$ and $K_{Tr}$ is the dimensionless growth factor for different durations $d$ and assigned return periods $T_r$.

### 6.3.3.5 Rainfall Intensity-Duration Frequency curve

The quantitative prevision of extreme rainfall at specific points is carried out by determining the rainfall Intensity-Duration Frequency (IDF) curve, i.e. the relation between the rainfall depth and its duration, for an assigned return period.

It is worth notice that the term "rainfall height", usually measured in mm, refers to the height of water that would be formed on the soil if the surface is horizontal and waterproof, during a certain time interval (duration of precipitation) and in absence of losses.

Therefore, from the rainfall height it is possible, through a logarithmic regression, to estimate the parameters $a$ and $n$ of the rainfall IDF curve according the relation:

$$h(t) = a \cdot t^n \tag{6.7}$$

$h$ is the rainfall height [mm], $t$ is the duration of precipitation [h]; $a$ and $n$ are the characteristics parameters of the curve and their values are function of the return period. In this study the standard expression of the IDF curve is used, so the $a, n$ parameters refer to the characteristic return periods (2, 5, 10, 20, 30, 50, 100, 150, 200, 500 years).

Knowing the values of the index rainfall for the different return periods over the whole Tuscany and the dimensionless growth factor $K_{Tr}$ for each of the four regions, the corresponding rainfall heights are detected in order to define the $a, n$ parameters. Finally, considering the five durations (1 hour, 3, 6, 12 and 24 hours) and the ten return periods (2, 5, 10, 20, 30, 50, 100, 150, 200, 500 years), 50 ASCII Grid file are obtained.

As a result of this work, the $a, n$ parameters for the whole Tuscany region are available in the format 1 km ASCII grid.

The Figure 6.18, as an example, shows the spatial distribution of the $a, n$ parameters for the return period of 50 years.

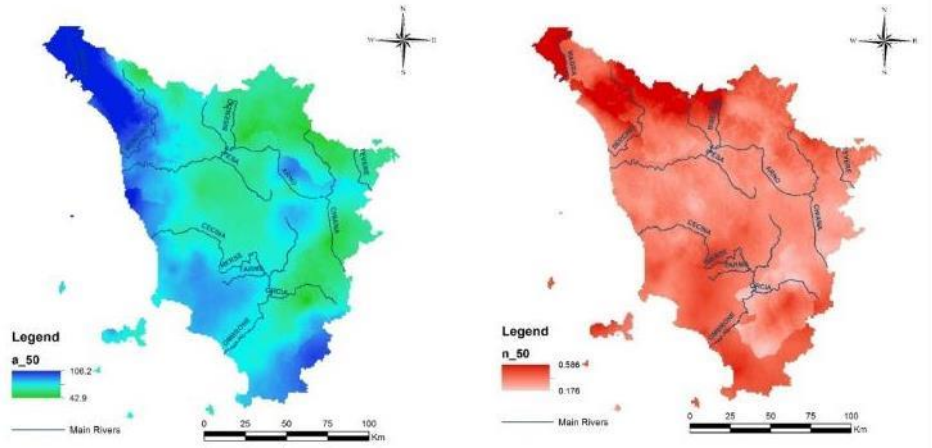


**Figure 6.18: Example of spatial distribution, 1 km grid, of parameters a and n for the return period of 50 years, of the Rainfall Intensity-Duration Frequency (IDF).**

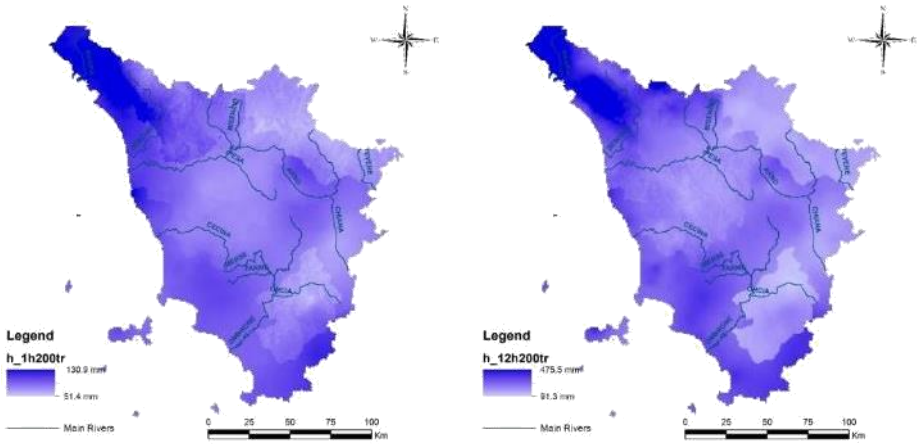


**Figure 6.19: Examples of maps of spatial distribution of the design rainfall height; (left) 1 hour (right) 12 hours duration, for 200-years return period.**

The outputs of this work are ASCII grid 1x1 km for the whole Tuscany region, while MOBIDIC model requires for design hydrograph application an ASCII table of parameters of the rainfall IDF curve for the Arno case study. The table is derivable from raster by using specific ArcGIS procedures. In Conversion toolbox, by means of *Raster to point* tool a raster dataset is converted to point features and in Data Management toolbox we can *add XY coordinates* to the new shapefile of virtual pluviometric stations (blue point in Figure 6.20). The execution of the hydrologic computation of the design hydrographs is a time consuming procedure, therefore only the rain gauges within the Arno river basin are selected and by means of *Point to raster* tool the point features are converted to a raster dataset with cell size 5 km assigning to the new cell the mean of the attributes of all the points within the cell (Cell assignment type Mean) (red square in Figure 6.20).

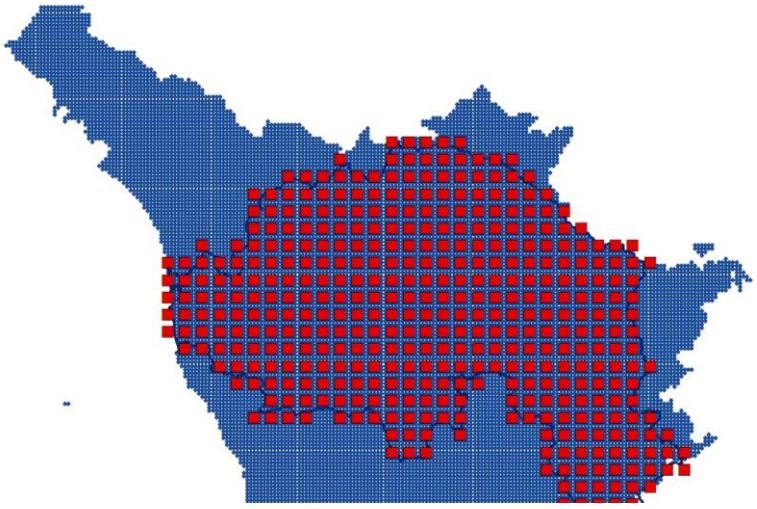

**Figure 6.20: ArcGIS procedure to get the ASCII table of the parameters *a* and *n* of the rainfall IDF curve for the Arno case study.**

### 6.4.3 The initial conditions

In a different way of the regional operational framework of MOBIDIC model where the hydrological model is run for real time forecast, then the initial conditions are updated in real time, the simulations here performed are characterized by the following initial conditions:

- Initial time of the simulation equal to zero $t_0 = 0$
- Streamflow equal to zero in the initial time ($Q = 0$ to $t_0 = 0$)
- Completely dry soil in $t_0 = 0$

Since the model starts to run considered zero initial conditions, a certain time to reach a steady-state condition is required. The total simulation time is 6 days for that reason, we take into account 3 days before the date of the flood event in order to allow to the model to reach this steady-state condition. This choice is based upon the fact that it is almost impossible to know the soil water content in the capillary and gravitational reservoirs at a generic time instant.

## 6.4 Global hydrologic parameters

Several numeric parameters used in various hydrologic conceptual schemes are global, i.e. constant in time and all over the basin, and hence they are not considered among the geographic data. In the configuration file, above the global hydrologic parameters categories are reported both required and optional parameters: $\alpha$, $\beta$, $\gamma$, $\kappa$ parameters control, respectively, the surface runoff and the hypodermic runoff, the percolation into the groundwater, the absorption by gravitational and capillary soils. These are parameters that affect the surface runoff and soil dynamics. In order to obtain good simulation results, sensitivity analysis, calibration and validation steps are required.

Some studies characterized by MOBIDIC application in the Arno river basin have been already performed (Castelli, 2014; Castelli et al., 2009; Tartaglia, 2005; Vanni, 2015). In particular, as reported in Castelli, 2014, a multi-objective sensitivity analysis and following calibration and validation stages have been performed for a pilot study considering that MOBIDIC contains twelve parameters which can be calibrated and potentially estimated (Table 6.6). The findings of this analysis reported that the parameters *wg_mult*, *wc_mult*, *Ks_mult*, *Celerfac*, *Cafac*, *CHfac* cannot be calibrated since they have been estimated on their physical basis.

**Table 6.6: MOBIDIC parameters, parameters units and parameters ranges.**

| Parameter | Meaning of the parameter | Units | Parameter range | |
|---|---|---|---|---|
| initinfo.wcsat | Initial relative saturation of capillary soil | (-) | 0.05 | 0.95 |
| initinfo.wgsat | Initial relative saturation of gravitational soil | (-) | 0.05 | 0.95 |
| wg_mult | Multiplying factor of maximum water holding capacity in soil large pores | (-) | 0.1 | 10 |
| wc_mult | Multiplying factor of maximum water holding capacity in soil small pores | (-) | 0.1 | 10 |
| Ks_mult | Multiplying factor of soil hydraulic conductivity | (-) | 0.1 | 10 |
| Celerfac | Flood wave celerity in channels | ($ms^{-1}$) | 0.1 | 10 |
| Chafac | Scale factor for fraction of channelized flow | (-) | 0.1 | 10 |
| CHfac | Multiplying factor of bulk turbulent exchange coefficient for heat | (-) | 0.1 | 10 |
| Alpha | Downhill routing coefficient | ($s^{-1}$) | 1.0e-7 | 1.0e-4 |
| Beta | Hypodermic flow coefficient | ($s^{-1}$) | 1.0e-7 | 1.0e-4 |
| Kappa | Soil adsorption coefficient | ($s^{-1}$) | 1.0e-7 | 1.0e-5 |
| Gamma | Soil percolation coefficient | ($s^{-1}$) | 1.0e-8 | 1.0e-6 |

# Chapter 7

# Parameter Identification of the MOBIDIC model

## 7.1 Motivation

The research activity focuses on the estimation of the uncertainty of the model parameters values, and its subsequent reduction. The parameter identification and the evolution of uncertainty in the model can be approached in different ways. Bayesian inference via MCS and MCMC sampling are becoming popular methods for uncertainty analysis in hydrological modelling. However, application of these methodologies requires significant computational costs therefore research is continuing for improving the efficiency of such methods. The aim of this part of dissertation is to show in principle how the model parameter identification can be done in hydrologic application. This part investigates the possibility to perform the Bayesian update describing RVs by functional approximation like PCE for improving the computational efficiency of MC sampling in the framework of hydrologic modelling. The relevant contribution of this study is related to proposing a statistically consistent simulation framework for uncertainty estimation which does not require model likelihood computation and simplification of the model structure.
To analyze the performance of this approach, various numerical experiments are implemented with different procedures: points for sampling are generated with different numerical integration rules (quasi-random points from a stream based on a leaping Halton sequence, normally distributed random points, Gauss-Hermite sparse grids) and the forward samples are computed by MC samples as well as by PCE samples. The assimilation process for the identification of three uncertain parameters of MOBIDIC model is carried out by means of the linear Bayesian method in its direct PCE and MC sampling (EnKF) form.

## 7.2 Numerical implementation to the Arno river basin

The calibration and validation steps are outside of the specific aim of this dissertation, they represent crucial procedures as long as perfect simulations of flood events want to be achieved (see for instance the flood forecasting simulations performed by Vanni, 2015). In the present study, the main goal is to show a methodology for the identification of uncertain parameters of MOBIDIC model, therefore the only information required is the preliminary estimation of the hydrologic parameters arising from expert knowledge. MOBIDIC simulations are

carried out with the aim to build the proxy model, i.e. compute the forward samples. We run 1000 times MOBIDIC with generated samples (each sample one run), see Section 7.3. MOBIDIC model does not use iterative method in order to calculate the output, so problems of convergence cannot arise. This information is useful because in case that the residual of a potentially iteration solver did not converge, such samples cannot be used for building PCE.

In the first step of the parameter identification procedure we decide which parameters are to be considered uncertain. A careful analysis is carried out in order to select the parameters to be identified more related with the runoff generation processes, at the end we decided to focus the attention on three parameters, the downhill routing coefficient $\alpha$, the hypodermic flow coefficient $\beta$ and the multiplying factor of soil hydraulic conductivity $K_{s\_mult}$. The prior information on parameters $\alpha$, $\beta$, $K_{s\_mult}$ comes from expert knowledge about their realistic values and can be modelled in a form of a prior probability density function (Table 7.1).

**Table 7.1: Distributions, means and variances used to define the prior samples.**

| Parameter | Initial estimation | Distribution | Mean | Variance |
|---|---|---|---|---|
| **β** | $2.0\text{x}10^{-5}$ [$1.0\text{x}10^{-7}$ - $1.0\text{x}10^{-4}$] | lognormal | 6 | 0.6 |
| **α** | $3.0\text{x}10^{-6}$ [$1.0\text{x}10^{-7}$ - $1.0\text{x}10^{-4}$] | lognormal | 5.5 | 0.8 |
| $\mathbf{K_{s\_mult}}$ | 1 [1 – 9] | lognormal | 2.5 | 1.3 |

Since the uncertain lumped parameters $\alpha$ and $\beta$ are always definite positive and ranges from [$1.0\text{x}10^{-7}$ - $1.0\text{x}10^{-4}$], we model these RVs according the lognormal distribution represented by

$$\mathcal{P}_i = c_1 \cdot exp(\mu + \sigma\theta_i) \tag{7.1}$$

Where

$\mathcal{P}_i$ are RVs samples, i.e. prior samples;

$\theta_i$ are the points in which is sampled, obtained by means of different numerical methods (see Section 7.3);

$\mu, \sigma$ mean and variance of the associated normal distribution;

$c_1$ the constant value $1.0\text{x}10^{-7}$.

In this way, the parameters are more or less in the bounds, obviously the upper bound is not limited but for the aim of this procedure it is fine.

It is called normal or Gaussian distributed a random variable distributed according to the probability density function

$$p(x) = \frac{1}{\sqrt{2\pi\sigma^2}} e^{-\frac{(x-\mu)^2}{2\sigma^2}} \tag{7.2}$$

The normal and lognormal distributions are closely related, a RV $X$ is lognormally distributed with parameters $\mu$ and $\sigma$ if the logarithm of $X$ is normally distributed with

mean $\mu$ and standard deviation $\sigma$. Thus, if the random variable $X$ is log-normally distributed, then $Y= ln(X)$ has a normal distribution. Likewise, if $Y$ has a normal distribution, then $X= exp(Y)$ has a lognormal distribution.
The lognormal probability density function is

$$p(x) = \frac{1}{x\sigma\sqrt{2\pi}} e^{-\frac{(\ln(x-\mu))^2}{2\sigma^2}} \quad (7.3)$$

The prior distribution is chosen as lognormal for $K_{s\_mult}$ parameter.
The choice to model only the multiplying factor of the soil hydraulic conductivity $K_s$ was achieved after a preliminary analysis on the possibility to model $K_s$ as a random field for a specific subset of soil type (Clay) and land cover (Urban area) layers in the Arno river basin. The idea was based on the assumption that the background data for this would be easy to obtain, unfortunately at river basin scale it represents a procedure very time demanding.
Focusing on the surface infiltration process, the physical properties of the soil are definitely a source of uncertainty as well as the intensity of rainfall. The hydraulic properties of the soil show a high variability even at very small spatial scales, for extensive areas this variability might not affect the simulations results considering the greater variability in the rainfall forcing both in time and in space. However, from the application point of view, i.e. when the infiltration process has to be represented inside a more general hydrologic distributed model, the presence of heterogeneity in the soil may be taken into account dealing with the multiplying factor of the hydraulic conductivity $K_{s\_mult}$ instead of directly the distributed parameter $K_s$.
$K_s$ depends on the soil texture and the soil moisture conditions. Study in details $K_s$, considering the soil texture on which depends the infiltration capacity, means work at a given domain which is smaller than the one used in hydrological model. In practice, we usually work at basin scale: the uncertainty and spatial variability of hydraulic soil properties as well as precipitation intensity it is so huge that maybe the uncertainty of the distributed parameter $K_s$ can be assumed to not influence significantly the runoff generation processes. For the sake of simplicity, in this dissertation we could consider only uncertainty the "lumped" hydraulic parameters. More precisely, the uncertainty due to the spatial variability of $K_s$ is not accounted for, because only limited information on the spatial variation of this parameter is available.
The assessment of hydraulic conductivity distributions through data assimilation procedure is very time-consuming and hardly applied to large simulation models in literature. (Pasetto et al., 2012) considered a catchment test case with a surface area of 1.62 km$^2$, DEM resolution 20x20 m, number of cells in the surface grid 50x81 – 4050, characterized by a homogeneous and isotropic saturated hydraulic conductivity field. (Crestani et al., 2015) considered the vertical distributions of Ks, using the data for the assimilation procedure provided by monitoring tracer tests with electrical

resistivity tomography (ERT). Their model domain has dimensions 16m×8m×8m, and is discretized along each direction into cells of side 0.25m. (Zarlenga et al., 2012) worked on anisotropic formations, never at basin scale. On the other hand, since it has hardly been done in the literature up to now, modelling the hydraulic conductivity $K_s$ as a random field could represent an original improvement for the hydrological modelling.

## 7.3 The numerical examples for parameter identification

The group of methods proposed in Chapter 5 is tested on few numerical examples in hydrological applications. Particularly, we present the methodology for Linear Bayesian update approach to inverse problem applying different methods, working in sampling and functional approximation. We propose for the assimilation process numerical implementations via Monte Carlo methods, i.e. the EnKF procedure, and PCE update without any sampling. Three MOBIDIC model parameters are described in a Bayesian way through a probabilistic model, they are considered as Random Variables (RVs). First, we present few concepts of pseudo-random number generators and the assessment of prior samples according to a given distribution. In order to represent the RVs, the Monte Carlo sampling techniques may be used. Then, the procedure to do prediction, i.e. to compute the forward samples since values for the parameters and the prior distribution are assumed. The numerical evaluation of the Linear Bayesian Update is the final step: since the measurements, both real and virtual, the predictions, the prior are known, the posterior is computed by the Kalman gain (EnKF function) and direct PCE updating.
Different numerical integration rules to build points and corresponding weights for sampling are surveyed:

- leaping Halton sequence (*qrand* Matlab function)
- normally distributed pseudo-random numbers (*randn* Matlab function)
- sparse grids (LIBpoints function in LIBERTY library - LInear BayEsian Random variable updaTing analysis Copyright (C) 2015 Bojana Rosic)

We remind that direct integration to compute the conditional expectation of the predictions $Q_f$ is performed with MC sampling or sparse grid according the equation

$$\mathbb{E}(Q_f) = \int_{\Omega} Q_f \mathbb{P}(d\omega) = \sum_{i=1}^{N} Q_f(\omega_i) \cdot W_i \tag{7.4}$$

Where usually $N \sim 10^6$.
Given the extreme importance of this step, an accurate analysis of the quality of the generators is carried out. In particular, we decided to build prior samples with the help of numerical integration by Smolyak sparse grids, type of Gaussian quadrature for integral with Gaussian weight (Gauss-Hermite). At the end of the comparison between the three numerical integration rules in terms of basic statistics on prior

distribution (Table 7.2), we decided to carry out MOBIDIC simulations to compute the proxy model with samples generated by means of normally distributed pseudo-random points and by means of leaping Halton sequence (each sample one run for a total of 1000 runs for procedure).

**Table 7.2: Basic statistics on prior distribution obtained by means of different numerical integration rules.**

| Parameter | Integration rules | μ | σ | Range | Pdf Max |
|---|---|---|---|---|---|
| β | randn | 5.56E-05 | 3.58E-09 | 3.91E-06 - 6.41E-04 | 2.32E-05 |
| | randn_PCE | 5.44E-05 | 2.44E-09 | 3.84E-06 -5.44E-04 | 2.10E-05 |
| | Halton sequence | 5.44E-05 | 2.34E-09 | 3.28E-06 - 4.62E-04 | 2.60E-05 |
| | Sparse grid | 3.12E-05 | 2.63E-10 | 7.12E-06 - 1.06E-04 | 2.42E-05 |
| α | randn | 3.77E-05 | 1.67E-09 | 1.42E-06 - 5.16E-04 | 1.27E-05 |
| | randn_PCE | 3.65E-05 | 1.60E-09 | 1.25E-06 - 4.94E-04 | 1.72E-05 |
| | Halton sequence | 3.64E-05 | 1.61E-09 | 1.35E-06 - 5.51E-04 | 1.49E-05 |
| | Sparse grid | 4.65E-06 | 1.07E-11 | 6.17E-07 - 2.25E-05 | 2.35E-06 |
| $K_{s\ mult}$ | randn | 2.52 | 1.36 | 0.52 - 10.80 | 2.12 |
| | randn_PCE | 2.50 | 1.30 | 0.44 - 10.65 | 2.12 |
| | Halton sequence | 2.50 | 1.30 | 0.58 - 9.37 | 1.90 |
| | Sparse grid | 3.00 | 0.90 | 0.89 - 9.10 | 2.57 |

It is worth to point out that select properly the prior probability density it is a difficult task because the whole range of parameters values should be considered, that means select a prior distribution with appropriate mean and variance, otherwise a reasonable representation of the posterior distribution will not be achieved. As already mentioned, the parameters to be identified are described as RVs, the randomness reflecting the uncertainty about the true values. The prior distributions are lognormal, but the code run differently in case the distribution is set lognormal or normal. Indeed, in case the simulations are run setting the prior distribution as lognormal, the prior is first transformed to normal and then the update is performed in normal space. After the update, the posterior is mapped by exponential back into parameter space. This means that the log transformation is applied to data, we work in normal space and then we return into parameter space by exponential transformation. Otherwise, in case the simulations are run setting the prior distribution as normal, this will not be done, prior distributions are still lognormal only it will not get transformed. So all computation are done with lognormal variables.

Figure 7.1 shows $\alpha$, $\beta$, $K_{s\_mult}$ pdfs, the probability density estimates for the prior with 1000 ensemble size sampling obtained by leaping Halton sequence as well as by randn points, the latter is selected as final prior to be used for Linear Bayesian update procedure. The prior is more or less lognormal, we expect that at the end of the assimilation period the update approach selected will moving the mean and reducing the variance and the posterior will be more or less Gaussian.

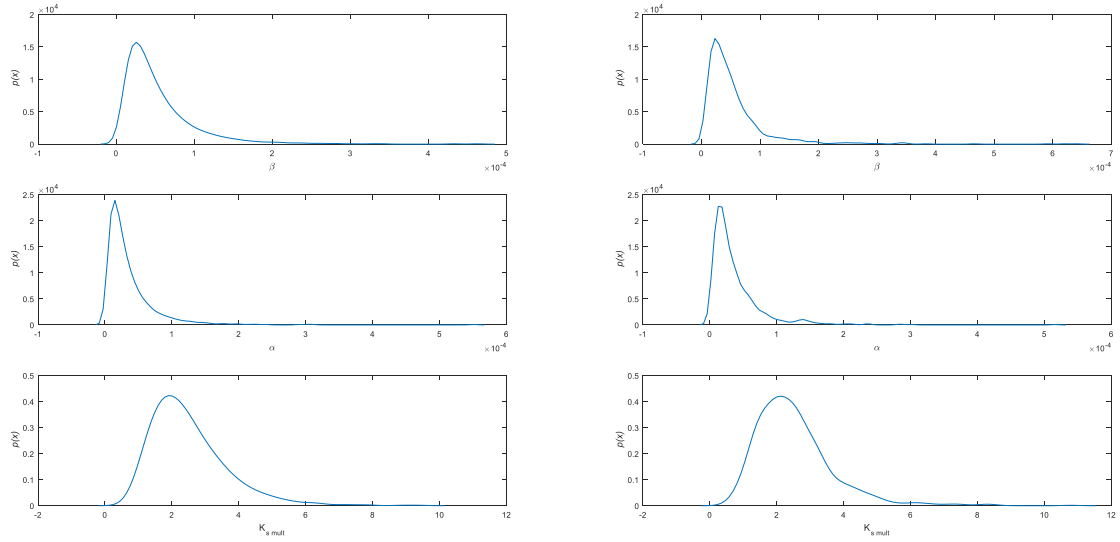

**Figure 7.1: Probability density estimates of β, α, $K_{s\_mult}$ (prior distribution) (left panel) MC sampling with leaping Halton sequence (right panel) MC sampling with randn points (selected as final prior).**

In the assimilation process via EnKF procedure only normally distributed pseudo-random points and prior sampled with this points are taken into account.
The first analyzed method is the EnKF procedure with forward samples computed by means of Monte Carlo sampling, we called this method MC_EnKF.
In addition, we propose the use of the proxy modelling in the assimilation process in order to reduce the required computational time. Indeed, to speed up the assimilation process one may introduce a proxy model for the forecasted (predicted) measurement (indicated here as $Q_f$ to remind that the predictions are discharge values). Usually, the proxy model is made with the help of a functional approximation of random variables entering the process. To this end, the predicted measurement $Q_f$may be represented in a PCE form as

$$Q_f(\omega) = \sum_{\mathcal{F}} Q_f^{(\alpha)} H_\alpha(\omega) \tag{7.5}$$

where $H_\alpha(\omega)$ represents the generalized orthogonal polynomials and $\mathcal{F}$ stands for the set of all finite non-negative integer sequences, i.e. multi-indices $\alpha$. Due to computational reasons, only a finite subset of $\mathcal{F}$ is taken, in other words the expansion in eq. (7.5) is truncated to a finite number of terms. Therefore, the forward model is substituted with a less accurate but computationally cheaper proxy model, in this manner the forward model is not individually solved for each MC sample, but a priori, increasing the efficiency of the update process.
In order to get new forward samples by PCE, different than those obtained by MCS, PCE have been computed. In this step, we work with multidimensional matrices like 768*10*25*286 dimension because for each time step (768) and each sensor (25) we compute for several orders (maximum order 10) the PCE coefficients (286). PCE coefficients are obtained using the points and samples of prior by the new numerical regression algorithm implemented by B. Rosić to compute PCE for this case study

where only such small number of samples is used. PCE for the 25 study stream gauges have been computed at certain time moment because in order to show the Bayesian updating procedure we can assume to update at any time moment, at the end of the first event (time index 768 corresponding to 01.12.2012 23:45:00), before the peak discharge, etc.
The realizations, i.e. the new forward samples, are computed by means of the tensor PCE coefficients, calculated for the best PCE order after an analysis of the error of the proxy model, and evaluating PCE in specified points taking the basis of PCE.
In that way, we got new forward samples, we called it PCE forward samples, and do the linear update using EnKF algorithm with this forward (PCE_EnKF method) for a comparison with the results of MC_EnKF approach. The other method taken into account is the PCE update without any sampling, by means it is possible to perform the Bayesian update of PCE of the a priori information to an a posteriori one without any sampling but in a direct, purely algebraic way by introducing the Hermite algebra as a sequel of ideas presented in (Rosić et al., 2012). PCE based methods is the focus of this part. We expect similar results to the EnKF procedure, the aim is to show that same results or even more accurate results can be achieved with this new PCE update procedure in order to decide which method is best applicable in practice. The theoretical framework is illustrated by presenting real-world case and synthetic case.
In order to obtain synthetic measurement, a sample of the forward is selected. Perturbation of this synthetic one is modeled for representing the modelling error adding a vector of RVs drawn from a normal distribution with a mean of 0 and a standard deviation of 1%. Moreover, we modeled the measurement error adding the noise by set the variance of the synthetic measurement equal to 2%. In the numerical implementation of the synthetic case the so called truth is an "artificial truth" represented by the parameter values by means we obtained synthetic measurement. In this way, the true value of the unknown parameters that are selected to be uncertain, are taken to be one realisation of the RVs described independently from the a priori distribution. Obviously, in real case the truth is unknown, we can only assume for the downhill routing coefficient $\alpha$, the hypodermic flow coefficient $\beta$, the multiplying factor of soil hydraulic conductivity $K_{s\_mult}$ representative values from expert knowledge and perform a validation procedure comparing measurements.

## 7.4 Analysis and comparison of the numerical results

In this section the comparison of numerical approaches to Bayesian updating is reported. First the results for synthetic case are shown, then some recommendations for the methodology application in real case, where measurements are represented by discharge time series recorded during the flood event occurs the 28.11.2012 in the Arno river basin, are reported.

For the purpose to update the three parameters $\alpha$, $\beta$, $K_{s\_mult}$, the simulations are run setting the prior distribution as lognormal, i.e. the prior is first transformed to normal and then the update is performed in normal space, and normal (Case log and n respectively) and the time step is both skipped and not skipped (Case 100 means skip=100 and 1 means skip=1 respectively). In summary, in Table 7.3 and Table 7.4 is shown the comparison of mean, maximum and variance for the posteriors $\alpha$, $\beta$, $K_{s\_mult}$ obtained by different update approaches, indicating the methods as

- MC_EnKF: EnKF with MC forward samples;
- PCE_EnKF: EnKF with PCE forward samples;
- PCE: direct PCE method;

and the case study as

- Clog1=prior distribution lognormal, skip=1;
- Cn1=prior distribution normal, skip=1;
- Clog100=prior distribution lognormal, skip=100;
- Cn100=prior distribution normal, skip=100;

Procedure with skip=1 is more time consuming, after all the result are more accurate, although sometimes is better to use all the data and sometimes to skip someone, especially in the real case. In real case, EnKF update using all the data it is worse than using only 192 measurements, for $\beta$ parameter we get truly bad posterior, only if less data are used EnKF is able to update $\beta$ parameter, maybe it is nonlinear process and EnKF uses only few samples in order to reduce variance. On the other hand, $K_{s\_mult}$ parameter is wrongly update in case if data are skipped and a normal distribution for prior is assumed. It is worth to point out the result of the update of $K_{s\_mult}$ parameter in real case: the posterior values, although the prior was modelled with a mean value equal to 2.5, are still in the range of the prior but in the tail of it. In particular, as we show in Chapter 8, the value of 8.32 and 8.46 (MC_EnKF and PCE_EnKF method respectively) is very similar to the one assumed for the design flood hydrograph application base on the calibration value found in Vanni, (2015). Maybe the prior for $K_{s\_mult}$ parameter has been "wrongly" assumed, it could be very interesting investigate more in details with further simulations this finding.
As we figured out the results are truly comparable, especially the findings of EnKF procedure with MC sampling and PCE sampling. The comparison is shown even more in Figure 7.2 and following where the probability density estimates of the prior and the posterior for the first EnKF and PCE update are represented. Particularly, in Figure 7.8 a), Figure 7.10 a), Figure 7.12 a) the results for the three update procedures in case of prior distribution lognormal and the time step skipped (case Clog100) are represented for real case. PCE updating give similar results to the other two if the model is linear for the update of parameter alpha, PCE is only better because does not drastically reduce the posterior variance. PCE approach performs better than

EnKF procedure for the update of $\beta$ parameter: in fact, a maximum value of posterior around $2x10^{-5}$ is obtained, very close to the one calibrated in previous study.
In synthetic case, it is possible to note that for all the approaches the Linear Bayesian update is able to reduce the variance as well as to move the mean towards the artificial truth. The posteriors are more or less Gaussian even if a slight skewness is presented in same case study. Considering the lognormal prior distribution, the results are slightly better for all the approaches, thus we decide to carry out simulations for direct PCE update only assuming this distribution for prior (see in Table 7.3 for PCE method the lack of values for Cn case studies). A clear improvement is achieved in posterior assessment for procedure carried out with all 19200 measurements (skip=1), the updated result is more accurate. We remind that in synthetic case the "truth" is plotted as parameter value by means synthetic measurements are obtained, in real case we never know the truth, one as to do validation comparing measurements.
In order to validate results, the maximum values of posterior are picked out and MOBIDIC model is run one time with these values, then the simulation output is compared to samples chosen as synthetic measurements (for synthetic case see the assessment of general errors reported in Table 7.5) and to real discharge measurements (see the relative error represented in Figure 7.20). Validation procedure in real case is performed only for the case Clog100 because for the other case studies both EnKF and PCE procedures fail to update at least one parameter, getting posterior values out of prior values range. Other tests for real case have been performed reducing measurement error to 1% and increasing up to 10% but the results are almost the same.
The comparison of predictions, obtained by run MOBIDIC with maximum posterior values for the different update methods, for synthetic case and case skip=1, is reported by the relative error expressed in percent over time (Figure 7.16 – 7.18 (a)) and the scatter plot between observed and simulated runoff values for each stream gauge (Figure 7.16- 7.18 (b)). It is worth to point out that we call *Qobserved* synthetic measurements of discharges. Moreover, the comparison of observed and simulated discharge values plotting all the measurements and the corresponding residuals both using all the 19200 measurements (skip=1) and the 192 measurements (skip=100) is reported in Figure 7.12 – 7.15. Finally, Figure 7.19 show the validation of the results in real case by the comparison of the simulated output (blu line) to real measurement (red line). Once is obtained by the EnKF procedure with forward samples computed by means of MC sampling in case of prior distribution lognormal and time step skipped (case Clog100) and the other one is obtained by the original update procedure without any sampling but by functional approximations using PCE. In this case, an improvement of the fitting especially in the sub-basins along the Arno river main stream (code from 4379 – 5191), Bisenzio (code 4782 – 4791) and Ombrone Pistoiese (code 4875) too is achieved. The validation for PCE_EnKF approach is not performed because the maximum values of posterior are more or less equal to the

maximum values found with MC_EnKF approach. In Figure 7.20 the comparisons are reported in terms of Relative error expressed in percentage. The error is very high in peak discharge occurrence for all the studied stream gauges. It is possible to note that smaller errors are found in the Arno sub-basins, with the exception of 4411-Subbiano catchment. On the other hand, the biggest errors are found in the Era river basin (code 5115 – 5131) and in other Arno tributaries rivers. In the PCE approach a slightly improvement is detected for the watersheds along the Arno river main stream.

**Table 7.3: Comparison of mean, maximum and variance for the posteriors α, β, Ks_mult obtained by different update approaches for synthetic case.**

| Synthetic case | | | | | | | | | | | |
|---|---|---|---|---|---|---|---|---|---|---|---|
| **Parameter** | **Method** | ***Mean*** | | | | ***Maximum*** | | | | ***Var*** | |
| | Case: | Clog1 | Cn1 | Clog100 | Cn100 | Clog1 | Cn1 | Clog100 | Cn100 | Clog1 | Clog100 |
| β | MC_EnKF | 8.00E-05 | 7.93E-05 | 6.96E-05 | 6.58E-05 | 8.00E-05 | 7.89E-05 | 6.61E-05 | 6.650E-05 | 3.40E-12 | 6.86E-10 |
| | PCE_EnKF | 7.83E-05 | 8.04E-05 | 6.60E-05 | 6.73E-05 | 7.80E-05 | 8.01E-05 | 6.34E-05 | 7.15E-05 | 2.30E-12 | 5.27E-10 |
| | PCE | 7.64E-05 | - | 6.85E-05 | - | 7.64E-05 | - | 7.44E-05 | - | 7.52E-11 | 8.93E-10 |

| **Parameter** | **Method** | ***Mean*** | | | | ***Maximum*** | | | | ***Var*** | |
|---|---|---|---|---|---|---|---|---|---|---|---|
| | Case: | Clog1 | Cn1 | Clog100 | Cn100 | Clog1 | Cn1 | Clog100 | Cn100 | Clog1 | Clog100 |
| α | MC_EnKF | 3.28E-05 | 3.33E-05 | 3.13E-05 | 2.70E-05 | 3.28E-05 | 3.34E-05 | 3.03E-05 | 2.920E-05 | 4.44E-14 | 3.93E-11 |
| | PCE_EnKF | 3.28E-05 | 3.31E-05 | 3.14E-05 | 2.83E-05 | 3.28E-05 | 3.31E-05 | 3.06E-05 | 2.88E-05 | 3.01E-14 | 4.41E-11 |
| | PCE | 3.23E-05 | - | 3.29E-05 | - | 3.24E-05 | - | 3.01E-05 | - | 1.11E-12 | 7.16E-11 |

| **Parameter** | **Method** | ***Mean*** | | | | ***Maximum*** | | | | ***Var*** | |
|---|---|---|---|---|---|---|---|---|---|---|---|
| | Case: | Clog1 | Cn1 | Clog100 | Cn100 | Clog1 | Cn1 | Clog100 | Cn100 | Clog1 | Clog100 |
| $K_{s\ mult}$ | MC_EnKF | 1.294 | 1.332 | 1.280 | 1.069 | 1.296 | 1.331 | 1.218 | 0.890 | 4.80E-05 | 4.49E-02 |
| | PCE_EnKF | 1.289 | 1.350 | 1.299 | 1.120 | 1.290 | 1.352 | 1.218 | 0.986 | 3.68E-05 | 4.57E-02 |
| | PCE | 1.289 | - | 1.286 | - | 1.288 | - | 1.185 | - | 6.30E-05 | 5.00E-02 |

**Table 7.4: Comparison of mean, maximum and variance for the posteriors α, β, Ks_mult obtained by different update approaches real case.**

| Real case | | | | | | | | | | | |
|---|---|---|---|---|---|---|---|---|---|---|---|
| **Parameter** | **Method** | ***Mean*** | | | | ***Maximum*** | | | | ***Var*** | |
| | Case: | Clog1 | Cn1 | Clog100 | Cn100 | Clog1 | Cn1 | Clog100 | Cn100 | Clog1 | Clog100 |
| β | MC_EnKF | 8.60E+05 | 2.23E-03 | 6.75E-05 | 4.00E-04 | 8.64E+05 | 2.23E-03 | 6.37E-05 | 4.017E-04 | 7.45E+08 | 5.65E-10 |
| | PCE_EnKF | 9.41E+06 | 2.20E-03 | 7.34E-05 | 3.85E-04 | 9.42E+06 | 2.20E-03 | 6.47E-05 | 3.85E-04 | 6.85E+10 | 7.12E-10 |
| | PCE | 1.16E+08 | 2.26E-03 | 2.69E-05 | 3.06E-04 | 1.16E+08 | 2.26E-03 | 2.85E-05 | 3.08E-04 | 3.99E+14 | 1.69E-10 |

| **Parameter** | **Method** | ***Mean*** | | | | ***Maximum*** | | | | ***Var*** | |
|---|---|---|---|---|---|---|---|---|---|---|---|
| | Case: | Clog1 | Cn1 | Clog100 | Cn100 | Clog1 | Cn1 | Clog100 | Cn100 | Clog1 | Clog100 |
| α | MC_EnKF | 1.29E-06 | 9.85E-05 | 4.78E-06 | 1.47E-04 | 1.29E-06 | 9.85E-05 | 4.51E-06 | 1.48E-04 | 5.16E-17 | 8.94E-13 |
| | PCE_EnKF | 1.47E-06 | 2.22E-05 | 5.39E-06 | 1.26E-04 | 1.47E-06 | 2.22E-05 | 5.19E-06 | 1.26E-04 | 6.04E-17 | 1.17E-12 |
| | PCE | 3.29E-05 | 9.12E-06 | 6.51E-06 | 7.38E-05 | 3.31E-05 | 8.89E-06 | 6.37E-06 | 7.29E-05 | 7.10E-13 | 2.30E-12 |

| **Parameter** | **Method** | ***Mean*** | | | | ***Maximum*** | | | | ***Var*** | |
|---|---|---|---|---|---|---|---|---|---|---|---|
| | Case: | Clog1 | Cn1 | Clog100 | Cn100 | Clog1 | Cn1 | Clog100 | Cn100 | Clog1 | Clog100 |
| $K_{s\ mult}$ | MC_EnKF | 1.892 | **8.32** | 0.45 | -1.555 | 1.890 | **8.32** | 0.419 | -1.696 | 2.02E-04 | 4.88E-03 |
| | PCE_EnKF | 2.673 | **8.46** | 0.440 | -1.598 | 2.675 | **8.46** | 0.425 | -1.638 | 3.65E-04 | 0.005 |
| | PCE | 1.371 | 5.97 | 0.297 | -2.946 | 1.371 | 5.97 | 0.281 | -3.144 | 1.29E-04 | 2.51E-03 |

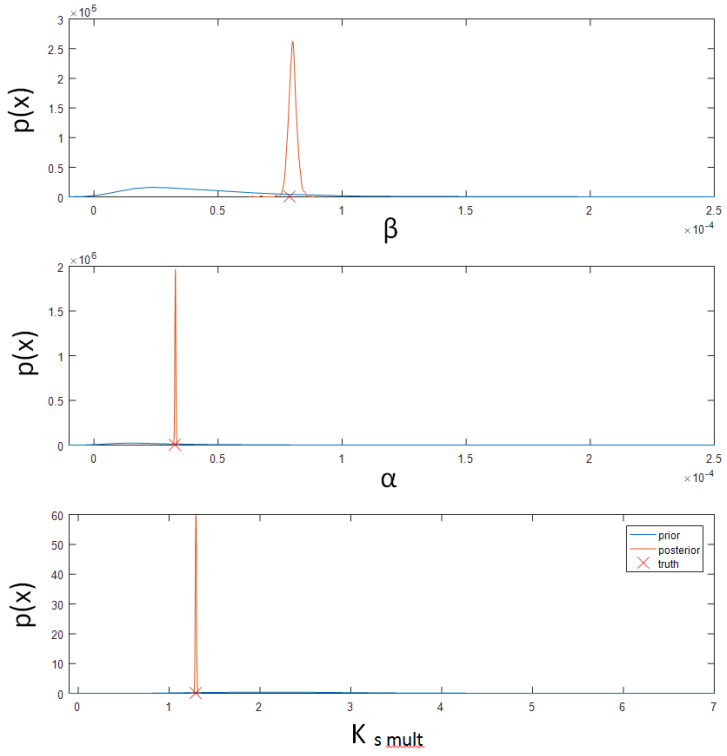


**a)**

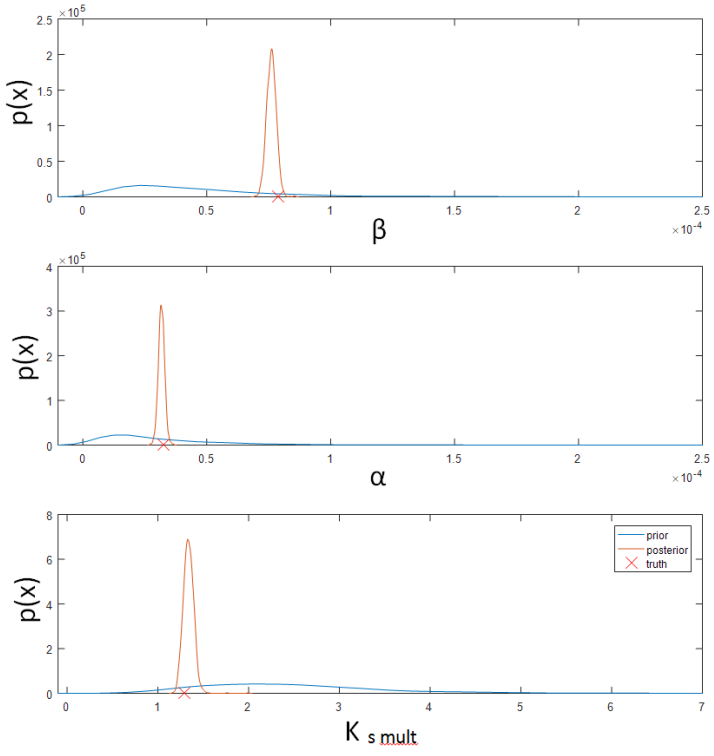


**b)**

**Figure 7.2: Synthetic case: probability density estimates of the prior and the posterior for the first MC_EnKF update in Case a) Clog1 b) Cn1. The blue line is the prior; the orange line is the posterior; the red X symbol is the value of the "truth".**

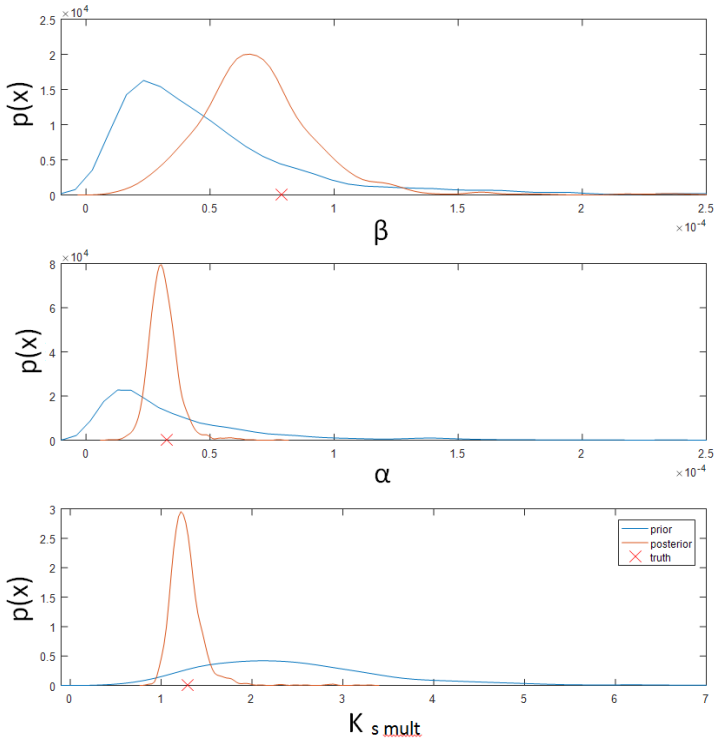


a)

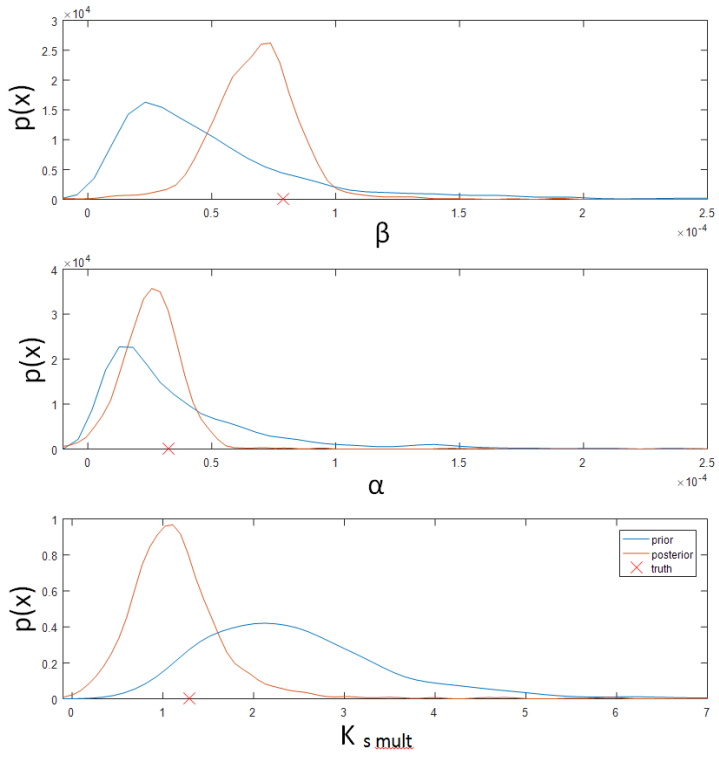


b)

**Figure 7.3: Synthetic case: probability density estimates of the prior and the posterior for the first MC_EnKF update in Case a) Clog100 b) Cn100.**

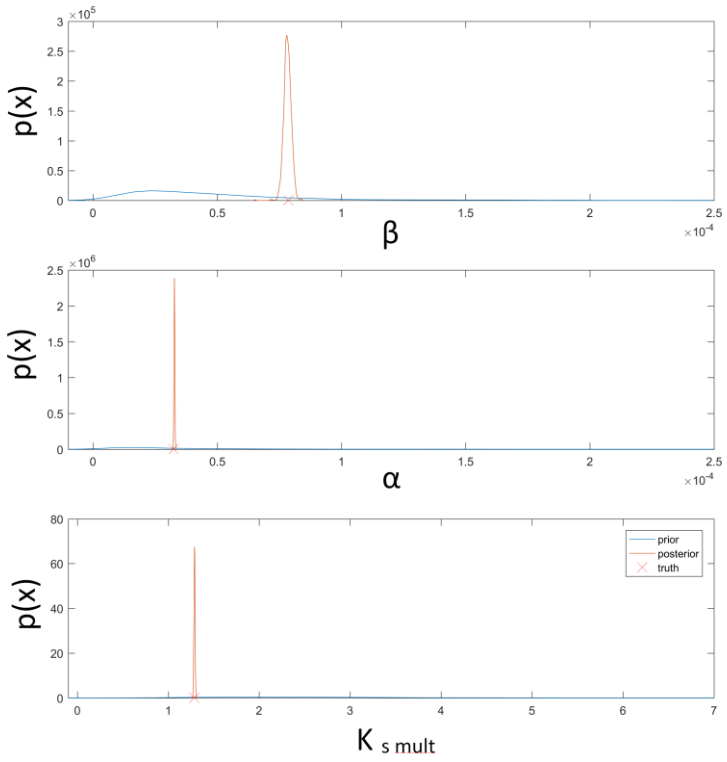


**a)**

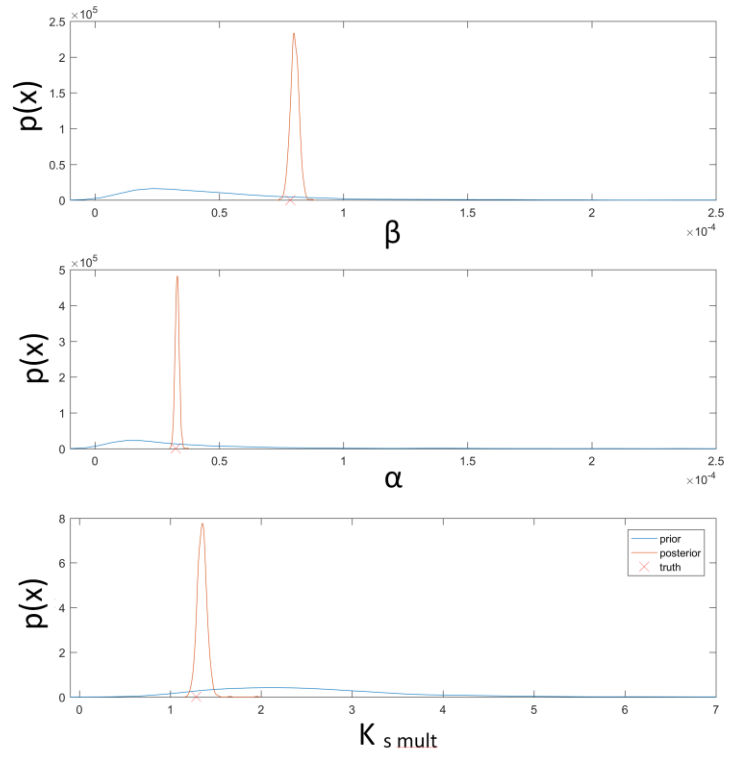


**b)**

**Figure 7.4: Synthetic case: probability density estimates of the prior and the posterior for the first PCE_EnKF update in Case a) Clog1 b) Cn1.**

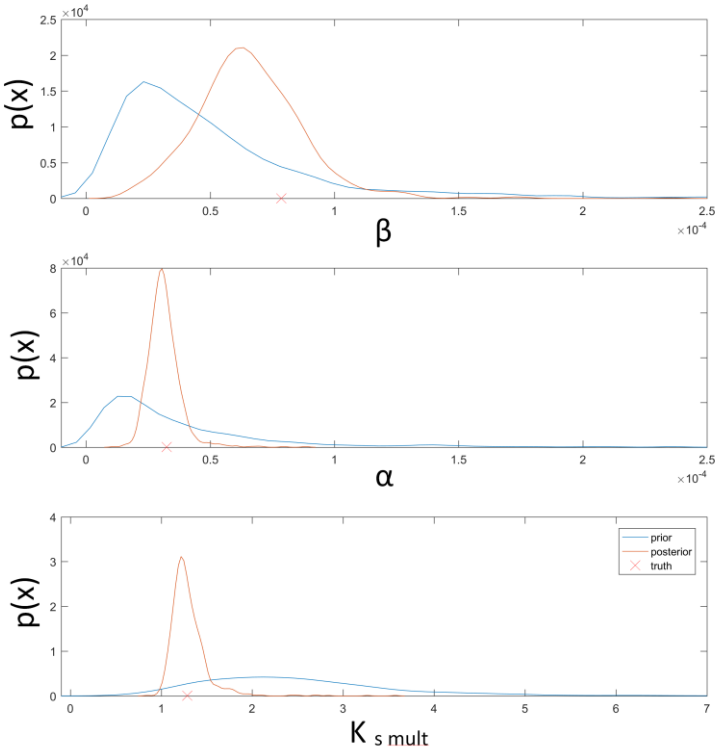


**a)**

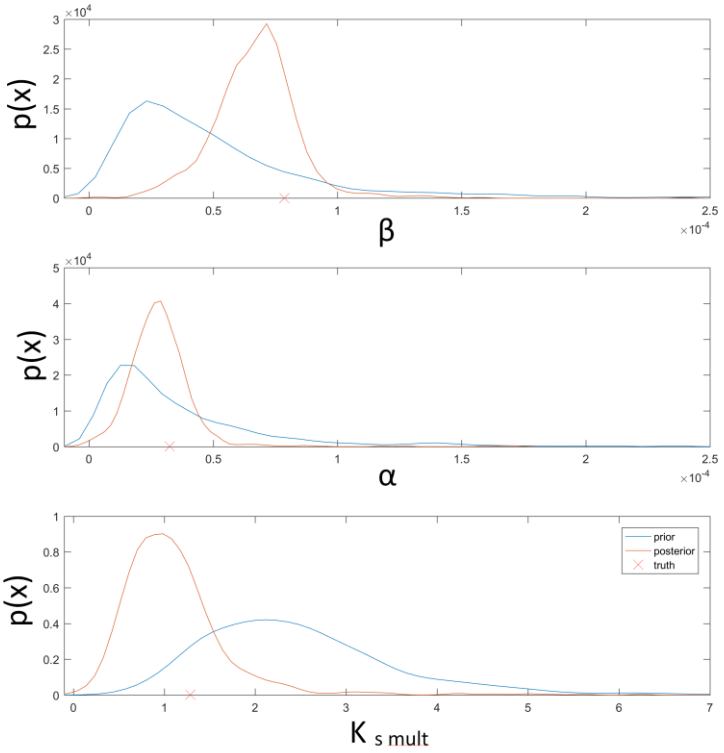


**b)**

**Figure 7.5: Synthetic case: probability density estimates of the prior and the posterior for the first PCE_EnKF update in Case a) Clog100 b) Cn100.**

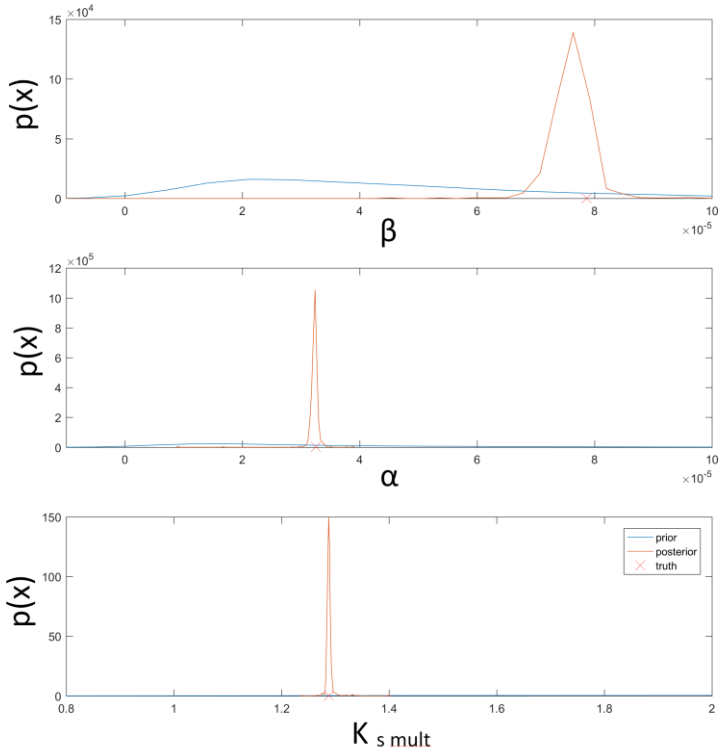


a)

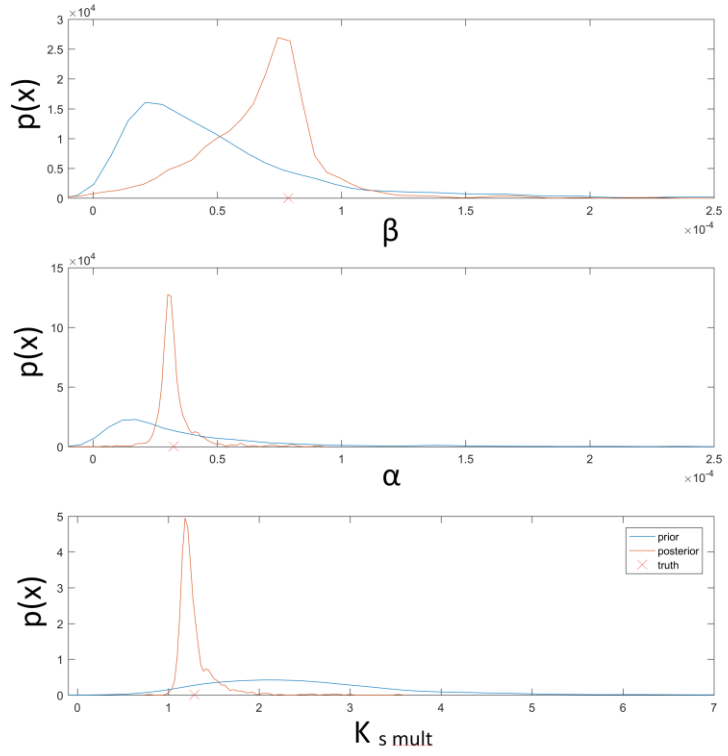


b)

**Figure 7.6: Synthetic case: probability density estimates of the prior and the posterior for the first PCE update in Case a) Clog1 b) Clog100.**

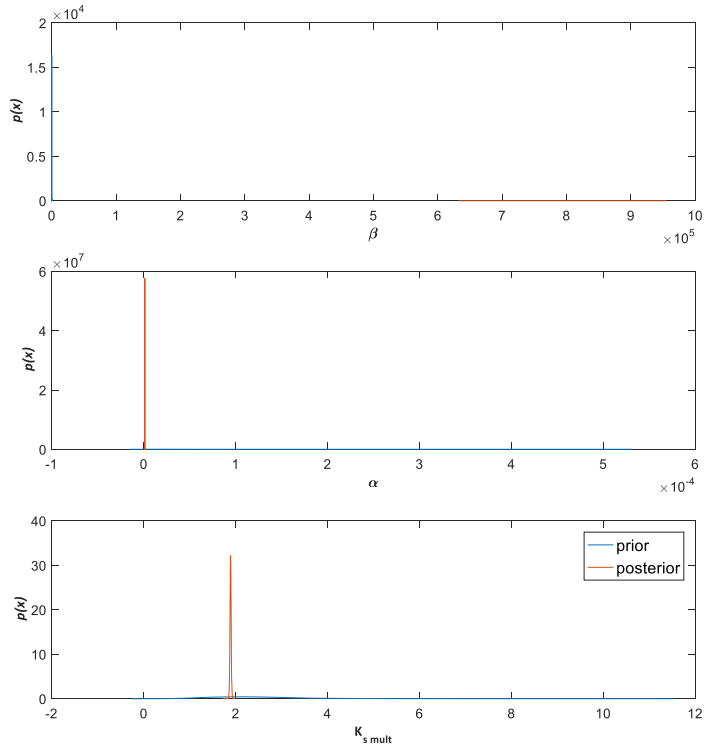


**a)**

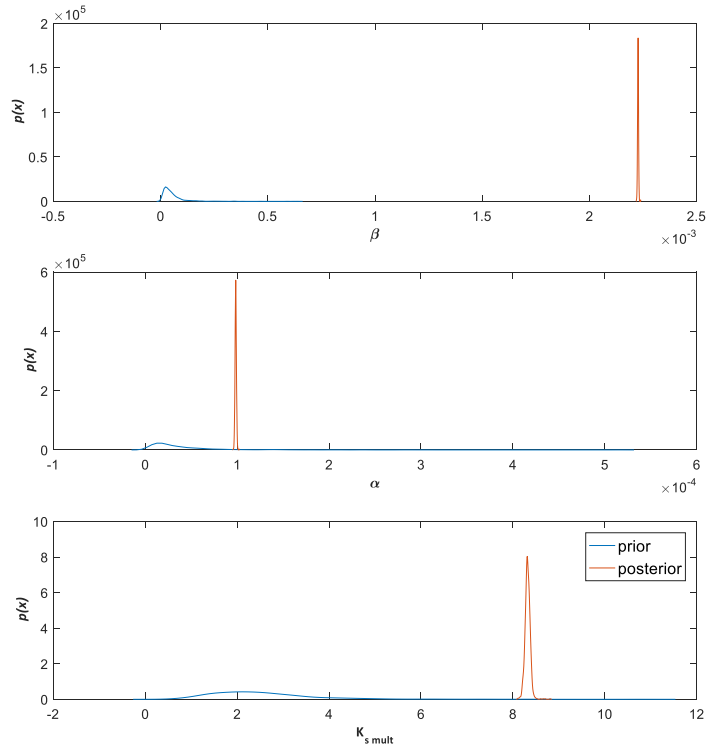


**b)**

**Figure 7.7: Real case: probability density estimates of the prior and the posterior for the first MC_EnKF update in Case a) Clog1 b) Cn1. The blue line is the prior and the orange line is the posterior.**

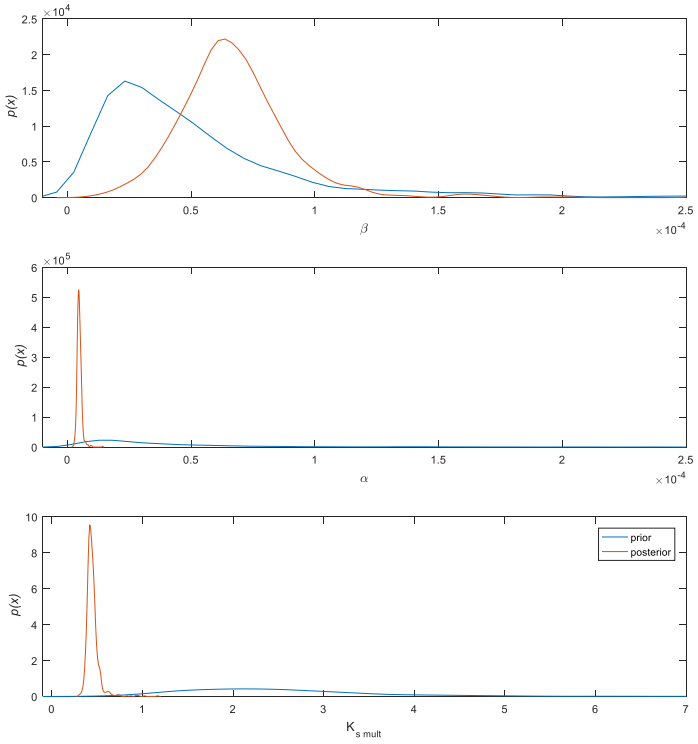


**a)**

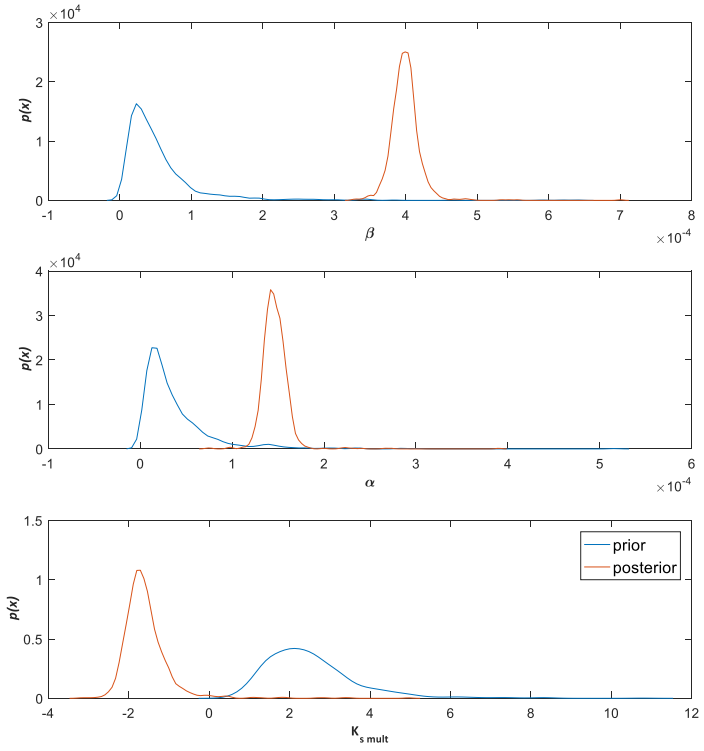


**b)**

**Figure 7.8: Real case: probability density estimates of the prior and the posterior for the first MC_EnKF update in Case a) Clog100 b) Cn100.**

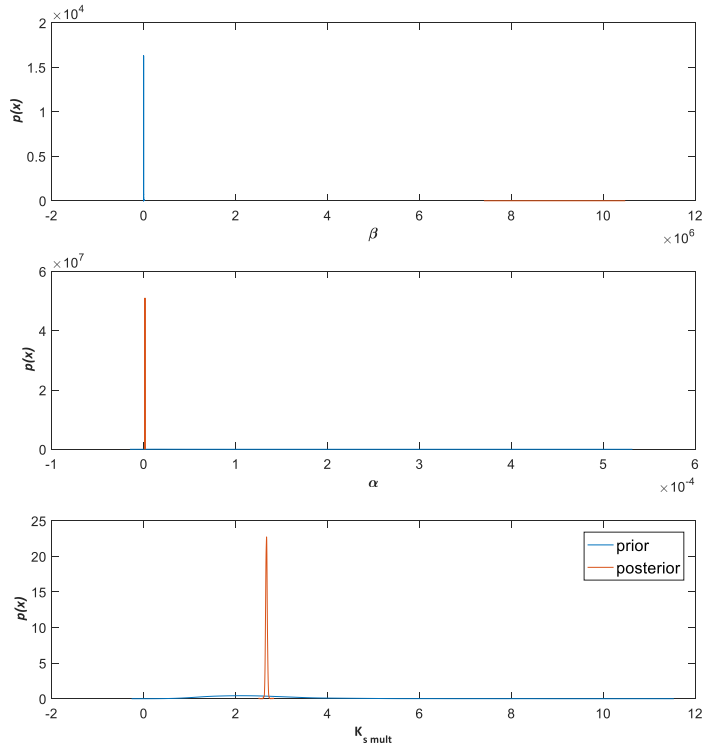


**a)**

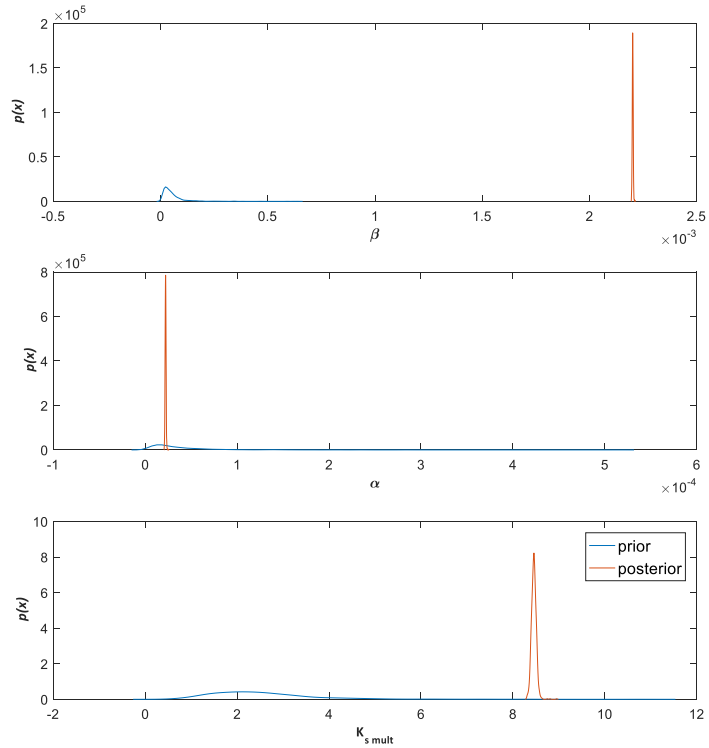


**b)**

**Figure 7.9: Real case: probability density estimates of the prior and the posterior for the first PCE_EnKF update in Case a) Clog1 b) Cn1.**

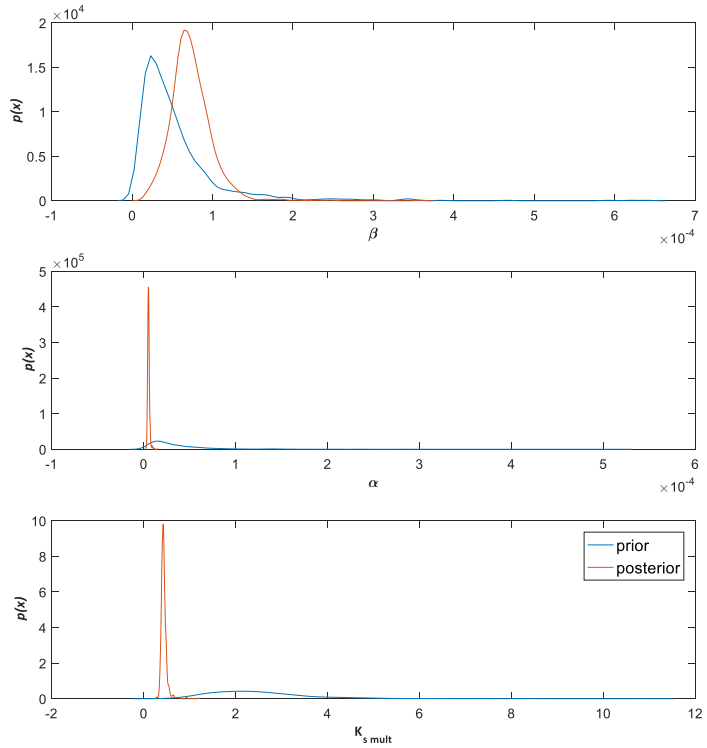


**a)**

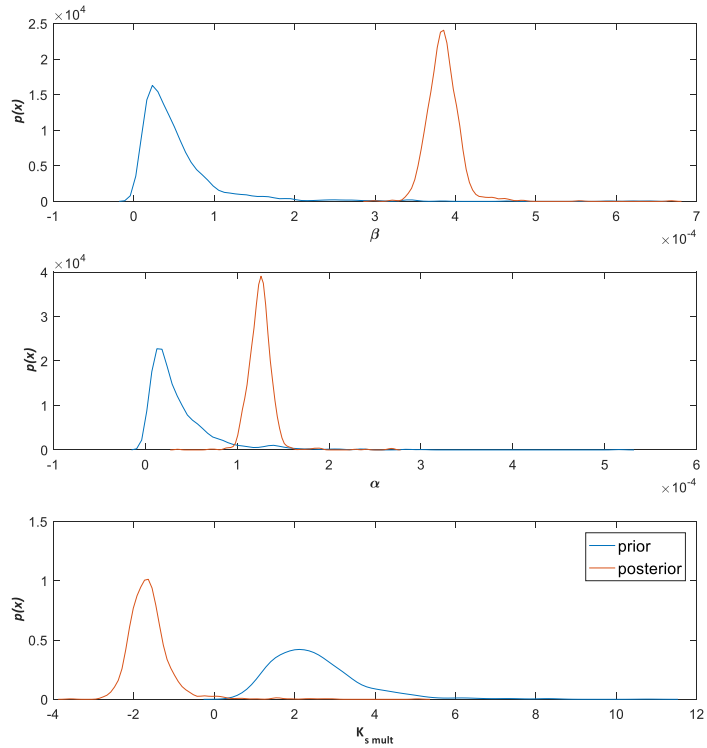


**b)**

**Figure 7.10: Real case: probability density estimates of the prior and the posterior for the first PCE_EnKF update in Case a) Clog100 b) Cn100.**

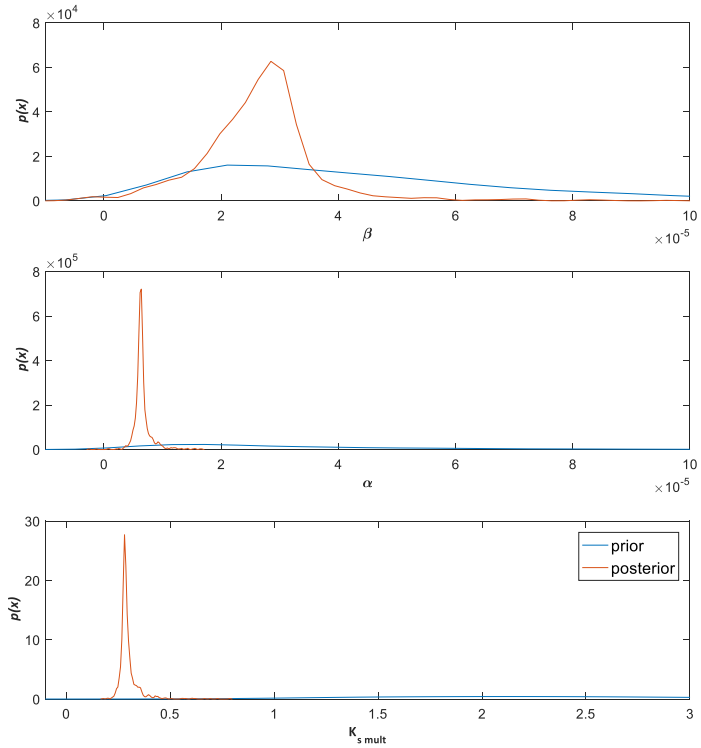


a)

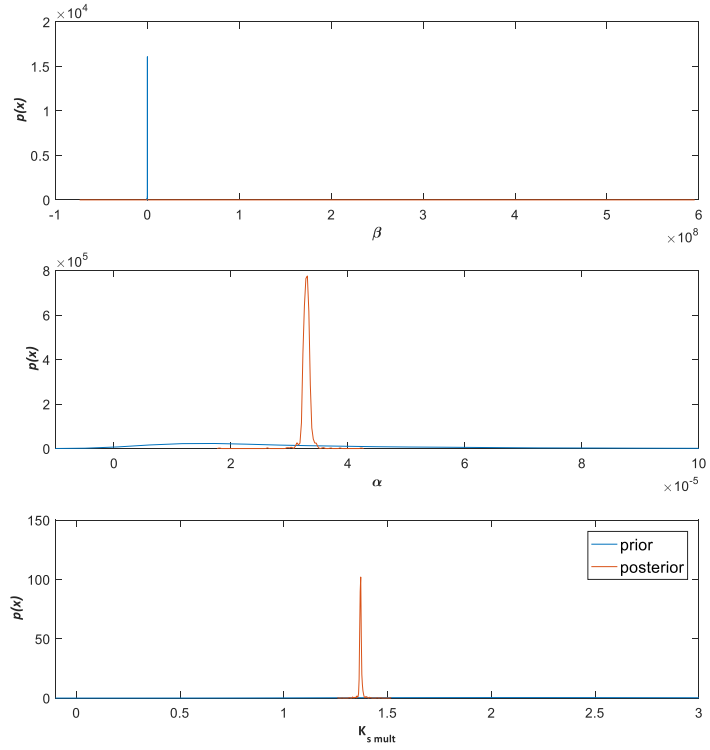


b)

**Figure 7.11: Real case: probability density estimates of the prior and the posterior for the first PCE update in Case a) Clog100 b) Clog1.**

**Table 7.5: Validation of the results for synthetic case in terms of mean error (ME), Mean Absolute Error (MAE), Root Mean Squared Error (RMSE), $R^2$, index of agreement (d).**

| Validation -Synthetic case | | | | | | | |
|---|---|---|---|---|---|---|---|
| | MC_EnKF | | | | PCE_EnKF | PCE | |
| Case | Clog1 | Cn1 | Clog100 | Cn100 | Cn100 | Clog1 | Clog100 |
| **μ (obs)** | 58.725 | 58.720 | 1.217 | 1.217 | 1.211 | 58.721 | 1.214 |
| **ME** | 0.470 | 1.160 | -0.067 | -0.490 | -0.343 | 0.376 | -0.100 |
| **MAE** | 0.777 | 1.250 | 0.067 | 0.491 | 0.344 | 0.746 | 0.100 |
| **RMSE** | 2.841 | 4.130 | 0.156 | 1.191 | 0.810 | 2.721 | 0.228 |
| **$R^2$** | 1.000 | 1.000 | 0.999 | 0.996 | 0.997 | 1.000 | 1.000 |
| **d** | 0.9999 | 0.9998 | 0.9993 | 0.9691 | 0.9839 | 0.9999 | 0.9985 |

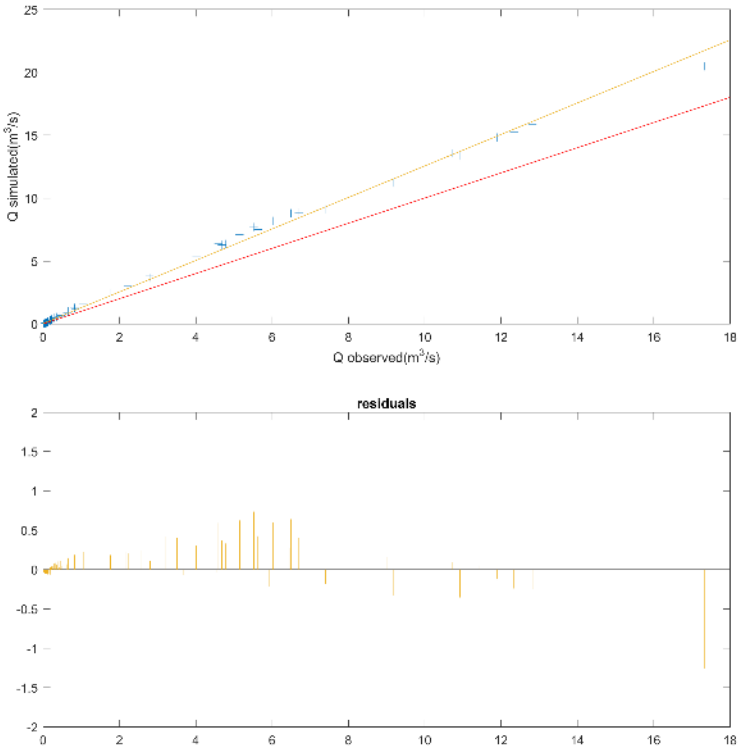


**Figure 7.12: Validation: comparison of synthetic measurement (Qobserved) with predictions obtained by run Mobidic with max posterior (Qsimulated) for the PCE_EnKF method in Case Cn100. Scatter plot with line 1:1 (red line) and linear interpolation (yellow line) (upper chart) and residuals (lower chart).**

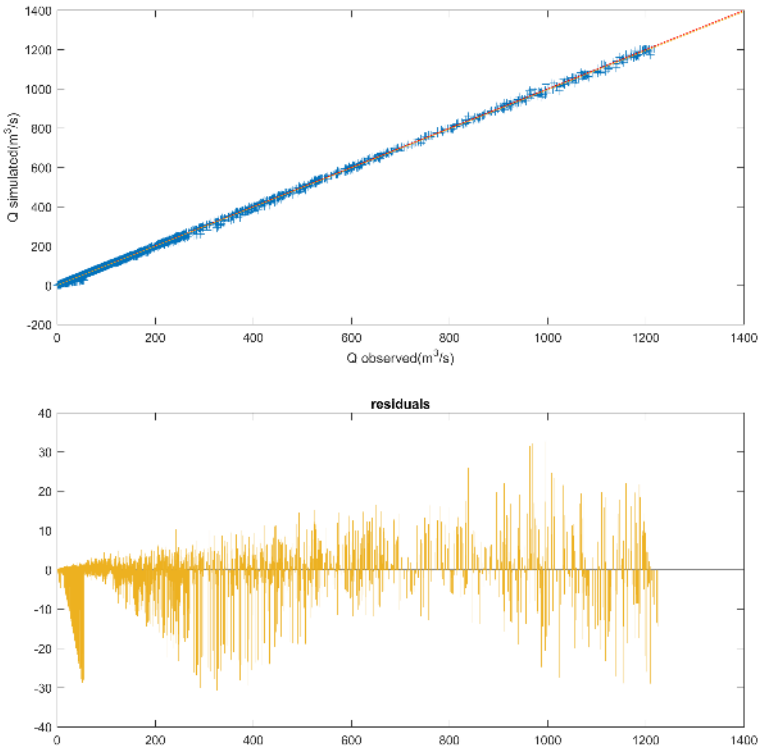


**a)**

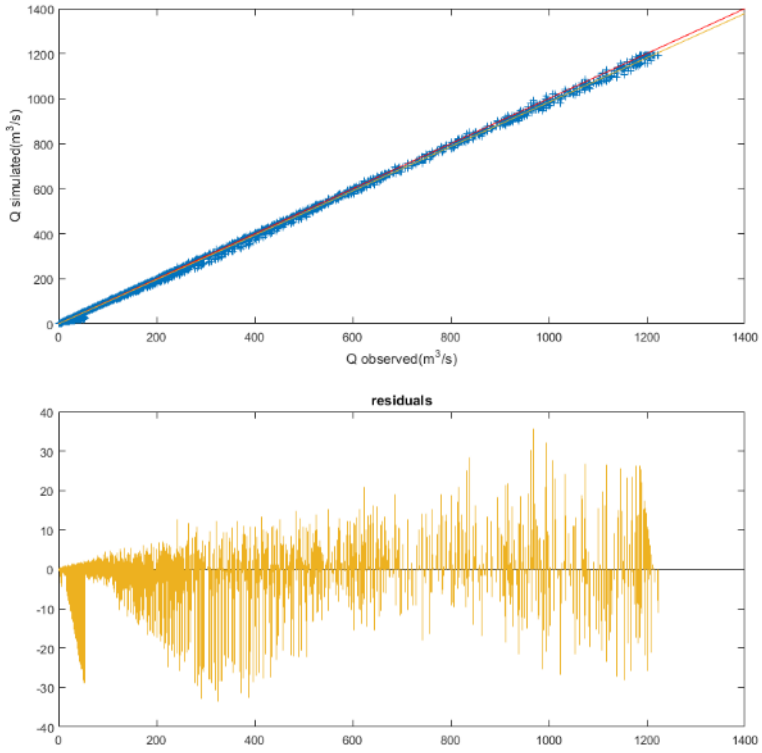


**b)**

**Figure 7.13: Validation: comparison of synthetic measurement (Qobserved) with predictions obtained by run Mobidic with max posterior (Qsimulated) for the MC_EnKF method in Case a) Clog1 b) Cn1.**

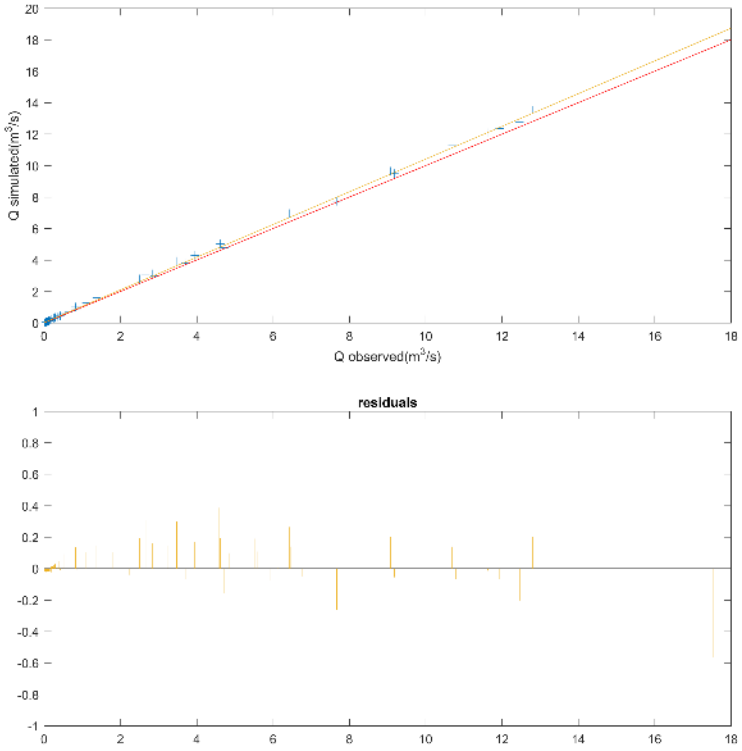


**a)**

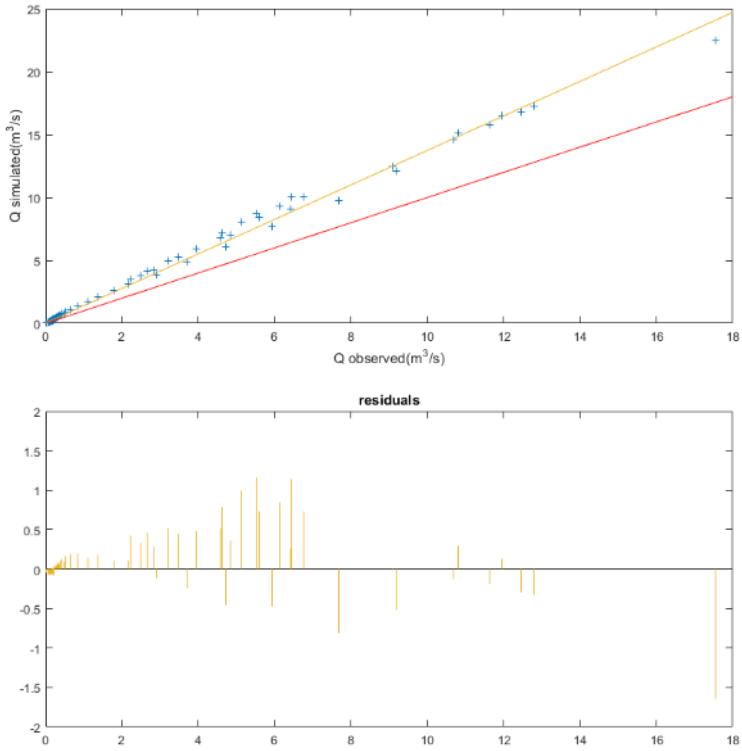


**b)**

**Figure 7.14: Validation: comparison of synthetic measurement (Qobserved) with predictions obtained by run Mobidic with max posterior (Qsimulated) for the MC_EnKF method in Case a) Clog100 b) Cn100.**

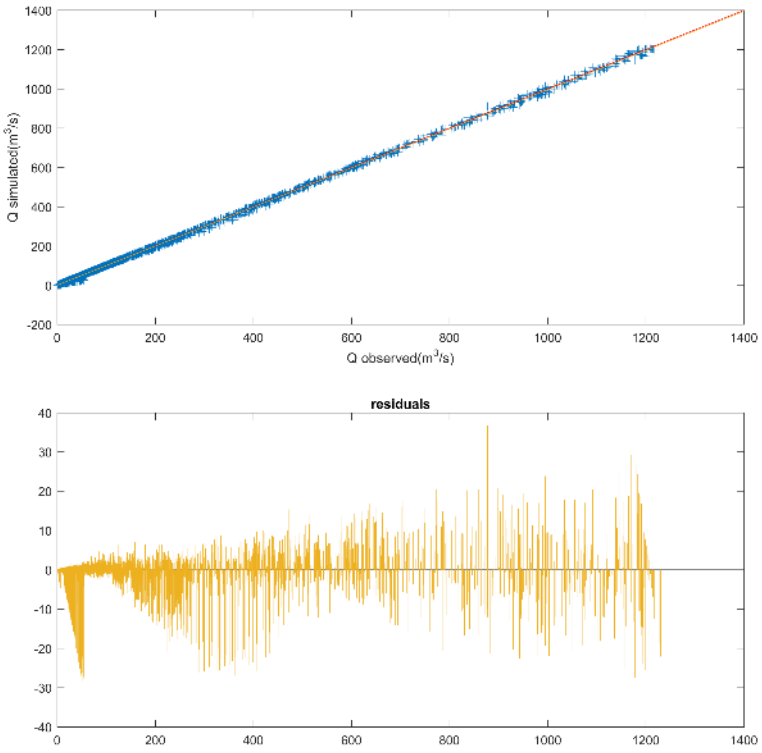


**a)**

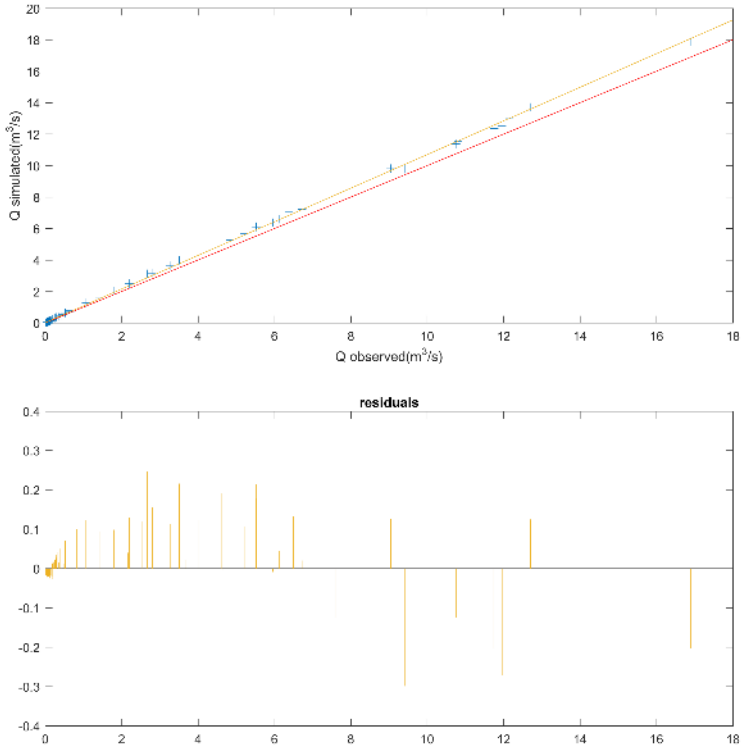


**b)**

**Figure 7.15: Validation: comparison of synthetic measurement (Qobserved) with predictions obtained by run Mobidic with max posterior (Qsimulated) for the PCE method in Case a) Clog1 b) Clog100.**

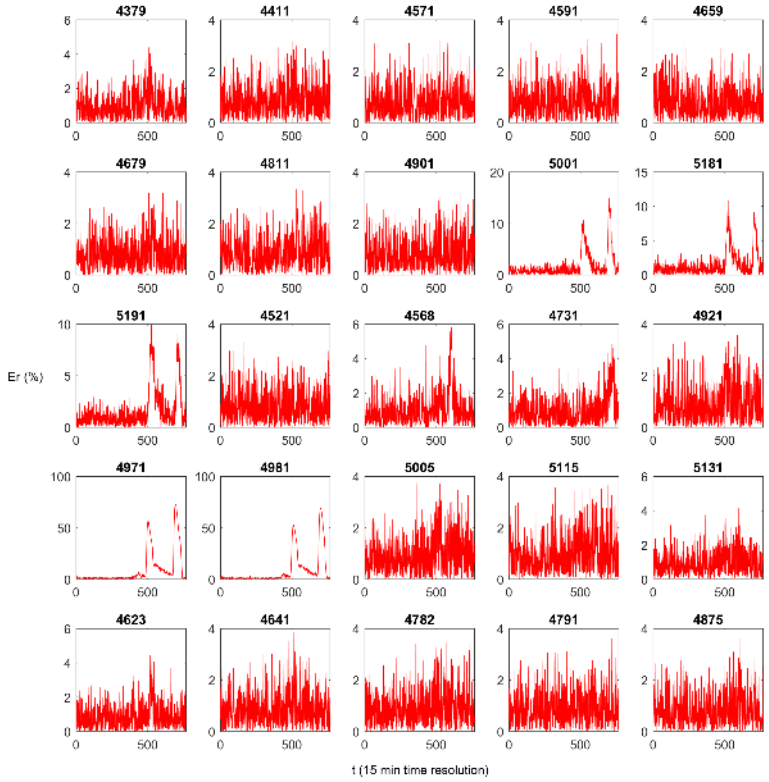


a)

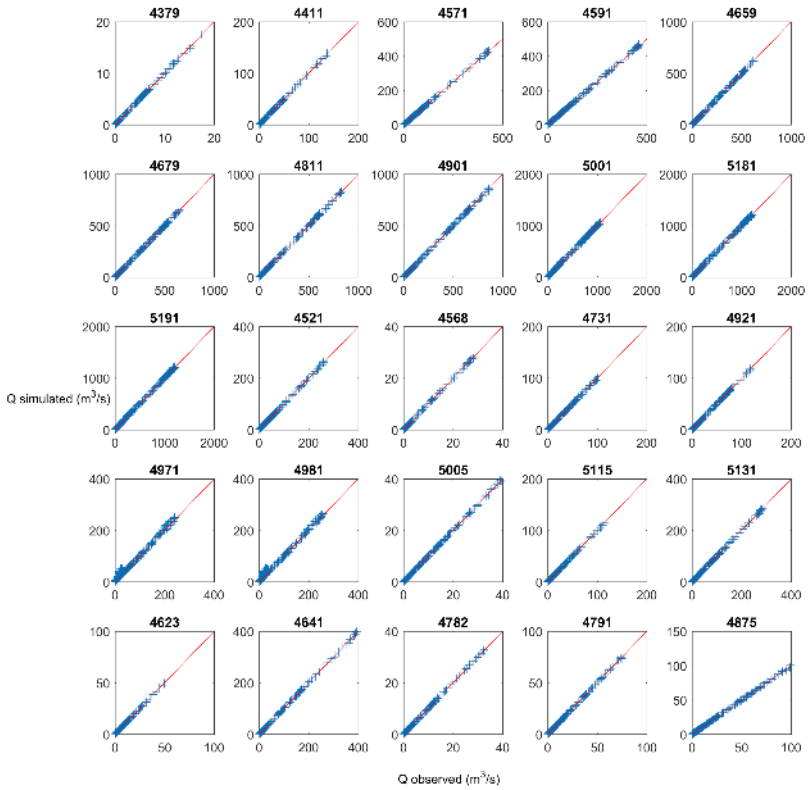


b)

**Figure 7.16: Validation: a) relative error expressed in percent over time for each stream gauge b) scatter plot where $Q_{observed}$ as x label are synthetic measurement for MC_EnKF method in case Clog1.**

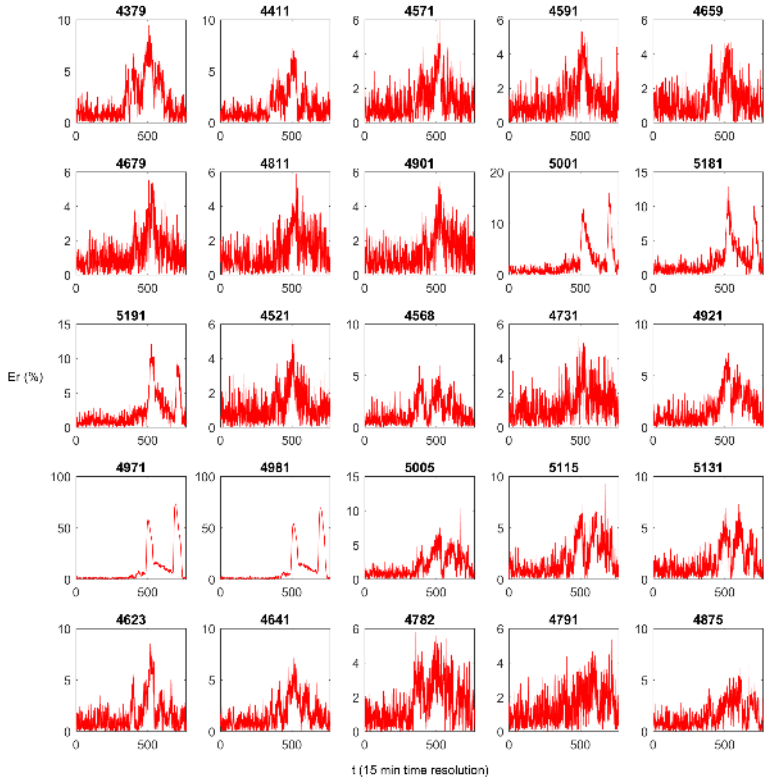


a)

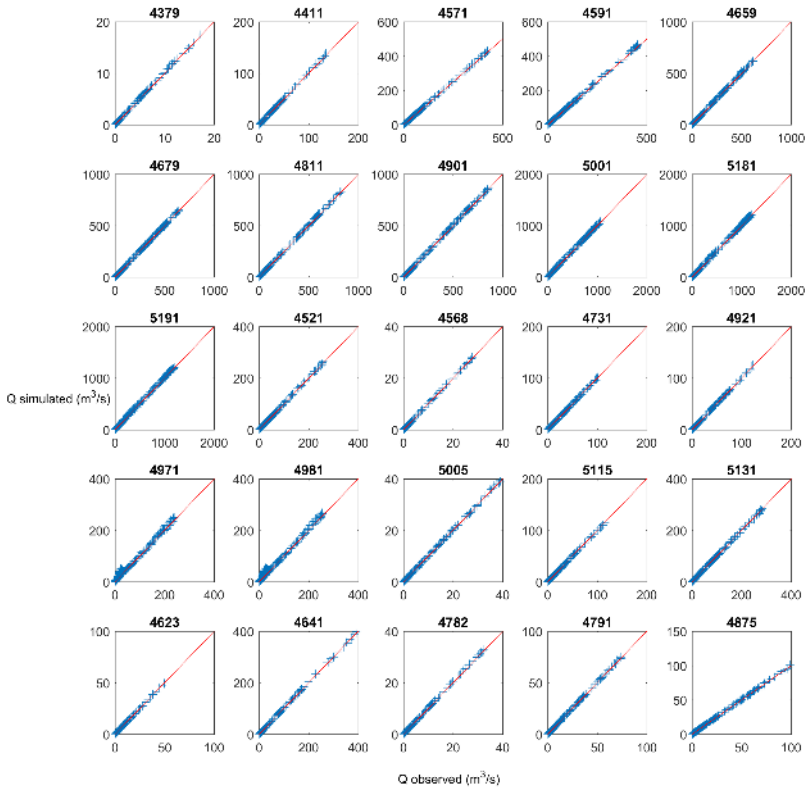


b)

**Figure 7.17: Validation: a) relative error expressed in percent over time for each stream gauge b) scatter plot where $Q_{observed}$ as x label are synthetic measurement for MC_EnKF method in case Cn1.**

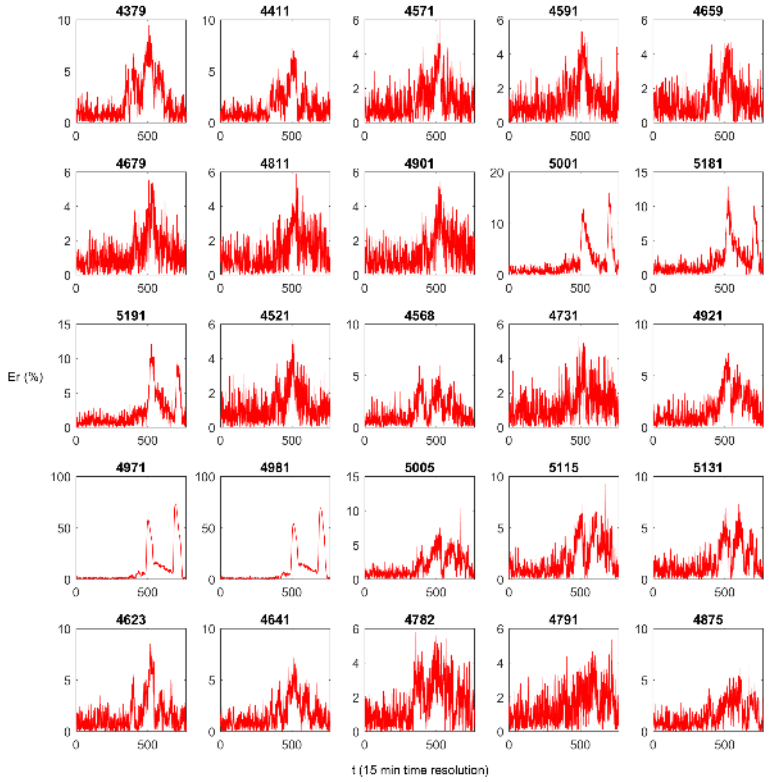


a)

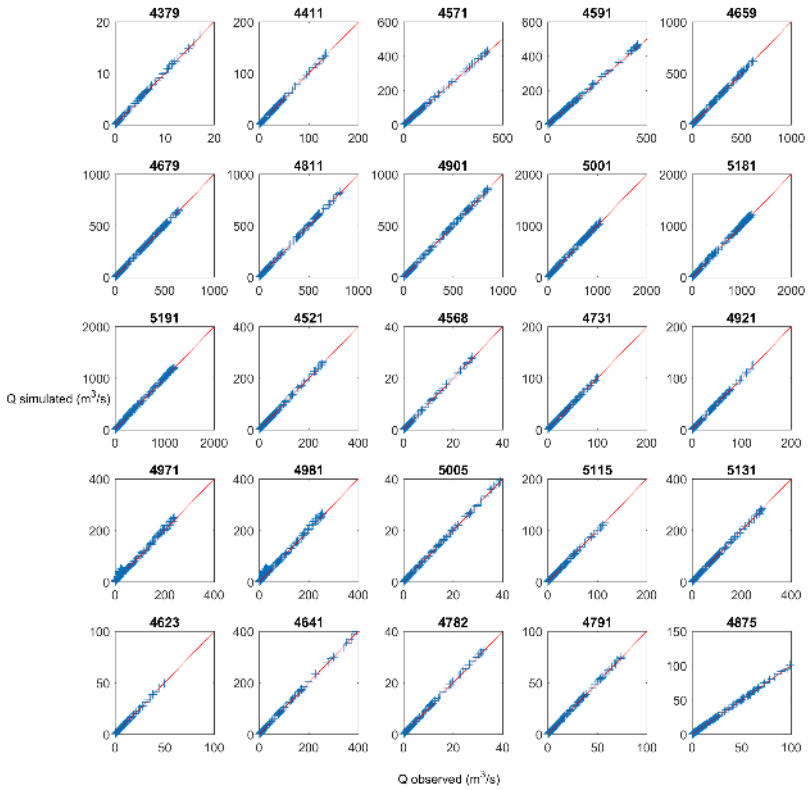


b)

**Figure 7.18: Validation: a) relative error expressed in percent over time for each stream gauge b) scatter plot where $Q_{observed}$ as x label are synthetic measurement for PCE method in case Clog1.**

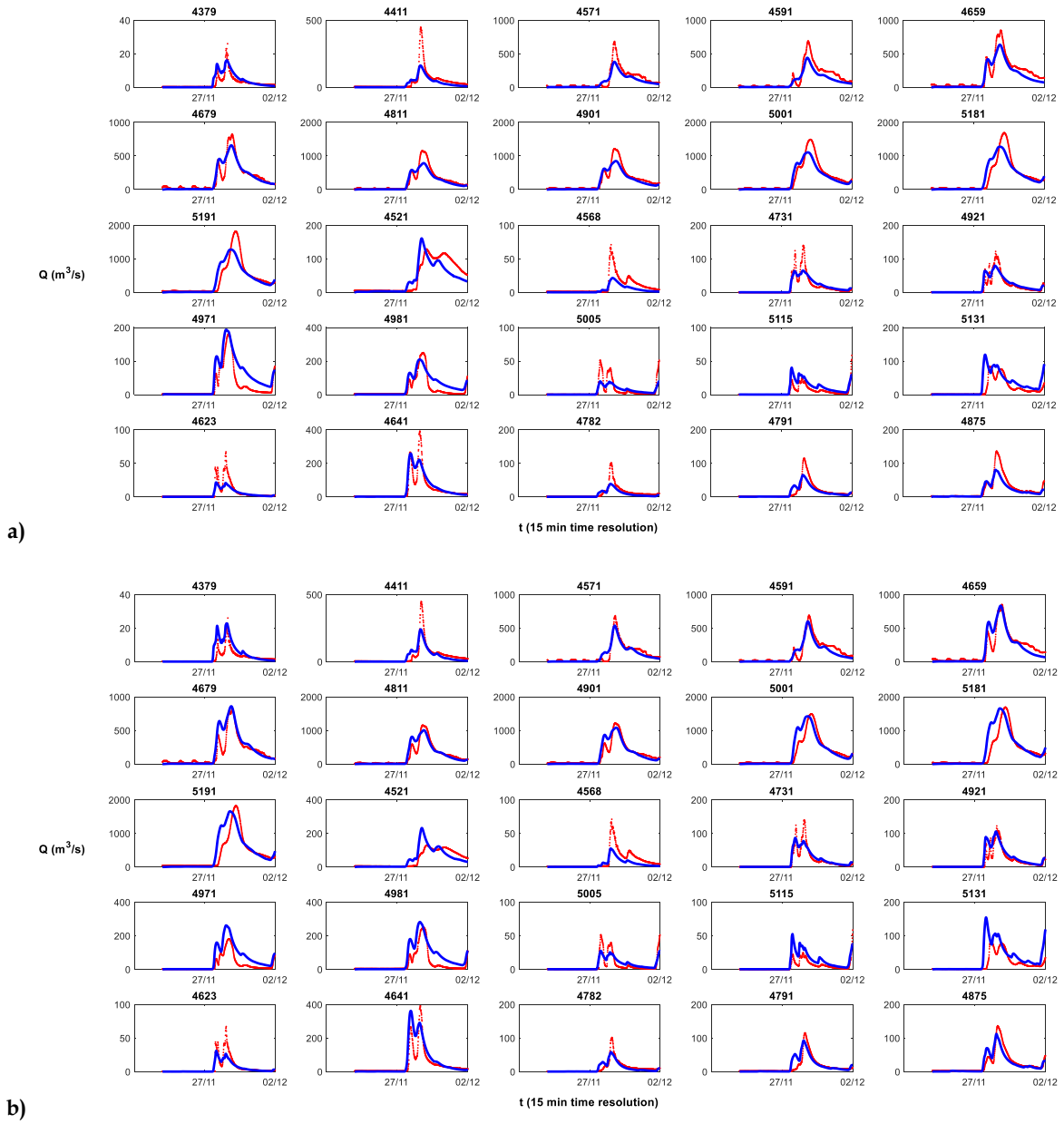


**Figure 7.19: Validation in real case: comparison of simulated output (blu line) to real discharge measurement recorded during the flood event occurs the 28.11.2012 (red line) for each stream gauge, case Clog100 a) MC_EnKF approach b) PCE approach.**

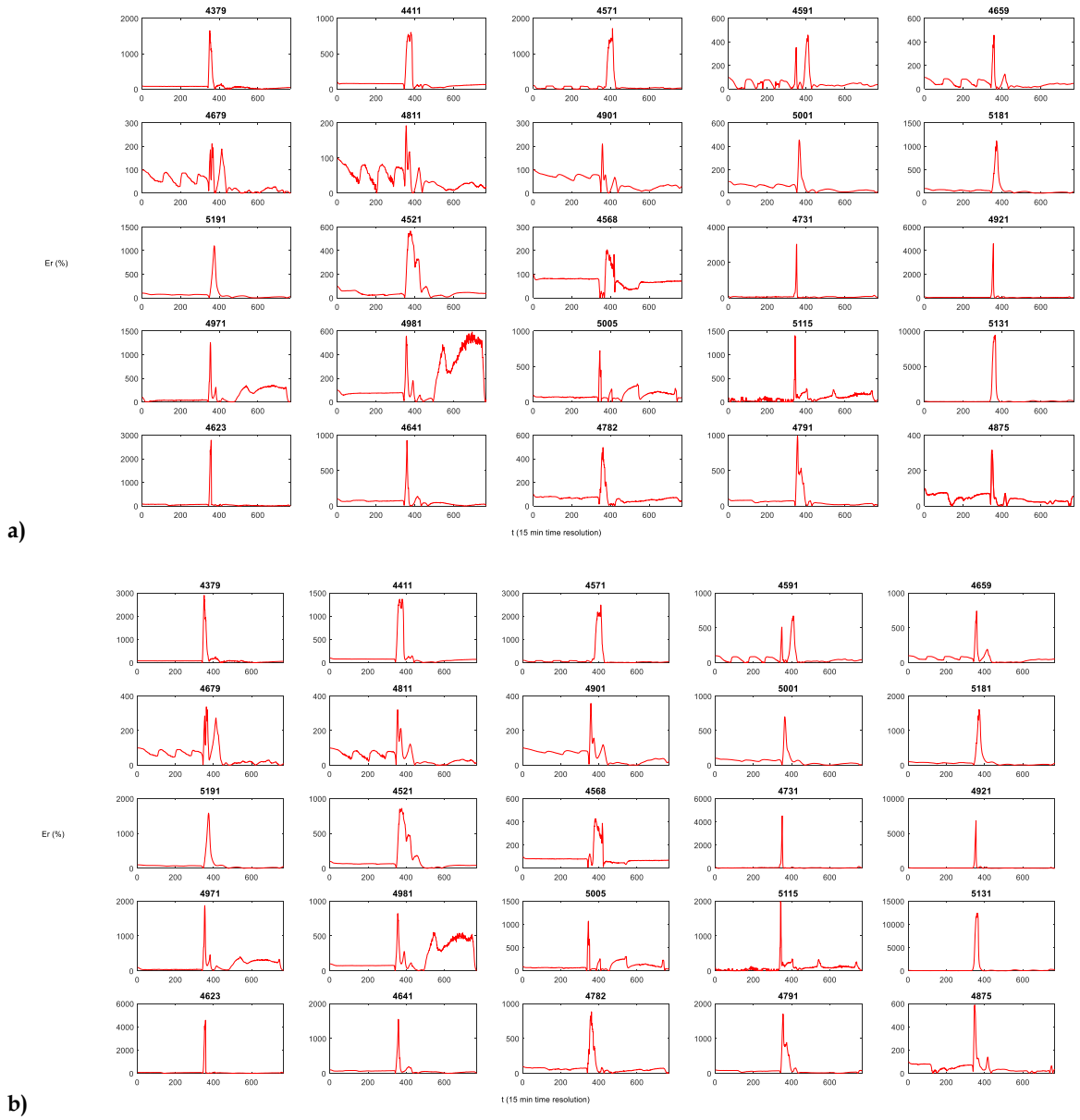


**Figure 7.20: Validation in real case: relative error expressed in percent over time for each stream gauge, case Clog100 a) MC_EnKF approach b) PCE approach.**

## 7.5 Conclusive remarks

How to update the state variable through data assimilation using EnKF in hydrological modeling? It is the question of a student on www.researchgate.net. In this dissertation we try to answer to this question, proposing the Linear Bayesian update of model parameters instead of taking into account only the state variable.
In this Chapter the group of methods proposed in Chapter 5 is applied for the uncertain parameters estimation of the distributed hydrological model MOBIDIC. The methodology is tested on numerical examples of water balance for a specific flood event occurs the 28.11.2012 in the Arno river basin, using synthetic measurement as well as real measurement of discharges. Even though the considered event is not long enough for a completely identification procedure, the effect of the input uncertainty on the system response is determined. In principle nothing would change in a more complete case, only the number of update would grow. The presented study was designed to determine the effect of the input uncertainty on the system response by considering two groups of update approaches: those based on the Monte Carlo techniques and those based on the Wiener's Polynomial Chaos Expansion (PCE) filter. The representation of the random variables is performed in a form of MC sampling with 1000 ensemble size as well as in a form of PCE as polynomial order 5.
Probability Density estimates for the prior and posterior for EnKF and PCE updates, are represented for synthetic case and real case. The update for both the approaches, as expected, moved the mean and reduced the variance. The prior as well as the posterior are more or less Gaussian even if a slight skewness is presented. In real case no one of the approaches is able to update $\beta$ parameter indeed we can see that the RV has effectively converged to a Dirac delta, which suggests that all variance has been lost and the number of samples and the polynomial order are clearly not sufficient for this case study. It is important to point out that the set reference of EnKF runs with 1000 ensemble members is not representing "the best we can do" in terms of Bayesian updating, so it is not possible to say which method is "better" by this direct comparison. All that can be done is to point out differences.
The validation of the results for synthetic case suggests that the methodology can be suitably applied in hydrological modelling, while in real case the detected high error in peak discharge occurrence suggests to further investigate the model errors.
The results show that, with the right hypothesis, the estimates by means of functional approximation are comparable or even better than that by means of the classic Monte Carlo techniques. The possibility to apply these methods for Bayesian updating in real case should be investigated in future studies.

# Chapter 8

# Conclusion

## 8.1 Quantification of the accuracy of the different models

The analysis of hydrological extreme events was carried out in Chapter 3 applying a geostatistical spatial interpolation technique and in this final part by the application of a distributed hydrological model. The flood quantiles associated with a given non-exceedance probability, with estimates of uncertainty, have been evaluated. Here a comparison of results from the Top-Kriging interpolation technique and from the hydrological model MOBIDIC is performed. The overall goodness of fit of the two methods is evaluated by the assessment of general errors between the empirical and predicted flood quantiles expressed in the same units of discharges. Since RMSE gives the standard deviation of the model prediction error, also the absolute error and the relative error expressed in percentage are reported. We remind that the results are streamflow indices, i.e. flood quantiles corresponding to 10, 50, 100, 200, 500-year return periods $T_r$, and empirical estimates of flood quantiles were determined by an at-site flood frequency analysis carried out at each station reported in Table 3.1 (`nsRFA` R-package).

As already mentioned in Chapter 6, an accurate calibration of MOBIDIC is missing, because the objective of the thesis is the methodological investigation of parameters identification. Moreover, the model is strongly influenced by soil saturation conditions. In order to estimate correctly the flood discharges, it became therefore fundamental the assessment and calibration of the soil saturation initial conditions. MOBIDIC simulations for design hydrograph application are here carried out considering initial relative saturation of capillary soil *initinfo.wcsat* equal to 0.6 and initial relative saturation of gravitational soil *initinfo.wcsat* equal to 0.2.

The computation of the design hydrographs has been implemented on the basis of parameters potentially identified in the analysis carried out in Chapter 7. One simulation for Q10 flood quantile is carried out considering as parameter values the maximum posterior values obtained in the synthetic case with all measurements (skip=1) and prior distribution normal, 7.89e-05 3.34e-05 1.30 for $\alpha$, $\beta$, $K_{s\_mult}$ respectively. Moreover, no initial condition for soil saturation have been set. Flood quantile values for these return periods affect by big error compared to empirical and Top-Kriging estimates and in some stream gauges unrealistic (e.g., in S. Giovanni alla vena watershed 7878 $m^3/s$, Brucianesi 5510 $m^3/s$, Nave di Rosano 4401 $m^3/s$ instead of Q10 values estimated around 1940 $m^3/s$, 1760 $m^3/s$, 1840 $m^3/s$ respectively) are obtained.

More simulation tests with parameters estimated in real case have been not performed yet considering that a complete identification of the uncertain parameters is not carried out. As already pointed out, the objective of the simulations for flood hydrograph application is not on event scale basis, i.e. on estimating the streamflow in certain Arno river sections for which records for the discharges are available. Rather, the objective of the simulation is to demonstrate the possibility of using the hydrological model MOBIDIC for the estimation of design streamflow as well as to show the methods for model errors assessment. Furthermore, the MOBIDIC module for flood hydrograph reconstruction has been recently implemented and applied for the moment only for the study case on Versilia river basin. The potentialities, the assets as well as the weaknesses are still not known.

Consequently, parameters values calibrated in previous analyses in the Arno river basin are considered. The downhill routing coefficient $\alpha$ is set equal to 3.00e-06, the hypodermic flow coefficient $\beta$ is set equal to 2.00e-05, the multiplying factor of soil hydraulic conductivity $K_{s\_mult}$ is set equal to 8.50.

As mentioned in Section 6.3.2 the hydrometeorological data for the computation of design hydrographs must be provided in the form of parameters $a$ and $n$ of the rainfall IDF curves for the 5 design recurrence intervals (10, 50, 100, 200, 500 years). The minimum and the maximum rainfall duration expressed in hours as well as the total time simulation to be considered in the simulations are defined as 6hours, 24hours and 40 hours respectively. These values for defining how the provided depth-duration curves are used according to the methodology implemented in this novelty MOBIDIC module for flood hydrograph application. The procedure consists in the generation of synthetic hyetographs for several rainfall durations and the computation of the hydrographs for all rainfall durations and return periods (Figure 8.1). Furthermore, the selection of the rainfall duration more critical for the maximum discharge $d(Q_{max})$ and for the maximum volume $d(V_{max})$ is performed. Finally, for each river section and each $T_r$ the maximum discharge values $Q_{max}$ and the maximum volume values $V_{max}$ are estimated.

Table 8.1 shows the Mean Error (ME), Mean Absolute Error (MAE), Root Mean Squared Error (RMSE) expressed in the same units of observations for comparing the estimate of flood quantiles by means Top-kriging method and MOBIDIC simulations.

**Table 8.1: The goodness of fit between Top-Kriging prediction and Mobidic prediction of flood quantile.**

| | Q10 [m³/s] | Q50 [m³/s] | Q100 [m³/s] | Q200 [m³/s] | Q500 [m³/s] |
|---|---|---|---|---|---|
| **μ (obs)** | 478.8 | 654.5 | 743.3 | 829.9 | 957.7 |
| **ME** | 35.5 | 117.1 | 155.5 | 199.7 | 244.8 |
| **MAE** | 203.8 | 374.6 | 450.8 | 544.2 | 684.3 |
| **RMSE** | 436.92 | 801.2 | 943.3 | 1130.6 | 1380.3 |
| **$R^2$** | 0.89 | 0.83 | 0.85 | 0.83 | 0.79 |

Table 8.2 shows the flood quantiles estimations, in each stream gauge considered in the Arno river basin, for the three method proposed as well as the absolute error and the relative error expressed as percentage.

**Table 8.2: Flood quantiles estimations, absolute error (EA), relative error (Er) for each stream gauges in the Arno river basin.**

| | | | Q10 [$m^3/s$] | | | | | Q50 [$m^3/s$] | | | | |
|---|---|---|---|---|---|---|---|---|---|---|---|---|
| **Name** | **A [$km^2$]** | **N° years** | **nsRFA** | **TK** | **Mobidic** | **Er (%)** | **EA** | **nsRFA** | **TK** | **Mobidic** | **Er (%)** | **EA** |
| Stia | 60.8 | 38 | 80.0 | 94.8 | 43.2 | 119.5 | 51.6 | 134.8 | 101.2 | 58.0 | 74.4 | 43.2 |
| Pollino | 457.2 | 10 | 390.7 | 560.9 | 349.8 | 60.4 | 211.1 | 408.0 | 843.9 | 472.2 | 78.7 | 371.7 |
| Subbiano | 748.2 | 76 | 908.7 | 573.2 | 580.5 | 1.3 | 7.4 | 1318.3 | 613.6 | 792.3 | 22.6 | 178.7 |
| Ponte ferrovia Fi-Roma | 1390.9 | 69 | 412.1 | 699.1 | 436.1 | 60.3 | 263.0 | 588.8 | 880.9 | 739.7 | 19.1 | 141.1 |
| Ponte Romito | 2400.1 | 13 | 1188.6 | 1174.0 | 1130.0 | 3.9 | 44.0 | 1532.7 | 1508.0 | 1719.8 | 12.3 | 211.8 |
| Bucine | 159.8 | 15 | 154.2 | 183.8 | 100.3 | 83.3 | 83.5 | 218.9 | 252.1 | 166.6 | 51.3 | 85.4 |
| Ponte del Bilancino | 150.2 | 18 | 475.7 | 247.7 | 6.9 | 3493.5 | 240.8 | 674.5 | 356.6 | 9.1 | 3799.7 | 347.4 |
| Fornacina | 824.8 | 71 | 699.6 | 787.1 | 436.0 | 80.5 | 351.0 | 950.3 | 1514.8 | 590.8 | 156.4 | 924.1 |
| Nave di Rosano | 4198.4 | 71 | 1837.9 | 1688.3 | 2016.3 | 16.3 | 327.9 | 2492.9 | 2022.7 | 3049.7 | 33.7 | 1027.0 |
| Ponte Falciani | 119.3 | 40 | 141.3 | 114.7 | 74.3 | 54.3 | 40.4 | 280.7 | 172.0 | 114.0 | 50.8 | 57.9 |
| Praticello | 37.3 | 17 | 92.3 | 74.7 | 17.9 | 316.2 | 56.7 | 128.8 | 107.3 | 26.7 | 301.7 | 80.6 |
| Carmignanello | 110.9 | 15 | 212.3 | 202.8 | 36.5 | 455.3 | 166.2 | 318.0 | 283.7 | 54.3 | 423.0 | 229.5 |
| Gamberame | 156.6 | 43 | 239.6 | 267.4 | 149.2 | 79.3 | 118.2 | 338.9 | 394.8 | 221.1 | 78.5 | 173.7 |
| S.Piero a Ponti | 267.9 | 17 | 385.3 | 379.1 | 208.8 | 81.5 | 170.3 | 570.1 | 532.3 | 308.9 | 72.3 | 223.4 |
| Ponte di Calcaiola | 17.5 | 12 | 98.9 | 49.4 | 4.8 | 917.9 | 44.5 | 152.9 | 89.1 | 7.4 | 1108.6 | 81.7 |
| Burgianico | 13.5 | 25 | 39.7 | 62.4 | 15.2 | 311.8 | 47.3 | 70.8 | 99.1 | 22.6 | 338.1 | 76.5 |
| Poggio a Caiano | 439.3 | 16 | 336.5 | 365.8 | 288.3 | 26.9 | 77.5 | 474.0 | 527.1 | 429.5 | 22.7 | 97.6 |
| Brucianesi | 5590.7 | 21 | 1764.6 | 1923.3 | 2722.9 | 29.4 | 799.7 | 2063.4 | 2622.1 | 4102.8 | 36.1 | 1480.7 |
| Sambuca | 118.0 | 25 | 115.2 | 142.2 | 78.3 | 81.8 | 64.0 | 227.3 | 251.7 | 123.2 | 104.4 | 128.6 |
| Castelfiorentino | 799.2 | 46 | 308.6 | 452.4 | 381.2 | 18.7 | 71.1 | 500.0 | 794.3 | 580.1 | 36.9 | 214.2 |
| Nievole Colonna | 38.0 | 33 | 35.7 | 41.4 | 33.3 | 24.3 | 8.1 | 54.4 | 64.2 | 49.9 | 28.7 | 14.3 |
| Molino Parlanti | 4.7 | 33 | 2.1 | 9.5 | 17.3 | 44.7 | 7.7 | 3.1 | 10.8 | 25.9 | 58.4 | 15.1 |
| Molino Narducci | 47.8 | 15 | 88.8 | 64.8 | 81.5 | 20.5 | 16.7 | 141.1 | 106.4 | 121.7 | 12.5 | 15.2 |
| Capannoli | 334.2 | 31 | 250.7 | 259.1 | 192.6 | 34.5 | 66.5 | 652.9 | 334.3 | 292.9 | 14.1 | 41.4 |
| San Giovanni alla Vena | 8631.4 | 75 | 1941.4 | 2013.9 | 3965.8 | 49.2 | 1951.9 | 2611.3 | 2510.1 | 5973.5 | 58.0 | 3463.4 |
| Cartiera Valgiano | 5.6 | 19 | 2.2 | 17.6 | 6.2 | 181.3 | 11.3 | 3.2 | 24.4 | 9.5 | 155.9 | 14.9 |

| | | Q100 [$m^3/s$] | | | | | Q200 [$m^3/s$] | | | | | Q500 [$m^3/s$] | | | | |
|---|---|---|---|---|---|---|---|---|---|---|---|---|---|---|---|---|
| **COD** | **Name** | **nsRFA** | **TK** | **Mobidic** | **Er (%)** | **EA** | **nsRFA** | **TK** | **Mobidic** | **Er (%)** | **EA** | **nsRFA** | **TK** | **Mobidic** | **Er (%)** | **EA** |
| 4379 | Stia | 165.5 | 99.8 | 65.0 | 53.5 | 34.7 | 201.8 | 100.2 | 72.4 | 38.4 | 27.8 | 260.3 | 99.4 | 82.6 | 20.3 | 16.8 |
| 4400 | Pollino | 411.2 | 973.7 | 530.5 | 83.6 | 443.3 | 413.3 | 1113.0 | 591.8 | 88.1 | 521.3 | 414.8 | 1314.5 | 676.5 | 94.3 | 637.9 |
| 4411 | Subbiano | 1503.3 | 637.7 | 894.0 | 28.7 | 256.3 | 1695.3 | 632.2 | 1000.8 | 36.8 | 368.6 | 1961.2 | 623.1 | 1148.0 | 45.7 | 524.9 |
| 4521 | Ponte ferrovia Fi-Roma | 663.5 | 948.8 | 892.9 | 6.3 | 55.9 | 737.9 | 1020.9 | 1045.8 | 2.4 | 24.8 | 836.1 | 1113.2 | 1241.8 | 10.4 | 128.5 |
| 4560 | Ponte Romito | 1676.6 | 1684.5 | 2014.5 | 16.4 | 330.0 | 1820.1 | 1877.1 | 2315.2 | 18.9 | 438.1 | 2010.6 | 2127.7 | 2712.3 | 21.6 | 584.7 |
| 4568 | Bucine | 246.2 | 284.9 | 200.2 | 42.4 | 84.8 | 273.4 | 315.1 | 234.0 | 34.7 | 81.1 | 309.3 | 355.8 | 278.1 | 27.9 | 77.7 |
| 4610 | Ponte del Bilancino | 763.0 | 405.1 | 10.3 | 3830.2 | 394.8 | 854.1 | 453.8 | 11.5 | 3836.5 | 442.3 | 979.2 | 520.1 | 13.2 | 3837.9 | 506.9 |
| 4641 | Fornacina | 1056.2 | 1668.7 | 664.6 | 151.1 | 1004.2 | 1161.8 | 1915.0 | 742.3 | 158.0 | 1172.7 | 1301.1 | 2252.2 | 850.6 | 164.8 | 1401.5 |
| 4659 | Nave di Rosano | 2769.8 | 2204.5 | 3563.6 | 38.1 | 1359.0 | 3045.7 | 2329.7 | 4089.7 | 43.0 | 1760.0 | 3409.6 | 2506.0 | 4787.0 | 47.7 | 2281.0 |
| 4710 | Ponte Falciani | 357.8 | 201.0 | 132.3 | 52.0 | 68.7 | 446.6 | 233.9 | 150.6 | 55.3 | 83.3 | 584.3 | 283.8 | 174.7 | 62.5 | 109.1 |
| 4750 | Praticello | 144.9 | 121.1 | 31.5 | 285.1 | 89.7 | 161.5 | 135.0 | 36.6 | 268.7 | 98.4 | 183.9 | 153.2 | 43.3 | 253.7 | 109.9 |
| 4760 | Carmignanello | 366.8 | 317.0 | 63.8 | 396.9 | 253.2 | 417.9 | 349.7 | 74.2 | 371.3 | 275.5 | 489.6 | 392.0 | 87.8 | 346.7 | 304.3 |
| 4779 | Gamberame | 380.5 | 453.8 | 259.8 | 74.7 | 194.0 | 421.5 | 515.2 | 301.6 | 70.8 | 213.6 | 475.3 | 600.9 | 356.5 | 68.6 | 244.4 |
| 4791 | S.Piero a Ponti | 654.7 | 593.8 | 362.5 | 63.8 | 231.3 | 743.1 | 656.4 | 420.6 | 56.1 | 235.8 | 866.3 | 737.6 | 496.9 | 48.4 | 240.7 |
| 4820 | Ponte di Calcaiola | 175.8 | 108.2 | 8.7 | 1139.8 | 99.5 | 198.5 | 130.5 | 10.2 | 1179.8 | 120.3 | 228.5 | 163.4 | 12.1 | 1247.1 | 151.3 |
| 4860 | Burgianico | 86.8 | 113.2 | 26.6 | 324.8 | 86.6 | 104.6 | 127.6 | 31.0 | 312.1 | 96.6 | 131.2 | 146.5 | 36.7 | 299.6 | 109.9 |
| 4875 | Poggio a Caiano | 532.5 | 633.9 | 504.9 | 25.6 | 129.0 | 590.8 | 751.8 | 585.7 | 28.4 | 166.1 | 667.5 | 926.6 | 691.7 | 34.0 | 234.9 |
| 4901 | Brucianesi | 2168.8 | 2840.9 | 4792.0 | 40.7 | 1951.1 | 2265.4 | 3128.0 | 5502.7 | 43.2 | 2374.7 | 2382.3 | 3484.3 | 6442.7 | 45.9 | 2958.4 |
| 4910 | Sambuca | 289.0 | 309.3 | 144.4 | 114.1 | 164.8 | 360.0 | 373.0 | 165.8 | 125.0 | 207.3 | 469.7 | 469.3 | 193.8 | 142.2 | 275.5 |
| 4971 | Castelfiorentino | 592.9 | 1051.2 | 669.4 | 57.0 | 381.8 | 692.9 | 1385.9 | 759.1 | 82.6 | 626.8 | 837.0 | 2014.2 | 876.7 | 129.7 | 1137.5 |
| 5040 | Nievole Colonna | 62.3 | 76.5 | 58.6 | 30.5 | 17.9 | 70.2 | 89.3 | 68.1 | 31.1 | 21.2 | 80.5 | 108.2 | 80.6 | 34.2 | 27.6 |
| 5050 | Molino Parlanti | 3.5 | 11.9 | 30.5 | 61.1 | 18.6 | 3.9 | 12.7 | 35.5 | 64.4 | 22.9 | 4.5 | 13.5 | 42.1 | 68.0 | 28.6 |
| 5070 | Molino Narducci | 166.2 | 120.6 | 143.3 | 15.9 | 22.8 | 193.0 | 137.0 | 166.8 | 17.9 | 29.8 | 231.4 | 157.9 | 197.8 | 20.2 | 39.9 |
| 5130 | Capannoli | 981.3 | 425.2 | 338.1 | 25.8 | 87.1 | 1474.0 | 451.0 | 383.4 | 17.6 | 67.6 | 2523.4 | 544.7 | 442.9 | 23.0 | 101.8 |
| 5191 | San Giovanni alla Vena | 2879.7 | 3010.0 | 6953.4 | 56.7 | 3943.4 | 3140.2 | 3309.1 | 7960.4 | 58.4 | 4651.2 | 3475.3 | 3751.9 | 9283.7 | 59.6 | 5531.8 |
| 5270 | Cartiera Valgiano | 3.7 | 29.2 | 11.3 | 158.5 | 17.9 | 4.1 | 33.9 | 13.2 | 156.2 | 20.6 | 4.7 | 40.8 | 15.7 | 159.2 | 25.0 |

The comparison between MOBIDIC and Top-kriging results have shown a relatively good agreement for the main Arno river sub-basin despite the simplifications of the numerical model. However, big relative error is found for the smallest catchments Ponte di Calcaiola, Praticello, Burgianico and Cartiera Valgiano as well as in Ponte del Bilancino, Carmignanello and Stia river sections. In the biggest catchments Nave di Rosano, Brucianesi, S. Giovanni alla Vena the absolute error is very high but we have to remind that the comparison is here carried out without consider the Areal Reduction Factors (ARF) for the Precipitation. Nevertheless, the influence of the ARF parameter in the design for hydrologic extremes is preliminary explored. It is assumed that the hydrographs for different $T_r$ are computed using hyetographs of 24 hours duration. In this way, the evaluation of ARF is performed by means of the empirical relation proposed by Moisello and Papiri (1986) finding for the precipitation of duration 24 hours the values shown in Table 8.3. Unfortunately, during the simulation runs the precipitation values for the critical duration are not stored (this is not implemented yet in the MOBIDIC module). Nevertheless, we can see for all $T_r$ a considerable reduction of flood quantile, even than 1500 $m^3/s$ for the highest $T_r$ in S. Giovanni alla Vena hydrometric station. In conclusion, for an accurate design flood estimate corresponding to a given risk level by MOBIDIC hydrological model the ARF parameter assessment should be considered.

**Table 8.3: Preliminary analysis on the evaluation of the Areal Reduction Factors (ARF) for the Precipitation in Nave di Rosano, Brucianesi, S. Giovanni alla Vena catchments.**

| | | Moisello e Papiri (1986) | | | | | | | | | | | |
|---|---|---|---|---|---|---|---|---|---|---|---|---|---|
| Hydrometric stations | Area ($km^2$) | β | ARF(24,A) | Q10 ($m^3/s$) | d(Q10) (h) | Q50 ($m^3/s$) | d(Q50) (h) | Q100 ($m^3/s$) | d(Q100) (h) | Q200 ($m^3/s$) | d(Q200) (h) | Q500 ($m^3/s$) | d(Q500) (h) |
| Nave di Rosano | 4198.4 | 0.6 | 0.88 | 2016.3 | 28.25 | 3049.7 | 28.00 | 3563.6 | 27.75 | 4089.7 | 27.75 | 4787.0 | 27.75 |
| | | | | 1830.5 | 24 | 2698.4 | 24 | 3149.2 | 24 | 3626.2 | 24 | 4274.9 | 24 |
| Brucianesi | 5590.7 | 0.6 | 0.87 | 2722.9 | 29.75 | 4102.8 | 29.25 | 4792.0 | 29.25 | 5502.7 | 29.25 | 6442.7 | 29.00 |
| | | | | 2427.1 | 24 | 3612.2 | 24 | 4189.6 | 24 | 4645.4 | 24 | 5708.9 | 24 |
| San Giovanni alla Vena | 8631.4 | 0.6 | 0.84 | 3965.8 | 31.75 | 5973.5 | 31.50 | 6953.4 | 31.25 | 7960.4 | 31.25 | 9283.7 | 31.25 |
| | | | | 3325.7 | 24 | 5033.9 | 24 | 5840.2 | 24 | 6714.8 | 24 | 7785.3 | 24 |

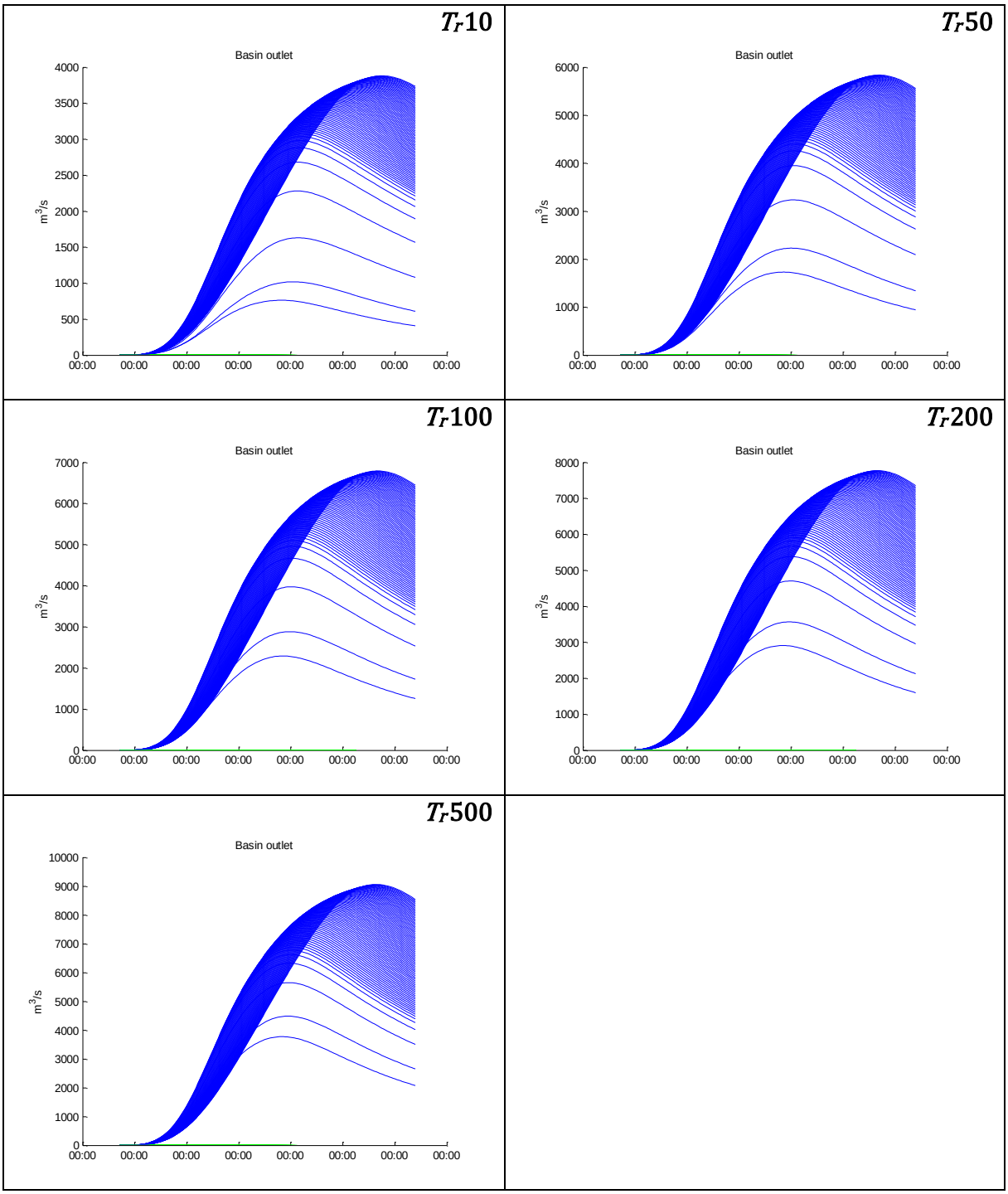


**Figure 8.1: Hydrographs computed by MOBIDIC module for flood hydrograph application for all rainfall durations (6-24h) and return periods (10, 50, 100, 200, 500 years).**

## 8.2 Flood risk assessment and uncertainty quantification

A preliminary discussion on the ways to convey the results of uncertainty quantification to stakeholders and to communicate the outcomes of this dissertation for flood risk assessment is here presented.

By a common definition, flood risk can be evaluated as a function of hazard, vulnerability and exposure (Crichton, 1999; Kron, 2002). Flood risk assessment is therefore comprised of two parts: a hazard and vulnerability assessment. The hazard assessment investigates the magnitude of flood events, which are associated to a certain exceedance probability, whereas the vulnerability part assesses the impact of the flooding on specified targets, e.g., building, people or infrastructure (Apel et al., 2008).

The flood risk assessment and subsequent development of mitigation strategies are at the centre of the Floods Directive (2007/60/EC), the legislation of the European Parliament on the management of flood risks. It requires Member States to engage their government departments, agencies and authorities to work for prevention and protection activities by means of flood hazard and risk maps evaluation. Flood Risk Management Plans (PGRA – Piano di Gestione Rischio Alluvioni) have been drawn up by the Unit of Management – UoM at the end of December 2015 with the aim to communicate to policy makers, stakeholders and the citizens, the prevention, protection, monitoring and post event measures proposed. In PGRA flood risk management is implemented through restraint actions of the negative consequences that a benchmark flood event may have on human health, environmental and cultural heritage, economic activities. The UoM of Northern Apennines River Basin District considered as benchmark event a flood having a 200-year recurrence interval or return period.

It is well known that hydrologists would prefer the use of recurrence interval terminology because tends to be more understandable for flood intensity comparisons, instead of return period because, scientifically, it is a misinterpretation of terminology that leads to a misconception of what a 200-year flood really is. For convenience's sake of representation, the $T_r$ is often used to replace the concept of probability of exceeding (or not exceeding) associated with flood events. The USGS instead often refer to the percent chance of occurrence as an Annual Exceedance Probability (AEP). For example, 0.5 AEP flood has a 50% chance of occurring in any given year, and this corresponds to a 2-year recurrence interval flood. The probability of the occurrence of a given flood event is estimated through a frequency analysis and the return period, that represents the average number of years between floods of a certain size, it is based on the probability that the given event will be equaled or exceeded in any given year. In fact, hazard is modelling with a probabilistic approach. Moreover, flood damage assessment is associated with large uncertainties. Given the enormous uncertainty of flood damage estimates the

refinement of flood damage data collection and modelling are major issues for further empirical and methodological improvements.

Therefore, flood risk assessment should always be accompanied by an uncertainty assessment (UA) in order to assist consequent decision properly. For this reason, the studies in quantification of uncertainties in flood risk assessments got increased attention.

In Apel et al. (2004) a stochastic flood risk model is used for risk and uncertainty analysis in a Monte Carlo framework. The Monte Carlo framework is hierarchically structured in two layers representing the two sources of uncertainty in the model system separated into aleatory uncertainty due to the variability of the system and epistemic uncertainty due to incomplete knowledge of the system. The model allows to calculate probabilities of occurrence for events of different magnitudes along with the expected economic damage in a target area in the first layer of the Monte Carlo framework, i.e. to assess the economic risks, and to derive uncertainty bounds associated with these risks in the second layer. It has been shown that the uncertainty caused by epistemic sources significantly alters the results obtained with aleatory uncertainty alone. The same authors in 2008 proposed a dynamic-probabilistic method which enables a cumulated flood risk assessment of a complete river reach considering dike failures at all dike locations. The model uses simple but computational efficient modules to simulate the complete process chain of flooding. These modules are embedded into a Monte Carlo framework enabling a risk assessment which is physically based, probabilistic and not based on scenarios because the real flooding process are modelled. The model also provides uncertainty estimates by quantifying various epistemic uncertainty sources of the hazard as well as the vulnerability part in a second layer of Monte Carlo simulations. These uncertainty estimates are associated to defined return intervals of the model outputs, i.e., the derived flood frequencies at the end of the reach and the risk curves for the complete reach, thus providing valuable information for the interpretation of the results. By separating single uncertainty sources a comparison of the contribution of different uncertainty sources to the overall predictive uncertainty in terms of derived flood frequencies and monetary risks could be performed. This revealed that the major uncertainties are extreme value statistics, respectively the length of the data series used and the stage-discharge relation used for the transformation of discharge into water levels in the river (Apel et al., 2008).

Up to now at national scale the uncertainty analysis during the drafting of PGRA has not been performed by the authorities, luckily this plan has a dynamic nature, precisely because of its content and its purpose, thus the proposed methodology for parameter identification here described could be applied in the future. Moreover, we assessed the predictive uncertainty of the models, explaining that the results are affected by huge uncertainty. Nevertheless, flood frequency analysis is still done without accounting for it, some works consider the uncertainties that might be affected the flood quantiles assessment highlighting the inaccuracy of the

measurements or the presence of short or discontinuous time series, although it is a crucial point the assessment of the confidence levels of the magnitude of the predictions or the associated error.

Despite uncertainty analysis is the subject of an increasing research activity by hydrologists, the application of UA methods is limited because the know-how transfer about uncertainty in hydrology from scientists to end-users is even now difficult. The researchers on the one hand are trying to fill the gap of a coherent terminology and a systematic approach and the decision maker on the other hand push to better quantify accuracy of model predictions. It is referred to as *linguistic uncertainty* affecting the UQ topic in hydrology (Beven, 2009a; Regan et al., 2003), it is the reason why some basic definitions are provided in the Chapter 4. Communicating uncertainty to end-users should not undermine their confidence in models (Beven, 2006; Faulkner et al., 2007; Pappenberger and Beven, 2006), but rather increase it through an improved perception of the underlying natural processes and an increased awareness of model reliability. Uncertainty does not mean lack of knowledge or lack of modeling capability but that the predicted value of a hydrological variable is uncertain. A proper estimation of uncertainty is the way forward to a reliable hydrological design and therefore a proper management of the environment and water resources (Montanari, 2011).

Flood risk management is defined by Beven and Hall (2014) a process of decision making under uncertainty. This book concludes with a Chapter on Translating Uncertainty in Flood Risk Science, affirming that scientific formulations of future risk are expressed in a complex language which is relatively inaccessible. The authors underline the different meaning of the communication, which can be understood as a means of transferring information from one to another or it may be viewed as a process of negotiation whereby testing or re-evaluating ideas with someone else. Communication also represents a learning process, but to do this it requires a system of transmission. The last step of translation, is the more complex: translating uncertainties into a set of different conceptualizations of risk, in order to communicate with stakeholders, it is a considerable additional challenge for the flood risk management professionals. Knowledge should be provided in a form that is accessible and useful to all the stakeholders because policy makers and public are not able in understanding uncertainty; moreover, the concepts of "uncertainty" and "risk" are perceived in different ways by different communities and different people. Only when both scientists and public institutions work together this gap may be bridged (Pappenberger and Beven, 2006). Being able to communicate in the right way is a very important key for the modeler because also a little misunderstanding in the confidence on the results can lead to a loss of credibility. In most cases the cascade of uncertainties through the multiple model components increase the overall uncertainty: therefore, a careful and detailed analysis of this issue is required in order to understand the different implications (such as limited data, model uncertainties, changes in the flooding system over the long term, etc.) that make difficult the task of

the decision makers. In the flood risk mapping there are several sources of uncertainty: uncertainties in rating curve extrapolation, in flood plain topography, in the model structure, in flood plain infrastructure and in the observations used in the model conditioning. Other sources of uncertainty could be in assessing the effects of future catchment change and climate change and uncertainty in fragility of defenses and mitigation measures.

Actually the practice of uncertainty analysis and use of the results of such analysis in decision making is not widespread for seven reasons according to the opinion of Pappenberger and Beven (2006):

- Uncertainty Analysis Is Not Necessary Given Physically Realistic Models;
- Uncertainty Analysis Is Not Useful in Understanding Hydrological and Hydraulic Processes;
- Uncertainty (Probability) Distributions Cannot Be Understood by Policy Makers and the Public;
- Uncertainty Analysis Cannot Be Incorporated into the Decision-Making Process;
- Uncertainty Analysis Is Too Subjective;
- Uncertainty Analysis Is Too Difficult to Perform;
- Uncertainty Does Not Really Matter in Making the Final Decision;

Moreover, an uncertainty analysis takes time, necessary data are not always available, so new data collection campaigns may need to be commissioned resulting in an increase of the risk analysis costs. In the final part of the paper, the authors suggest to follow a Code of Practice that makes uncertainty analysis an integral part of the modeling process, guidance needed to define best practice across all stakeholder groups. However, it remains the critical point of the discussion of the results: in fact, the uncertainty analysis requires careful interpretation in order to understand the meaning and significance of the results. It is through this process of scrutiny and discussion that the most useful insights for decision makers are obtained (Hall and Solomatine, 2008).

The success of collaborative knowledge products has been assessed in the global environmental change research community and the experience in the communication of uncertainty to the decision makers and public institutions is growing. In particular in van der Sluijs et al. (2005) it is highlighted the importance of engaging stakeholders from the first step of the work, identifying the target audiences and then using appropriate language to communicate with them about the uncertainties. Beside the numerical results and their implications for the decision makers, the limits of the data set and the analysis methods should be made clear; moreover, the areas of ignorance should be highlighted. This step probably is the most critical as well as

important, because without it the technical analysis will not be used by anyone else except by the scientific community.
Another good method to simplify the communication between the parties could be to explain, directly in the flood risk maps, what the return period exactly is: with this aim, it should be draft a Guidelines for Probabilistic Flood Risk Mapping as suggested by Beven and Hall (2014). For example, under a risk map should be written that the $T_r$ is the average amount of time in years that you would expect a flood of a particular size to occur once. I.e. a flood with 100 years $T_r$ would be expected to occur 10 times in a century. Or, if there is the possibility to choose a probability of flooding, expressed as a percent value, it may be useful to explain what corresponds to the entered value. For example, 90% correspond to 90% chance that the 100 years flood will be larger than the extent shown in the map. Also other considerations could be added to further simplify the understanding of the maps. If these kinds of information are contained in the risk maps, the decision makers may be able to interpret the results in the right way, limiting the understanding and communication problems. Uncertainty estimation is a means of maintaining integrity (and avoiding being wrong) but it requires a correct translation that could allow us to successfully reach a better communication between scientists and end users.

## 8.3 Outlook

The proper analysis of the accuracy of the proposed methods for parameter identification is performed. However, we have not properly analyzed the computation time as well as the memory consumption, in future studies an analysis of the computation cost might be conducted in order to know which method could be best applicable in practice.
Modelling the soil saturation hydraulic conductivity $Ks$ as a random field at the river basin scale, at least in a pilot case characterized by the worst soil characteristics related to runoff process generation, could represent an original improvement in the hydrological modelling.
As reported in section 6.2, for practical utilization a complete procedure of identification should be described with the help of more measurements of flood events. Moreover, usually in a complete update procedure both the coefficients and the state should be updated. Here it is shown in principle the model parameter identification procedure in hydrologic modelling. However, at the start of the research activity in this field, the numerical evaluation of the Bayesian updating methods analyzed has been carried out considering the Lorenz-84 model. This is defined by a set of three state variables $x,y,z$ and the state evolution of this model is described by a set of ordinary differential equations (ODEs). In this work we update both the state and the parameters instead of only update the parameters starting integration from the beginning until the hypothetic next moment when the update is done. Besides, in hydrological modelling the current state might be updated and

integration may continue from that step to the next if it is possible to start from a given time to another one and to know what the state is. MOBIDIC is very feasible for this purpose because for every hydrologic balance it allow to save the state for every time moment according the data resolution, for example every 15 min. Numerical simulations with this sequential update approach, assuming to collect time series of discharges longer than 6 days, might be investigated in order to perform a complete identification procedure comparing two different approaches.

Since MCMC method is one of the most commonly used techniques for parameter estimation of the types considered in this hydrologic application, we tried to implement MCMC update according Metropolis-Hastings algorithm. In MCMC methods, the Markov chain is constructed such that the asymptotic distribution of the chain is the Bayesian posterior distribution that means the posterior as an equilibrium distribution. According the Metropolis scheme, a sequence of samples is generated depending on the previous sample in the chain, due to this, the speed of the convergence greatly depends on the initial choice. However, it is a method slowly convergent and often computationally infeasible especially when one deals with large-scale problems. During the runs it happened that the initial point for implemented the algorithm is not properly identified, the error saying none of proposed samples and the update procedure fails because the posterior remains exactly the same as the prior. Unfortunately, more time is necessary to better understand the complexity of the procedure, therefore in this dissertation a comparison with MCMC approach is not carried out. MCMC approach might be analyzed in future research activities to complete the investigation of numerical approaches to Bayesian updating in hydrological modelling.

Regarding the couple Uncertainty Quantification-Flood Risk mitigation, the work could be extended in order to develop a Code of Practice that makes uncertainty analysis an integral part of the modeling process providing guide lines for the Flood risk mapping. Finally, a complete flood risk assessment methodology for making the final decision by policymaker, wherein the importance to use uncertainty analysis findings should be highlighted, could be introduced.

# References


Ajami, N.K., Duan, Q., Sorooshian, S., 2007. An integrated hydrologic Bayesian multimodel combination framework: Confronting input, parameter, and model structural uncertainty in hydrologic prediction. J. Hydrometeorol. 8, 755–768. doi:10.1029/2005WR004745

Ali, G., Tetzlaff, D., Soulsby, C., McDonnell, J.J., Capell, R., 2012. A comparison of similarity indices for catchment classification using a cross-regional dataset. Adv. Water Resour. 40, 11–22. doi:10.1016/j.advwatres.2012.01.008

Apel, H., Merz, B., Thieken, A.H., 2008. Quantification of uncertainties in flood risk assessments. Int. J. River Basin Manag. 6, 149–162. doi:10.1080/15715124.2008.9635344

Apel, H., Thieken, A.H., Merz, B., Blöschl, G., 2004. Flood risk assessment and associated uncertainty. Nat. Hazards Earth Syst. Sci. 4, 295–308. doi:10.5194/nhess-4-295-2004

Archfield, S.A., Pugliese, A., Castellarin, A., Skøien, J.O., Kiang, J.E., 2013. Topological and canonical kriging for design flood prediction in ungauged catchments: An improvement over a traditional regional regression approach? Hydrol. Earth Syst. Sci. 17, 1575–1588. doi:10.5194/hess-17-1575-2013

Archfield, S.A., Vogel, R.M., 2010. Map correlation method: Selection of a reference streamgage to estimate daily streamflow at ungaged catchments. Water Resour. Res. 46. doi:10.1029/2009WR008481

Aronica, G.T., Apel, H., Di Baldassarre, G., Schumann, G.J.P., 2013. HP - Special Issue on Flood Risk and Uncertainty. Hydrol. Process. 27, 1291–1291. doi:10.1002/hyp.9812

Bárdossy, A., 2006. Copula-based geostatistical models for groundwater quality parameters. Water Resour. Res. 42, W11416. doi:10.1029/2005WR004754

Bárdossy, A., Li, J., 2008. Geostatistical interpolation using copulas. Water Resour. Res. 44, W07412. doi:10.1029/2007WR006115

Bárdossy, A., Pegram, G.G.S., Samaniego, L., 2005. Modeling data relationships with a local variance reducing technique: Applications in hydrology. Water Resour. Res. 41. doi:10.1029/2004WR003851

Bazargan, H., Christie, M., Tchelepi, H., 2013. Efficient Markov Chain Monte Carlo Sampling Using Polynomial Chaos Expansion, in: Proceedings of the SPE Reservoir Simulation Symposium. Society of Petroleum Engineers, The Woodlands, Texas, United States. doi:10.2118/163663-MS

Beran, M., Hosking, J.R.M., Arnell, N., 1986. Comment on "Two-Component Extreme Value Distribution for Flood Frequency Analysis" by Fabio Rossi, Mauro Florentino, and Pasquale Versace. Water Resour. Res. 22, 263–266. doi:10.1029/WR022i002p00263

Beven, K.J., 2009a. Environmental Modelling: An Uncertain Future? An Introduction to Techniques for Uncertainty Estimation in Environmental Prediction, Routledge Taylor and Francis group. London and New York.

Beven, K.J., 2009b. Comment on "Equifinality of formal (DREAM) and informal (GLUE) Bayesian approaches in hydrologic modeling?" by J. A. Vrugt, C. J. F. ter Braak, H. V. Gupta and B.A. Robinson. Stoch. Environ. Res. Risk Assess. 23, 1059–1060. doi:10.1007/s00477-008-0283-x

Beven, K.J., 2006. On undermining the science? Hydrol. Process. 20, 3141–3146. doi:10.1002/hyp.6396

Beven, K.J., 1993. Prophecy, reality and uncertainty in distributed hydrological modelling. Adv. Water Resour. 16, 41–51. doi:http://dx.doi.org/10.1016/0309-1708(93)90028-E

Beven, K.J., Binley, A., 2014. GLUE: 20 years on. Hydrol. Process. 28, 5897–5918. doi:10.1002/hyp.10082

Beven, K.J., Binley, A., 1992. The future of distributed models: Model calibration and uncertainty prediction. Hydrol. Process. 6, 279–298. doi:10.1002/hyp.3360060305
Beven, K.J., Hall, J., 2014. Applied Uncertainty Analysis for flood Risk Management. Imperial College Press, London, 663 pp.
Bivand, R.S., Pebesma, E., Gómez-Rubio, V., 2013. Applied Spatial Data Analysis with R, 2nd ed. ed, Applied Spatial Data Analysis with R. UseR! Series, Springer-Verlag New York. doi:10.1007/978-0-387-78171-6
Blöschl, G., 2016. Predictions in ungauged basins - where do we stand?, in: Proceedings of the IAHS. pp. 373, 57–60. doi:10.5194/piahs-373-57-2016
Blöschl, G., Sivapalan, M., Wagener, T., Viglione, A., Savenije, H.H.G., 2013. Runoff prediction in ungauged basins : synthesis across processes, places and scales. Cambridge University Press, Cambridge, UK, 465 pp.
Bonham-Carter, G., 1994. Geographic information systems for geoscientists: modelling with GIS. Pergamon, 398 pp.
Brath, A., Castellarin, A., Montanari, A., 2003. Assessing the reliability of regional depth-duration-frequency equations for gaged and ungaged sites. Water Resour. Res. 39. doi:10.1029/2003WR002399
Bulygina, N., Gupta, H.V., 2009. Estimating the uncertain mathematical structure of a water balance model via Bayesian data assimilation. Water Resour. Res. 45, W00B13. doi:10.1029/2007WR006749
Burn, D.H., 1990. Evaluation of Regional Flood Frequency Analysis With a Region of Influence Approach. Water Resour. Res. 26, 2257–2265.
Burn, D.H., Goel, N.K., 2000. The formation of groups for regional flood frequency analysis. Hydrol. Sci. J. 45, 97–112. doi:10.1080/02626660009492308
Campo, L., Caparrini, F., Castelli, F., 2006. Use of multi-platform, multi-temporal remote-sensing data for calibration of a distributed hydrological model: an application in the Arno basin, Italy. Hydrol. Process. 20, 2693–2712. doi:10.1002/hyp.6061
Caporali, E., Cavigli, E., Petrucci, A., 2008. The index rainfall in the regional frequency analysis of extreme events in Tuscany (Italy). Environmetrics 19, 714–724. doi:10.1002/env.949
Caporali, E., Chiarello, V., Rossi, G., 2014. Analisi di frequenza regionale delle precipitazioni estreme. In Accordo di collaborazione scientifica RT-UNIFI per attività di ricerca per la mitigazione del rischio idraulico nella regione Toscana. Macroattività B - Modellazione idrologica Attività B1: Regionalizzazione precipitazioni. Scientific report (in Italian language).
Castellarin, A., Burn, D.H., Brath, A., 2001. Assessing the effectiveness of hydrological similarity measures for flood frequency analysis. J. Hydrol. 241, 270–285. doi:10.1016/S0022-1694(00)00383-8
Castelli, F., 2014. Implementazione modello distribuito per la Toscana MOBIDIC. In Accordo di collaborazione scientifica RT-UNIFI per attività di ricerca per la mitigazione del rischio idraulico nella regione Toscana. Macroattività B-Modellazione idrologica, Attività B2: Modellazione idrologica caso pilota. Scientific report (in Italian language).
Castelli, F., Menduni, G., Mazzanti, B., 2009. A distributed package for sustainable water management: a case study in the Arno basin, in: The Role of Hydrology in Water Resoures Management (Proceedings of a Symposium Held on the Island of Capri, Italy, October 2008), IAHS Publ. 327. pp. 52–61.
Castiglioni, S., Castellarin, A., Montanari, A., 2009. Prediction of low-flow indices in ungauged basins through physiographical space-based interpolation. J. Hydrol. 378, 272–280. doi:10.1016/j.jhydrol.2009.09.032
Castiglioni, S., Castellarin, A., Montanari, A., Skøien, J.O., Laaha, G., Blöschl, G., 2011. Smooth regional estimation of low-flow indices: physiographical space based interpolation and top-kriging. Hydrol. Earth Syst. Sci. 15, 715–727. doi:10.5194/hess-15-

715-2011
Castillo, A., Castelli, F., Entekhabi, D., 2014. Gravitational and capillary soil moisture dynamics for hillslope-resolving models. Hydrol. Earth Syst. Sci. Discuss. 11, 7133–7168. doi:10.5194/hessd-11-7133-2014
Castrignanò, A., 2010. Introduction to spatial data processing. Aracne editrice Srl, 112 pp.
CFR, 2013. hydro-meteorological event report on 23-24.10.2013.
Chebana, F., Ouarda, T.B.M.J., 2011a. Multivariate quantiles in hydrological frequency analysis. Environmetrics 22, 63–78. doi:10.1002/env.1027
Chebana, F., Ouarda, T.B.M.J., 2011b. Multivariate extreme value identification using depth functions. Environmetrics 22, 441–455. doi:10.1002/env.1089
Chokmani, K., Ouarda, T.B.M.J., 2004. Physiographical space-based kriging for regional flood frequency estimation at ungauged sites. Water Resour. Res. 40, W12514. doi:10.1029/2003WR002983
Claps, P., Fiorentino, M., Laio, F., 2003. Scale di deflusso di piena di corsi d'acqua naturali, in: La Difesa Idraulica Del Territorio 2003. (in Italian language), pp. 1–11.
Crestani, E., Camporese, M., Salandin, P., 2015. Assessment of hydraulic conductivity distributions through assimilation of travel time data from ERT-monitored tracer tests. Adv. Water Resour. 84, 23–36. doi:10.1016/j.advwatres.2015.07.022
Crichton, D., 1999. The risk triangle. Nat. Disaster Manag. 102–103.
Cunderlik, J.M., Burn, D.H., 2006. Switching the pooling similarity distances: Mahalanobis for Euclidean. Water Resour. Res. 42, W03409. doi:10.1029/2005WR004245
Dalrymple, T., 1960. Flood-Frequency Analyses. Part 3. Flood-flow techniques. Man. Hydrol. 80.
Daviau, J.-L., Adamowski, K., Patry, G.G., 2000. Regional flood frequency analysis using GIS, L-moment and geostatistical methods. Hydrol. Process. 14, 2731–2753.
De Marsily, G., Ahmed, S., 1987. Application of kriging techniques in groundwater hydrology. J. Geol. Soc. India 29, 57–82.
De Michele, C., Salvadori, G., 2003. A Generalized Pareto intensity-duration model of storm rainfall exploiting 2-Copulas. J. Geophys. Res. 108, 1–11. doi:10.1029/2002JD002534
Domeneghetti, A., Castellarin, A., Brath, A., 2012. Assessing rating-curve uncertainty and its effects on hydraulic model calibration. Hydrol. Earth Syst. Sci. 16, 1191–1202. doi:10.5194/hess-16-1191-2012
Engl, H.W., Hanke, M., Neubauer, A., 1996. Regularization of inverse problems. Dordrecht, Kluwer. doi:10.1007/978-94-009-1740-8
Faulkner, H., Parker, D., Green, C., Beven, K.J., 2007. Developing a translational discourse to communicate uncertainty in flood risk between science and the practitioner. AMBIO A J. Hum. Environ. 36, 692–703. doi:10.1579/0044-7447(2007)36[692:DATDTC]2.0.CO;2
Favre, A.-C., El Adlouni, S., Perreault, L., Thiémonge, N., Bobée, B., 2004. Multivariate hydrological frequency analysis using copulas. Water Resour. Res. 40, 1–12. doi:10.1029/2003WR002456
Fenton, J.D., Keller, R.J., 2001. The Calculation of Streamflow from Measurements of Stage. Technical Report 01/6, Cooperative Research Centre for Catchment Hydrology, Melbourne, Australia, p. 77.
Fiorentino, M., Gabriele, S., Rossi, F., Versace, P., 1987. Hierarchical approach for regional flood frequency analysis. Reg. Flood Freq. Anal.
FitzPatrick, E.A., 1980. Soils, their formation, classification and distribution. Longman, London, New York.
Freer, J., Beven, K.J., Ambroise, B., 1996. Bayesian estimation of uncertainty in runoff production and the value of data: An application of the GLUE approach. Water Resour. Res. 32, 2161–2173.
Gaál, L., Kysel, J., Szolgay, J., 2008. Region-of-influence approach to a frequency analysis of heavy precipitation in Slovakia. Hydrol. Earth Syst. Sci 12, 825–839. doi:10.5194/hess-

12-825-2008
Gabriele, S., Iiritano, G., 1994. Analisi regionale delle piogge in Basilicata. Rapporto interno n. 414, CNR-IRPI, Rende (Cs).
Gamerman, D., Lopes, H.F., 2006. Markov Chain Monte Carlo: Stochastic Simulation for Bayesian Inference, Second Edition.
Gingras, D., Adamowski, K., 1993. Homogeneous region delineation based on annual flood generation mechanisms. Hydrol. Sci. J. 38, 103–121. doi:10.1080/02626669309492649
Goovaerts, P., 1997. Geostatistics for Natural Resources Evaluation. Oxford University Press, New York, 483 pp.
Gottschalk, L., 1993a. Correlation and covariance of runoff. Stoch. Hydrol. Hydraul. 7, 85–101.
Gottschalk, L., 1993b. Interpolation of runoff applying objective methods. Stoch. Hydrol. Hydraul. 7, 269–281.
Gottschalk, L., Leblois, E., Skøien, J.O., 2011. Correlation and covariance of runoff revisited. J. Hydrol. 398, 76–90. doi:10.1016/j.jhydrol.2010.12.011
Götzinger, J., Bárdossy, A., 2008. Generic error model for calibration and uncertainty estimation of hydrological models. Water Resour. Res. 44, W00B07. doi:10.1029/2007WR006691
Gräler, B., Pebesma, E., 2011. The pair-copula construction for spatial data: a new approach to model spatial dependency. Procedia Environ. Sci. 7, 206–211. doi:10.1016/j.proenv.2011.07.036
Grayson, R., Blöschl, G., 2000. Spatial Patterns in Catchment Hydrology Observations and Modelling, Cambridge University Press. Cambridge, 404 pp.
GREHYS, G. de recherche en hydrologie statistique, 1996a. Presentation and review of some methods for regional flood frequency analysis. J. Hydrol. 186, 63–84. doi:10.1016/S0022-1694(96)03042-9
GREHYS, G. de recherche en hydrologie statistique, 1996b. Inter-comparison of regional flood frequency procedures for Canadian rivers. J. Hydrol. 186, 85–103. doi:10.1016/S0022-1694(96)03043-0
Hall, J.W., Solomatine, D., 2008. A framework for uncertainty analysis in flood risk management decisions. Int. J. River Basin Manag. 6, 85–98. doi:10.1080/15715124.2008.9635339
Herschy, R.W., 2002. The uncertainty in a current meter measurement. Flow Meas. Instrum. 13, 281–284. doi:10.1016/S0955-5986(02)00047-X
Herschy, R.W., 1999. Hydrometry: Principles and Practice, 2nd Edn. ed. John Wiley and Sons, New York, NY, p. 376.
Hoeting, J.A., Madigan, D., Raftery, A.E., Volinsky, C.T., 1999. Bayesian model averaging: a tutorial. Stat. Sci. 14, 382–401. doi:10.1214/ss/1009212519
Hosking, J.R.M., Wallis, J.R., 1997. Regional frequency analysis, an approach based on L-moments. Cambridge University Press, Cambridge, UK, 224 pp.
Hosking, J.R.M., Wallis, J.R., 1993. Some statistics useful in regional flood frequency analysis. Water Resour. Res. 29, 271–281.
Hosking, J.R.M., Wallis, J.R., Wood, E.F., 2009. An appraisal of the regional flood frequency procedure in the UK Flood Studies Report. Hydrol. Sci. J. 30, 85–109. doi:10.1080/02626668509490973
Hrachowitz, M., Savenije, H.H.G., Blöschl, G., McDonnell, J.J., Sivapalan, M., Pomeroy, J.W., Arheimer, B., Blume, T., Clark, M.P., Ehret, U., Fenicia, F., Freer, J.E., Gelfan, A., Gupta, H.V., Hughes, D.A., Hut, R.W., Montanari, A., Pande, S., Tetzlaff, D., Troch, P.A., Uhlenbrook, S., Wagener, T., Winsemius, H.C., Woods, R.A., Zehe, E., Cudennec, C., 2013. A decade of Predictions in Ungauged Basins (PUB)—a review. Hydrol. Sci. J. 58, 1198–1255. doi:10.1080/02626667.2013.803183
IPCC, 2012. Managing the Risks of Extreme Events and Disasters to Advance Climate

Change Adaptation. A Special Report of Working Groups I and II of the Intergovernmental Panel on Climate Change [Field, C.B., V. Barros, T.F. Stocker, D. Qin]. Cambridge University Press, Cambridge, UK, and New York, NY, USA, 582 pp.
Isaaks, E.H., Srivastava, R.M., 1989. An Introduction to Applied Geostatistics. Oxford University Press, Toronto, 561 pp.
Jaynes, E.T., 2003. Probability theory. The logic of science. Cambridge University Press, New York, 727 pp.
Jonkman, S.N., 2005. Global Perspectives on Loss of Human Life Caused by Floods. Nat. Hazards 34, 151–175. doi:10.1007/s11069-004-8891-3
Journel, A., Huijbregts, C., 1878. Mining Geostatistics. Academic Press, London, 600 pp.
Katz, R.W., Parlange, M.B., Naveau, P., 2002. Statistics of extremes in hydrology. Adv. Water Resour. 25, 1287–1304.
Kavetski, D., Kuczera, G., Franks, S.W., 2006. Bayesian analysis of input uncertainty in hydrological modeling: 1. Theory. Water Resour. Res. 42, 1–9. doi:10.1029/2005WR004368
Kazianka, H., Pilz, J., 2011. Bayesian spatial modeling and interpolation using copulas. Comput. Geosci. 37, 310–319. doi:10.1016/j.cageo.2010.06.005
Koutsoyiannis, D., Makropoulos, C., Langousis, A., Baki, S., Efstratiadis, A., Christofides, A., Karavokiros, G., Mamassis, N., 2009. HESS Opinions: Climate, hydrology, energy, water: recognizing uncertainty and seeking sustainability. Hydrol. Earth Syst. Sci. 13, 247–257. doi:10.5194/hessd-5-2927-2008
Krause, P., Boyle, D.P., Bäse, F., 2005. Comparison of different efficiency criteria for hydrological model assessment. Adv. Geosci. 5, 89–97. doi:10.5194/adgeo-5-89-2005
Krige, D.G., 1951. A statistical approach to some mine valuations problems at the Witwatersrand. J. Chem. Metall. Min. Soc. South Africa 52, 119–139.
Kron, W., 2002. Keynote lecture: Flood risk = hazard x Exposure x Vulnerability, in: Flood Defence. Wu et al. (eds)© 2002 Science Press, New York Ltd, pp. 82–97.
Krzysztofowicz, R., 2002. Bayesian system for probabilistic river stage forecasting. J. Hydrol. 268, 16–40. doi:10.1016/S0022-1694(02)00106-3
Kučerová, A., Sýkora, J., Rosić, B. V., Matthies, H.G., 2012. Acceleration of uncertainty updating in the description of transport processes in heterogeneous materials. J Comput Appl Math 236, 4862–72.
Laaha, G., Skøien, J.O., Blöschl, G., 2014. Spatial prediction on river networks: comparison of top-kriging with regional regression. Hydrol. Process. 28, 315–324. doi:10.1002/hyp.9578
Laio, F., Di Baldassarre, G., Montanari, A., 2009. Model selection techniques for the frequency analysis of hydrological extremes. Water Resour. Res. 45, 1–11. doi:10.1029/2007WR006666
Leclerc, M., Ouarda, T.B.M.J., 2007. Non-stationary regional flood frequency analysis at ungauged sites. J. Hydrol. 343, 254–265. doi:10.1016/j.jhydrol.2007.06.021
Legates, D.R., McCabe Jr., G.J., 1999. Evaluating the Use of "Goodness of Fit" Measures in Hydrologic and Hydroclimatic Model Validation. Water Resour. Manag. 35 (1), 233–241.
Li, J., Heap, A.D., 2008. A Review of Spatial Interpolation Methods for Environmental Scientists, Geoscience Australia. Canberra, 154 pp.
Liu, Y., Gupta, H.V., 2007. Uncertainty in hydrologic modeling: Toward an integrated data assimilation framework. Water Resour. Res. 43, W07401. doi:10.1029/2006WR005756
Lombardi, L., Toth, E., Castellarin, A., Montanari, A., Brath, A., 2012. Calibration of a rainfall-runoff model at regional scale by optimising river discharge statistics: Performance analysis for the average/low flow regime. Phys. Chem. Earth 42–44, 77–84. doi:10.1016/j.pce.2011.05.013
Marzouk, Y., Xiu, D., 2009. A stochastic collocation approach to Bayesian inference in inverse problems. Commun Comput Phys 6, 826–47.

Marzouk, Y.M., Najm, H.N., Rahn, L.A., 2007. Stochastic spectral methods for efficient Bayesian solution of inverse problems. J. Comput. Phys. 224, 560–586. doi:10.1016/j.jcp.2006.10.010

Matheron, G., 1963. Principles of geostatistics. Econ. Geol. 58, 1246–1266.

Matott, L.S., Babendreier, J.E., Purucker, S.T., 2009. Evaluating uncertainty in integrated environmental models: A review of concepts and tools. Water Resour. Res. 45, W06421. doi:10.1029/2008WR007301

Mcmillan, H., Krueger, T., Freer, J., 2012. Benchmarking observational uncertainties for hydrology: Rainfall, river discharge and water quality. Hydrol. Process. 26, 4078–4111. doi:10.1002/hyp.9384

Merz, R., Blöschl, G., Humer, G., 2008. National flood discharge mapping in Austria. Nat. Hazards 46(1), 53–72. doi:10.1007/s11069-007-9181-7

Milly, P.C.D., Betancourt, J., Falkenmark, M., Hirsch, R.M., Kundzewicz, Z.W., Lettenmaier, D.P., Stouffer, R.J., 2008. Stationarity is dead: Whither water management? Science (80-. ). 319 (5863), 573–574.

Moisello, U., Papiri, S., 1986. "Relazione tra altezza di pioggia puntuale e ragguagliata," in: XX Convegno Nazionale Di Idraulica E Costruzioni Idrauliche. Padova.

Montanari, A., 2011. Uncertainty of hydrological predictions, in: Peter Wilderer (ed.) Treatise on Water Science (Ed.), . Oxford: Academic Press, vol. 2, pp. 459–478.

Montanari, A., 2007. What do we mean by "uncertainty"? The need for a consistent wording about uncertainty assessment in hydrology. Hydrol. Process. 21, 841–845. doi:10.1002/hyp.6623

Montanari, A., Brath, A., 2004. A stochastic approach for assessing the uncertainty of rainfall-runoff simulations. Water Resour. Res. 40, 1–11. doi:10.1029/2003WR002540

Montanari, A., Koutsoyiannis, D., 2012. A blueprint for process-based modeling of uncertain hydrological systems. Water Resour. Res. 48, 1–15. doi:10.1029/2011WR011412

Montanari, A., Shoemaker, C.A., Van De Giesen, N., 2009. Introduction to special section on uncertainty assessment in surface and subsurface hydrology: An overview of issues and challenges. Water Resour. Res. 45, 2005–2008. doi:10.1029/2009WR008471

Montanari, A., Young, G., Savenije, H.H.G., Hughes, D., Wagener, T., Ren, L.L., Koutsoyiannis, D., Cudennec, C., Toth, E., Grimaldi, S., Blöschl, G., Sivapalan, M., Beven, K.J., Gupta, H.V., Hipsey, M., Schaefli, B., Arheimer, B., Boegh, E., Schymanski, S.J., Di Baldassarre, G., Yu, B., Hubert, P., Huang, Y., Schumann, A., Post, D. a., Srinivasan, V., Harman, C., Thompson, S., Rogger, M., Viglione, A., McMillan, H., Characklis, G., Pang, Z., Belyaev, V., 2013. "Panta Rhei—Everything Flows": Change in hydrology and society—The IAHS Scientific Decade 2013–2022. Hydrol. Sci. J. 58, 1256–1275. doi:10.1080/02626667.2013.809088

National Academies of Sciences, 2012. Building Resilience to Disasters of Natural and Technological Origin, G-Science Resilience Statement, in: Science Academies Issue "G-Science" Statements to Call World Leaders' Attention to How Science and Technology Can Help Solve Global Challenges. https://rsc-src.ca/en/node/278.

Neuman, S.P., 2003. Maximum likelihood Bayesian averaging of uncertain model predictions. Stoch. Environ. Res. Risk Assess. 17, 291–305. doi:10.1007/s00477-003-0151-7

Nezhad, M.K., Chokmani, K., Ouarda, T.B.M.J., Barbet, M., Bruneau, P., 2010. Regional flood frequency analysis using residual kriging in physiographical space. Hydrol. Process. 24, 2045–2055. doi:10.1002/hyp.7631

NRC (National Research Council), 2000. Risk Analysis and Uncertainty in Flood Damage Reduction Studies. National Academy Press, Washington, DC.

Ouarda, T.B.M.J., Girard, C., Cavadias, G.S., Bobée, B., 2001. Regional flood frequency estimation with canonical correlation analysis. J. Hydrol. 254, 157–173.

Pajonk, O., Rosić, B. V., Litvinenko, A., Matthies, H.G., 2012. A deterministic filter for non-

Gaussian Bayesian estimation— Applications to dynamical system estimation with noisy measurements. Phys. D Nonlinear Phenom. 241, 775–788. doi:10.1016/j.physd.2012.01.001

Pajonk, O., Rosić, B. V., Matthies, H.G., 2013. Sampling-free linear Bayesian updating of model state and parameters using a square root approach. Comput. Geosci. 55, 70–83.

Pandey, G.R., Nguyen, V.T.V., 1999. A comparative study of regression based methods in regional flood frequency analysis. J. Hydrol. 225, 92–101. doi:10.1016/S0022-1694(99)00135-3

Pappenberger, F., Beven, K.J., 2006. Ignorance is bliss: Or seven reasons not to use uncertainty analysis. Water Resour. Res. 42, 1–8. doi:10.1029/2005WR004820

Parajka, J., Merz, R., Skøien, J.O., Viglione, A., 2015. The role of station density for predicting daily runoff by top-kriging interpolation in Austria. J. Hydrol. Hydromechanics 63, 228–234. doi:10.1515/johh-2015-0024

Parajka, J., Viglione, A., Rogger, M., Salinas, J.L., Sivapalan, M., Blöschl, G., 2013. Comparative assessment of predictions in ungauged basins – Part 1: Runoff-hydrograph studies. Hydrol. Earth Syst. Sci. 17, 1783–1795. doi:10.5194/hess-17-1783-2013

Pasetto, D., Camporese, M., Putti, M., 2012. Ensemble Kalman filter versus particle filter for a physically-based coupled surface-subsurface model. Adv. Water Resour. 47, 1–13. doi:10.1016/j.advwatres.2012.06.009

Pugliese, A., Castellarin, A., Brath, A., 2014. Geostatistical prediction of flow-duration curves in an index-flow framework. Hydrol. Earth Syst. Sci. 18, 3801–3816. doi:10.5194/hess-18-3801-2014

R Core Team, 2013. R: a language and environment for statistical computing. R Foundation for Statistical Computing, Vienna, Austria.

Reed, D.W., Jakob, D., Robson, A.J., Faulkner, D.S., Stewart, E.J., 1999. Regional frequency analysis : a new vocabulary, in: Hydrological Extremes: Understanding, Predicting, Mitigating (Proceedings of IUGG 99 Symposium HSI, Birmingham) IAHS Publ. No. 255. pp. 237–243.

Regan, H.M., Akçakaya, H.R., Ferson, S., Root, K. V, Carroll, S., Ginzburg, L.R., 2003. Treatments of Uncertainty and Variability in Ecological Risk Assessment of Single-Species Populations. Hum. Ecol. Risk Assess. An Int. J. 9, 889–906. doi:10.1080/713610015

Rosbjerg, D., Madsen, H., 1995. Uncertainty measures of regional flood frequency estimators. J. Hydrol. 167, 209–224. doi:10.1016/0022-1694(94)02624-K

Rosić, B., Sýkora, J., Pajonk, O., Kučerová, A., Matthies, H.G., 2014. Comparison of Numerical Approaches To Bayesian Updating. doi:http://www.digibib.tu-bs.de/?docid=00057895

Rosić, B. V., Kučerová, A., Sýkora, J., Pajonk, O., Litvinenko, A., Matthies, H.G., 2013. Parameter identification in a probabilistic setting. Eng. Struct. 50, 179–196. doi:10.1016/j.engstruct.2012.12.029

Rosić, B. V., Litvinenko, A., Pajonk, O., Matthies, H.G., 2012. Sampling-free linear Bayesian update of polynomial chaos representations. J. Comput. Phys. 231, 5761–87.

Rossi, F., Fiorentino, M., Versace, P., 1984. Two-Component Extreme Value Distribution for Flood Frequency Analysis. Water Resour. Res. 20, 847–856. doi:10.1029/WR020i007p00847

Saad, G., Ghanem, R., 2009. Characterization of reservoir simulation models using a polynomial chaos-based ensemble Kalman filter. Water Resour. Res. 45, 1–19. doi:10.1029/2008WR007148

Salinas, J.L., Laaha, G., Rogger, M., Parajka, J., Viglione, a., Sivapalan, M., Blöschl, G., 2013. Comparative assessment of predictions in ungauged basins – Part 2: Flood and low flow studies. Hydrol. Earth Syst. Sci. 17, 2637–2652. doi:10.5194/hess-17-2637-2013

Salvadori, G., De Michele, C., 2007. On the use of copulas in hydrology: theory and practice.

J. Hydrol. Eng. 369–380.
Salvadori, G., De Michele, C., Durante, F., 2011. On the return period and design in a multivariate framework. Hydrol. Earth Syst. Sci. 15, 3293–3305. doi:10.5194/hess-15-3293-2011
Samaniego, L., Bárdossy, A., Kumar, R., 2010. Streamflow prediction in ungauged catchments using copula-based dissimilarity measures. Water Resour. Res. 46, W02506. doi:10.1029/2008WR007695
Sauquet, E., 2006. Mapping mean annual river discharges: Geostatistical developments for incorporating river network dependencies. J. Hydrol. 331(1–2), 300–314. doi:10.1016/j.jhydrol.2006.05.018
Sauquet, E., Gottschalk, L., Leblois, E., 2000. Mapping average annual runoff: a hierarchical approach applying a stochastic interpolation scheme. Hydrol. Sci. J. 45, 799–815. doi:10.1080/02626660009492385
Shrestha, D.L., Kayastha, N., Solomatine, D.P., 2009. A novel approach to parameter uncertainty analysis of hydrological models using neural networks. Hydrol. Earth Syst. Sci. 13, 1235–1248. doi:10.5194/hess-13-1235-2009
Shrestha, D.L., Solomatine, D.P., 2008. Data-driven approaches for estimating uncertainty in rainfall-runoff modelling. Int. J. River Basin Manag. 6, 109–122. doi:10.1080/15715124.2008.9635341
Shu, C., Burn, D.H., 2004a. Homogeneous pooling group delineation for flood frequency analysis using a fuzzy expert system with genetic enhancement. J. Hydrol. 291, 132–149. doi:10.1016/j.jhydrol.2003.12.011
Shu, C., Burn, D.H., 2004b. Artificial neural network ensembles and their application in pooled flood frequency analysis. Water Resour. Res. 40, 1–10. doi:10.1029/2003WR002816
Sivapalan, M., Takeuchi, K., Franks, S.W., Gupta, V.K., Karambiri, H., Lakshmi, V., Liang, X., McDonnell, J.J., Mendiondo, E.M., O'Conell, P.E., Oki, T., Pomeroy, J.W., Schertzer, D., Uhlenbrook, S., Zehe, E., 2003. IAHS Decade on Predictions in Ungauged Basins (PUB), 2003–2012: Shaping an exciting future for the hydrological sciences. Hydrol. Sci. J. 48 (6), 857–880. doi:10.1623/hysj.48.6.857.51421
Skøien, J.O., Blöschl, G., 2007. Spatiotemporal topological kriging of runoff time series. Water Resour. Res. 43, W09419. doi:10.1029/2006WR005760
Skøien, J.O., Blöschl, G., Laaha, G., Pebesma, E., Parajka, J., Viglione, A., 2014. rtop: An R package for interpolation of data with a variable spatial support, with an example from river networks. Comput. Geosci. 67, 180–190. doi:10.1016/j.cageo.2014.02.009
Skøien, J.O., Merz, R., Blöschl, G., 2006. Top-kriging – geostatistics on stream networks. Hydrol. Earth Syst. Sci. 10 (2), 277–287. doi:10.5194/hess-10-277-2006
Skøien, J.O., Pebesma, E., Blöschl, G., 2008. Geostatistics for automatic estimation of environmental variables - some simple solutions. Georisk 2 (4), 257–270.
Stephenson, D.B., 2008. Definition, diagnosis and origin of extreme weather and climate events, in: Climate Extremes and Society. ed. H. F. Diaz and R. J. Murnane. Published by Cambridge University Press., New York, p. 340. doi:10.1017/CBO9780511535840.003
Stuart, A.M., 2010. Inverse problems: A Bayesian perspective, Acta Numerica. doi:10.1017/S0962492910000061
Szolgay, J., Parajka, J., Kohnová, S., Hlavčová, K., 2009. Comparison of mapping approaches of design annual maximum daily precipitation. Atmos. Res. 92, 289–307. doi:10.1016/j.atmosres.2009.01.009
Tarantola, A., 2004. Inverse problem theory and methods for model parameter estimation. Philadelphia.
Tartaglia, V., 2005. EnKF. School of Engineering, Università degli Studi di Firenze, PhD thesis, 250 pp (in Italian language).
Thyer, M., Renard, B., Kavetski, D., Kuczera, G., Franks, S.W., Srikanthan, S., 2009. Critical

evaluation of parameter consistency and predictive uncertainty in hydrological modeling: A case study using Bayesian total error analysis. Water Resour. Res. 45. doi:10.1029/2008WR006825

van der Sluijs, J.P., Craye, M., Funtowicz, M., Kloprogge, P., Ravetz, J., Risbey, J., 2005. Combining quantitative and qualitative measures of uncertainty in model-based environmental assessment: the NUSAP system. Risk Anal. 25, 481–492.

Vanni, M., 2015. Analysis of flood forecasting errors in an operative hydrological model. School of Engineering, Università degli Studi di Firenze, MSc degree, 133 pp (in Italian language).

Viglione, A., Parajka, J., Rogger, M., Salinas, J.L., Laaha, G., Sivapalan, M., Blöschl, G., 2013. Comparative assessment of predictions in ungauged basins - Part 3: Runoff signatures in Austria. Hydrol. Earth Syst. Sci. 17, 2263–2279. doi:10.5194/hess-17-2263-2013

Vrugt, J.A., Gupta, H.V., Bastidas, L.A., Bouten, W., Sorooshian, S., 2003a. Effective and efficient algorithm for multiobjective optimization of hydrologic models. Water Resour. Res. 39, 1–19. doi:10.1029/2002WR001746

Vrugt, J.A., Gupta, H.V., Bouten, W., Sorooshian, S., 2003b. A Shuffled Complex Evolution Metropolis algorithm for optimization and uncertainty assessment of hydrologic model parameters. Water Resour. Res. 39, 1201. doi:10.1029/2002WR001642

Vrugt, J.A., Robinson, B.A., 2007. Improved evolutionary optimization from genetically adaptive multimethod search. Proc. Natl. Acad. Sci. U. S. A. 104, 708–711. doi:10.1073/pnas.0610471104

Vrugt, J.A., ter Braak, C.J.F., Gupta, H.V., Robinson, B.A., 2009. Equifinality of formal (DREAM) and informal (GLUE) Bayesian approaches in hydrologic modeling? Stoch. Environ. Res. Risk Assess. 23, 1011–1026. doi:10.1007/s00477-008-0274-y

Wagener, T., McIntyre, N., Lees, M.J., Wheater, H.S., Gupta, H. V., 2003. Towards reduced uncertainty in conceptual rainfall-runoff modelling: Dynamic identifiability analysis. Hydrol. Process. 17, 455–476. doi:10.1002/hyp.1135

Webster, R., Oliver, M., 2001. Geostatistics for Environmental Scientists. John Wiley & Sons, Ltd, Chichester, UK, 271 pp.

Wiener, N., 1938. The Homogeneous Chaos. Am. J. Math. 60, 897–936.

Willmott, C.J., 1981. On the validation of models. Phys. Geogr. 2, 184–194. doi:10.1080/02723646.1981.10642213

Wiltshire, S.E., 1986. Identification of homogeneous regions for flood frequency analysis. J. Hydrol. 84, 287–302. doi:10.1016/0022-1694(86)90128-9

Xiu, D., 2010. Numerical Methods for Stochastic Computations: A Spectral Method Approach, Princeton University Press. Princeton.

Yang, J., Castelli, F., Chen, Y., 2014. Multiobjective sensitivity analysis and optimization of distributed hydrologic model MOBIDIC. Hydrol. Earth Syst. Sci. 18, 4101–4112. doi:10.5194/hess-18-4101-2014

Ye, M., Meyer, P.D., Neuman, S.P., 2008. On model selection criteria in multimodel analysis. Water Resour. Res. 44, 1–12. doi:10.1029/2008WR006803

Zarlenga, A., Fiori, A., Soffia, C., Janković, I., 2012. Flow velocity statistics for uniform flow through 3D anisotropic formations. Adv. Water Resour. 40, 37–45. doi:10.1016/j.advwatres.2012.01.011

APPENDIX A1:

| COD | Name | E UTM [m] | N UTM [m] | E GB [m] | N GB [m] | A [km$^2$] | 1st year | Last year | N° years | Max AM [m$^3$/s] | Distribution | Q10 [m$^3$/s] | Q50 [m$^3$/s] | Q100 [m$^3$/s] | Q200 [m$^3$/s] | Q500 [m$^3$/s] |
|---|---|---|---|---|---|---|---|---|---|---|---|---|---|---|---|---|
| 4379 | Stia | 713353 | 4856143 | 1717111 | 4853769 | 60.8 | 1939 | 2010 | 38 | 312.0 | GEV | 80.0 | 134.8 | 165.5 | 201.8 | 260.3 |
| 4400 | Pollino | 719489 | 4848871 | 1727624 | 4841105 | 457.2 | 1933 | 1942 | 10 | 417.0 | P3 | 390.7 | 408.0 | 411.2 | 413.3 | 414.8 |
| 4411 | Subbiano | 723539 | 4844721 | 1731587 | 4828203 | 748.2 | 1930 | 2011 | 76 | 2250.0 | LN | 908.7 | 1318.3 | 1503.3 | 1695.3 | 1961.2 |
| 4521 | Ponte ferrovia Fi-Roma | 731853 | 4787826 | 1728495 | 4816533 | 1390.9 | 1926 | 2010 | 69 | 567.0 | GUMBEL | 412.1 | 588.8 | 663.5 | 737.9 | 836.1 |
| 4560 | Ponte Romito | 716499 | 4819851 | 1716446 | 4819671 | 2400.1 | 1936 | 1955 | 13 | 1440.0 | LN | 1188.6 | 1532.7 | 1676.6 | 1820.1 | 2010.6 |
| 4568 | Bucine | 710910 | 4810455 | 1711804 | 4817854 | 159.8 | 1996 | 2010 | 15 | 176.1 | GUMBEL | 154.2 | 218.9 | 246.2 | 273.4 | 309.3 |
| 4610 | Ponte del Bilancino | 679735 | 4876691 | 1683714 | 4871656 | 150.2 | 1965 | 1984 | 18 | 585.6 | LN | 475.7 | 674.5 | 763.0 | 854.1 | 979.2 |
| 4641 | Fornacina | 694196 | 4868377 | 1698537 | 4852775 | 824.8 | 1931 | 2005 | 71 | 1340.0 | GUMBEL | 699.6 | 950.3 | 1056.2 | 1161.8 | 1301.1 |
| 4659 | Nave di Rosano | 717076 | 4825164 | 1694862 | 4849357 | 4198.4 | 1931 | 2011 | 71 | 3540.0 | GUMBEL | 1837.9 | 2492.9 | 2769.8 | 3045.7 | 3409.6 |
| 4710 | Ponte Falciani | 685450 | 4831021 | 1678509 | 4838252 | 119.3 | 1933 | 1992 | 40 | 258.5 | LN | 141.3 | 280.7 | 357.8 | 446.6 | 584.3 |
| 4750 | Praticello | 666994 | 4875953 | 1666941 | 4875773 | 37.3 | 1960 | 1976 | 17 | 121.0 | LN | 92.3 | 128.8 | 144.9 | 161.5 | 183.9 |
| 4760 | Carmignanello | 670124 | 4878366 | 1670071 | 4878186 | 110.9 | 1937 | 1960 | 15 | 278.0 | LN | 212.3 | 318.0 | 366.8 | 417.9 | 489.6 |
| 4779 | Gamberame | 670329 | 4875978 | 1670737 | 4865309 | 156.6 | 1959 | 2009 | 43 | 302.0 | P3 | 239.6 | 338.9 | 380.5 | 421.5 | 475.3 |
| 4791 | S.Piero a Ponti | 672065 | 4870200 | 1671422 | 4852276 | 267.9 | 1992 | 2010 | 17 | 408.8 | LN | 385.3 | 570.1 | 654.7 | 743.1 | 866.3 |
| 4820 | Ponte di Calcaiola | 652879 | 4875998 | 1651720 | 4875059 | 17.5 | 1986 | 2000 | 12 | 103.0 | P3 | 98.9 | 152.9 | 175.8 | 198.5 | 228.5 |
| 4860 | Burgianico | 654496 | 4872442 | 1653342 | 4868986 | 13.5 | 1940 | 2001 | 25 | 68.3 | LN | 39.7 | 70.8 | 86.8 | 104.6 | 131.2 |
| 4875 | Poggio a Caiano | 657693 | 4864958 | 1665817 | 4853340 | 439.3 | 1992 | 2010 | 16 | 433.0 | P3 | 336.5 | 474.0 | 532.5 | 590.8 | 667.5 |
| 4901 | Brucianesi | 706035 | 4832968 | 1665905 | 4848361 | 5590.7 | 1928 | 2008 | 21 | 1980.0 | NORM | 1764.6 | 2063.4 | 2168.8 | 2265.4 | 2382.3 |
| 4910 | Sambuca | 687398 | 4821518 | 1679247 | 4825920 | 118.0 | 1973 | 2001 | 25 | 339.0 | LN | 115.2 | 227.3 | 289.0 | 360.0 | 469.7 |
| 4971 | Castelfiorentino | 670908 | 4813963 | 1658971 | 4829611 | 799.2 | 1950 | 2000 | 46 | 612.0 | LN | 308.6 | 500.0 | 592.9 | 692.9 | 837.0 |
| 5040 | Nievole Colonna | 644699 | 4864855 | 1645436 | 4860137 | 38.0 | 1954 | 1998 | 33 | 44.3 | P3 | 35.7 | 54.4 | 62.3 | 70.2 | 80.5 |
| 5050 | Molino Parlanti | 645621 | 4858701 | 1645551 | 4859985 | 4.7 | 1965 | 2002 | 33 | 2.9 | P3 | 2.1 | 3.1 | 3.5 | 3.9 | 4.5 |
| 5070 | Molino Narducci | 639008 | 4871058 | 1637162 | 4868346 | 47.8 | 1936 | 1955 | 15 | 112.0 | LN | 88.8 | 141.1 | 166.2 | 193.0 | 231.4 |
| 5130 | Capannoli | 644164 | 4813110 | 1635916 | 4827789 | 334.2 | 1933 | 2002 | 31 | 311.0 | GEV | 250.7 | 652.9 | 981.3 | 1474.0 | 2523.4 |
| 5191 | San Giovanni alla Vena | 687744 | 4832315 | 1627771 | 4838082 | 8631.4 | 1924 | 2000 | 75 | 2290.0 | P3 | 1941.4 | 2611.3 | 2879.7 | 3140.2 | 3475.3 |
| 5270 | Cartiera Valgiano | 628548 | 4864242 | 1627546 | 4863116 | 5.6 | 1961 | 1981 | 19 | 2.5 | P3 | 2.2 | 3.2 | 3.7 | 4.1 | 4.7 |